MEDICAL UNIVERSITY OF VIENNA

Nucleic Acid Sensing in the Cytosol

Doctoral thesis at the Medical University of Vienna
for obtaining the academic degree

Doctor of Philosophy

Submitted by

Mag. Evelyn Dixit

Supervisor:
Prof. Dr. Giulio Superti-Furga
CeMM - Research Center for Molecular Medicine
of the Austrian Academy of Sciences
Lazarettgasse 14, AKH BT 25.3, A-1090 Vienna

Vienna, 10/2011

To Annika

Who teaches me the most important lessons in life

ACKNOWLEDGEMENTS

I am grateful to those who guided, supported and encouraged me throughout the pursuit of my PhD. I consider myself extremely fortunate to be surrounded by many wonderful people who directly or indirectly contributed to my success. I would like to express my gratitude to all the helpful people I met over the course of my PhD, particularly to:

My supervisor *Prof. Dr. Giulio Superti-Furga* for the great opportunity to work on fascinating projects in an innovative research environment, for his ceaseless scientific and career advice, but above all his tremendous patience with an individualistic student, a longer than planned stay abroad and a tough pregnancy during the compilation of this thesis.

Dr. Tilmann Bürckstümmer for excellent day to day supervision, countless scientific discussions and the freedom to work independently.

Prof. Dr. Jonathan Kagan – my senior partner of Team Peroxisome – who hosted me for a year, let me investigate 'a crazy idea' that turned into a scientific goldmine, hooked me up to many a source to help me complete the project in record time, picked up all loose ends after I had to leave and taught me how much fun it is to talk science.

Team Peroxisome was never short of enthusiastic encouragement, technical support and scientific advice provided by my Boston lab colleagues: Lorri Marek, Christoph Glanemann, Ivan Zanoni, Muriel Schneider, Sky Brubaker and Kevin Bonham. Special thanks go to Steeve Boulant and Bennett Shum who diligently and repeatedly lysed virus-infected cells in the dead of the night for me.

I also thank all past and present members of CeMM, especially those who shared the lab with me and created such a friendly, pleasant and neat work environment.

Last, but not least, I thank my family and friends who were there for me when science was no fun: Sunil, for his love, loyalty and patience, Babsi for her insistence on realizing my potential, Los Haselsteineros for good food and good spirits, my parents and sister Karin for their support throughout the years and excessive babysitting more recently.

The results presented in this thesis constitute the major part of the following publication:

Dixit, E., Boulant, S., Zhang, Y., Lee, A.S., Odendall, C., Shum, B., Hacohen, N., Chen, Z.J., Whelan, S.P., Fransen, M., Nibert, M.L., Superti-Furga, G. & Kagan, J.C.

Peroxisomes are signaling platforms for antiviral innate immunity.

Cell 141, 668-681.

SUMMARY

Peroxisomes have long been established to play a central role in regulating various metabolic activities in mammalian cells. These organelles act in concert with mitochondria to control the synthesis and degradation of lipids and reactive oxygen species. However, while mitochondria have emerged as an important site of antiviral signal transduction, a role for peroxisomes in immune defense is unknown. The innate immune system typically detects viral infections by the presence of pathogen-derived nucleic acids. The RIG-I-like receptors, one family of so-called pathogen recognition receptors, sense viral RNA in the cytosol of infected cells and initiate a signal transduction cascade that depends on the adapter protein MAVS and ultimately leads to induction of type I interferon and interferon-stimulated genes. Collectively these defense factors establish an antiviral state in infected and adjacent cells.

In this study I show that MAVS – in addition to its known localization on mitochondria – is also expressed on peroxisomes. Several lines of evidence indicate the presence of MAVS on peroxisomes. First, MAVS co-localizes with peroxisomal marker proteins in human and murine cells. Second, MAVS co-purifies with peroxisomal proteins in cell fractionation experiments. To determine the functional significance of these findings, I generated cell lines that differ only in their subcellular localization of MAVS to peroxisomes and/or mitochondria. I find that peroxisomal and mitochondrial MAVS act sequentially to create an antiviral cellular state. Upon viral infection, peroxisomal MAVS induces the rapid interferon-independent expression of defense factors that provides short-term protection, whereas mitochondrial MAVS activates an interferon-dependent signaling pathway with delayed kinetics, which amplifies and stabilizes the antiviral response.

These results establish that peroxisomes are not solely metabolic organelles, but are an important site of antiviral signal transduction.

ZUSAMMENFASSUNG

Es ist seit langem bekannt, dass Peroxisomen eine zentrale Rolle bei der Regulation verschiedener metabolischer Prozesse in Säugerzellen einnehmen. Diese Organellen steuern in enger Kooperation mit Mitochondrien die Synthese und den Abbau von Lipiden und reaktiven Sauerstoffspezies. Während Mitochondrien als Ort von antiviraler Signaltransduktion bereits etabliert sind, ist eine Rolle für Peroxisomen in der Immunantwort unbekannt. Das angeborene Immunsystem detektiert Virusinfektionen zumeist über die Anwesenheit der Nukleinsäuren des Erregers mit Hilfe sogenannter *pattern recognition*-Rezeptoren. Die Familie der RIG-I-ähnlichen Rezeptoren erkennt virale RNA im Zytosol infizierter Zellen und löst unter Verwendung des Adaptorproteins MAVS eine Signaltransduktionskaskade aus, die letztlich zur Induktion von Typ I Interferon und Interferon-stimulierten Genen führt. Die Gesamtheit dieser Abwehrfaktoren ermöglicht einen antiviralen Zustand der befallenen und benachbarten Zellen.

Ich zeige in dieser Studie, dass MAVS – zusätzlich zur bekannten Lokalisation auf Mitochondrien – auch auf Peroxisomen zu finden ist. Mehrere unabhängige Befunde belegen die Anwesenheit von MAVS auf Peroxisomen: Erstens, MAVS ist mit peroxisomalen Markerproteinen in humanen und murinen Zellen kolokalisiert. Zweitens, nach Zellfraktionierung sedimentiert MAVS in der gleichen Fraktion wie andere peroxisomale Proteine. Um die funktionelle Signifikanz der Lokalisationsdaten zu beurteilen, wurden Zelllinien generiert, die sich einzig durch die Lokalisation von MAVS auf Peroxisomen und/oder Mitochondrien unterscheiden. Ich zeige hier, dass peroximales und mitochondriales MAVS nacheinander agieren, um einen antiviralen Zustand herbeizuführen. Nach viraler Infektion induziert peroxisomales MAVS eine schnelle Interferon-unabhängige Expression von Abwehrfaktoren, wodurch ein vorübergehender Schutz gewährleistet wird. Mitochondriales MAVS hingegen aktiviert Interferon-abhängige Signaltransduktionswege mit langsamerer Kinetik, die die antivirale Antwort verstärken und stabilisieren.

Diese Forschungsergebnisse belegen, dass Peroxisomen nicht nur metabolischen Zwecken dienen, sondern auch einen wichtigen Ort der antiviralen Signaltransduktion darstellen.

TABLE OF CONTENTS

ABBREVIATIONS

AIM2A	Absent in melanoma 2
AP-1	Activator protein 1
APC	Antigen presenting cell
CARD	Caspase activation and recruitment domain
cDC	Conventional dendritic cell
CLR	C-type lectin receptor
CpG-DNA	DNA sequence rich in unmethylated 2′-deoxyribo cytidine-phosphateguanosine (TLR9 ligand)
CTL	Cytotoxic T lymphocytes
DC	Dentritic cell
ds	Double-stranded
EBV	Epstein–Barr virus
EMCV	Encephalomyocarditis virus
Fis1	Fission 1 (mitochondrial outer membrane) homolog (S. cerevisiae)
fw	Forward
GAS	Interferon-gamma-activated sequence
GFP	Green fluorescent protein
HCMV	Human cytomegalovirus
HCV	Hepatitis C virus
HIV	Human immunodeficiency virus
HSV	Herpes simplex virus
iE-DAP	D-glutamyl-meso-diaminopimelic acid (NOD1 ligand)
IFN	Interferon
IFNAR	Interferon alpha/beta receptor
IFNGR	Interferon gamma receptor
IKK	IκB kinase
IL	Interleukin
IRF	Interferon regulatory factor
ISG	Interferon stimulated gene
ISGF3	Interferon-stimulated gene factor 3
ISRE	Interferon-stimulated response element
JAK	Janus kinase

JEV	Japanese encephalitis virus
LeTx	Anthrax lethal toxin
LGP2	Laboratory of genetics and physiology 2
LPS	Lipopolysaccharide
MAPK	Mitogen-activated protein kinase
MAVS	Mitochondrial antiviral signaling protein
MCMV	Mouse cytomegalovirus virus
MDA-5	Melanoma differentiation-associated gene 5
MDP	Muraml dipeptide (NOD2 ligand)
MEF	Mouse embryonic fibroblasts
Mϕ	Macrophage
Mff	Mitochondrial fission factor
MINCLE	Macrophage-inducible C-type lectin
MMTV	Mouse mammary tumor virus
MYD88	Myeloid differentiation primary response protein 88
NDV	Newcastle disease virus
NF-κB	Nuclear factor kappa B
NLR	NOD-like receptor
NLRC4	NLR family, CARD domain containing protein 4
NLRP1, NLRP3, NLRP6	NLR family, pyrin domain containing protein 1, 3 and 6
NLRX1	NLR family member X1
NLS	Nuclear localization signal
NOD1 , NOD2	Nucleotide-binding oligomerization domain containing protein 1 and 2
OAS	2',5'-oligoadenylate synthetase
PAMP	Pathogen-associated molecular pattern
PARP	Poly (ADP-ribose) polymerase
PBS	Phosphate buffered saline
PCR	Polymerase chain reaction
pDC	Plasmacytoid dentritic cell
PFA	Paraformaldehyde
PIP2	Phosphatidylinositol 4,5 bisphosphate
PKR	Protein kinase R
polyI:C	Polyinosinic-polycytidylic acid (TLR3/MDA-5 ligand)
PRR	Pattern recognition receptor

RD	Repressor domain
rev	Reverse
RIG-I	Retinoic acid inducible gene I
Riplet	RING finger protein leading to RIG-I activation
RLR	RIG-I-like receptor
RLR	RIG-I-like receptors
ROS	Reactive oxygen species
RSV	Respiratory syncytial virus
SDS-PAGE	Sodium dodecyl sulfate-polyacrylamide gel electrophoresis
SeV	Sendai virus
ss	Single-stranded
STAT	Signal transducers and activators of transcription
STING	Stimulator of interferon genes
TAE	Tris-acetate-ethylene diamine tetra acetic acid-buffer
TBK1	TANK binding kinase 1
TIRAP	TIR domain-containing adapter protein
TLR	Toll-like receptor
TNFα	Tumer necrosis factor alpha
TRAM	TRIF-related adapter molecule
TRIF	TIR domain-containing adapter protein inducing IFN beta
TRIM25	Tripartite motif-containing protein 25
VSV	Vesicular stomatatis virus
WNV	West Nile virus
ZAPS	Zincfinger antiviral protein shorter isoform

INTRODUCTION

Innate immunity provides the first line of protection against viruses

Viruses are obligate intracellular parasites and thus strictly depend on the biosynthetic machinery of the host in order to replicate and spread. Exploitation of the host cell's metabolic pathways and reprogramming of cellular processes by the virus often lead to cell death [1]. The struggle for survival between virus and host cell is ancient and as a consequence both organisms have evolved multiple strategies to antagonize each other. While mammalian hosts developed sophisticated mechanisms of antiviral immunity, viruses acquired strategies to evade the immune response [2]. It is mandatory for the host to mount an effective innate and adaptive immune response immediately upon infection to successfully combat the pathogen.

The innate immune response constitutes the earliest phase of the host's defense against viruses. It attenuates viral replication and ensures cell survival until the specialized adaptive response has formed [3]. Type I interferons (IFN), i. e. IFN-α and IFN-β, are secreted within few hours after infection, which is imperative for an efficient antiviral defense. Interferons - named after their fundamental ability to interfere with virus infection [4] - exhibit antiviral, antiproliferative and immunomodulatory functions [5]. The IFN circuit constitutes of a 2-step process: First, viruses are detected by so-called pattern recognition receptors (PRR) which trigger IFN secretion. Second, binding of secreted IFN to the IFN-α receptor (IFNAR) on the surface of infected and neighbouring cells results in the expression of hundreds of interferon-stimulated genes (ISG) [6]. These ISGs collectively establish an antiviral state that limits viral replication and prevents further spread of the infection (Figure 1) [7]. The importance of the IFN system for antiviral immunity is underscored by the enhanced susceptibility of IFNAR-deficient mice to virus infection [8, 9] and the numerous evasion mechanisms devised by viruses to interfere with IFN or ISG production and function [7].

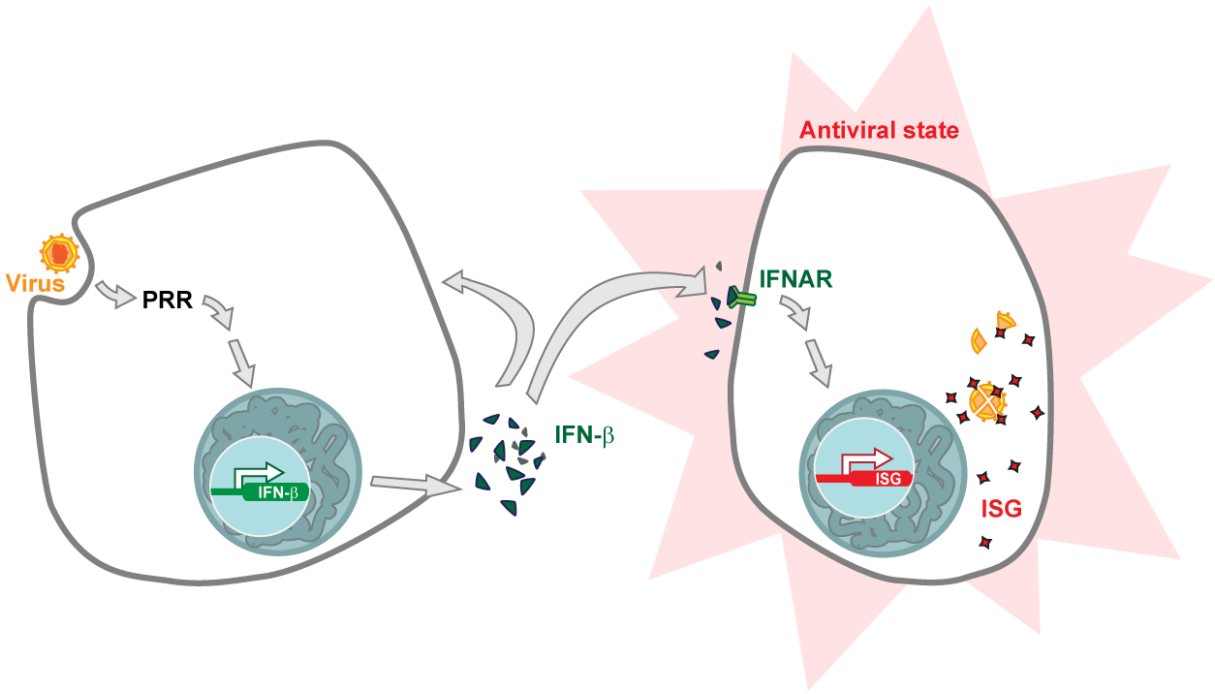

Figure 1. Type I IFN secretion is the hallmark of antiviral immunity

A variety of PRR detect viral infections and trigger the production of type I IFN. IFN acts on the same and neighbouring cells to induce ISG expression, which in turn establishes an antiviral state in the cell.

Pathogen recognition triggers an inflammatory response

Janeway's pattern recognition theory

Two decades ago at the 3rd Cold Spring Harbor Symposium dedicated to immune recognition, the late Charles Janeway Jr. held a provocative speech pointing out a gross oversight in immunology. At the time Burnet's clonal selection theory had been accepted as the central paradigm of immunology, B and T lymphocytes had been identified as major players, the molecules involved – antibodies, B and T cell receptors – as well as the generation thereof by genetic rearrangement had been discovered, and the principle of major histocompatibility complex (MHC) restriction was known. However, the question of immunogenicity had not been addressed to Janeway's satisfaction. He proposed the existence of signaling events beyond the known interaction between antigen and lymphocyte receptor and postulated the requirement for such signaling as a prerequisite for an effective immune response. He described the features of this second costimulatory signal as follows: Antigen presenting cells (APC) like dentritic cells (DC) and macrophages (Mϕ) express germ line-encoded pattern recognition receptors (PRR) that recognize highly conserved molecular structures shared by many microbes, but absent on mammalian cells. These so-called pathogen-associated

molecular patterns (PAMP) are products of biosynthetic pathways that are essential for the survival of the pathogen and therefore lack the potential for variability. The second signal culminates in cytokine secretion that allows lymphocyte activation, clonal expansion and generation of an immune response. This distinct type of immune recognition is phylogenetically older and thus operates as the only defense mechanism against pathogens in invertebrates [10].

Janeway's pattern recognition theory not only outlined the general principle of innate immune recognition, it also placed the initiation of the adaptive immune response under control of the pathogen sensing mechanisms of the innate immune system [11]. Certainly Janeway's theory laid the groundwork for modern innate immunity research. It would take ten years until the identification of the first pattern recognition receptor – Toll-like receptor 4 (TLR4), but since then a complex network of receptors and signaling pathways aimed at detecting and eliminating pathogens has emerged.

Pattern recognition receptors sense microbial infection

PRRs have evolved to recognize PAMPs - signature components that represent broad classes of microbes - and thus detect a wide variety of pathogens including viruses, bacteria, fungi and protozoan as well as helminth parasites. Invariably the specificities of PRRs are germ line-encoded and as a consequence they are limited in number. In general pattern recognition receptors harbor a "recognition domain" for ligand binding and an "interaction domain" to initiate downstream signaling [12]. Based on their domain architecture PRRs are grouped into four different classes, two of which include transmembrane proteins such as the Toll-like receptors (TLR) and C-type lectin receptors (CLR). The other two – RIG-I-like receptors (RLR) and NOD-like receptors (NLR) – are comprised of cytosolic proteins. Many of these receptors are not only expressed in Mϕs and DCs, but also in non-professional immune cells. Overall, engagement of PRRs leads to the activation of signaling cascades that culminate in the transcription of genes responsible for an inflammatory response. Among these genes are proinflammatory cytokines such as tumor necrosis factor alpha (TNFα), interleukin (IL)-1 and IL-6, type I IFN, chemokines and antimicrobial peptides. However, the inflammatory output is determined by the identity of both the recognition receptor and the cell type [13]. The ligand specificities of the major PRR families are listed in Table 1. It is important to note, that a given pathogen is composed of several PAMPs and that one PAMP may be detected by

more than one PRR. Therefore the innate immune response is the sum of pathogen-specific and cell type-specific responses.

PRRs	Subcellular Compartment	Ligand	Origin of the Ligand	Output (Source)
TLRs				
TLR2-TLR1 heterodimer	Plasma membrane	Triacyl lipoprotein	Gram-negative bacteria Mycoplasma	Proinflammatory cytokines (DC and Mϕ)
TLR2-TLR6 heterodimer	Plasma membrane	Diacyl lipoprotein	Gram-positive bacteria Mycoplasma	Proinflammatory cytokines (DC and Mϕ)
TLR2	Plasma membrane	Unknown	Vaccinia virus	Type I IFN (Inflammatory monocytes)
TLR3	Endolysosome	dsRNA	Reovirus, EMCV, WNV, RSV	Cytokines and IFN (cDC and Mϕ)
TLR4	Plasma membrane	LPS Pneumolysin RSV fusion protein MMTV envelope protein	Gram-negative bacteria *Streptococcus pneumoniae* RSV MMTV	Cytokines and IFN (cDC and Mϕ)
TLR5	Plasma membrane	Flagellin	Bacteria	Proinflammatory cytokines (Lamina propria DC)
TLR7 (human TLR8)	Endolysosome	ssRNA Imiquimod, R-848	RNA viruses: VSV, Influenza virus, HIV	Proinflammatory cytokines (cDC and Mϕ) IFN-α (pDC)
TLR9	Endolysosome	CpG-DNA Crystal hemozoin	DNA viruses: MCMV, HSV-1, HSV-2 bacteria, protozoa *Plasmodium falciparum*	Proinflammatory cytokines (cDC and Mϕ) IFN-α (pDC)
RLRs				
RIG-I	Cytoplasm	Short dsRNA, 5'-triphosphate RNA	RNA viruses: Influenza virus, NDV, SeV, VSV, HCV, WNV Dengue virus, reovirus DNA viruses: Adenovirus, HSV, EBV	Cytokines and IFN (most cell types)
MDA-5	Cytoplasm	Long dsRNA	RNA viruses: EMCV, poliovirus, Theiler's virus, WNV, Dengue virus, reovirus	Cytokines and IFN (most cell types)
NLRs				
NOD1	Cytoplasm	Peptidoglycan (iE-DAP)	Bacteria	Proinflammatory cytokines (APC, epithelial cell subsets)
NOD2	Cytoplasm	Peptidoglycan (MDP)	Bacteria	Proinflammatory cytokines (APC, other hematopoietic cells, Paneth cells)
NLR-Inflammasomes				
NLRP1	Cytoplasm	LeTx Peptidoglycan (MDP)	*Bacillus anthracis* Bacteria	IL-1β, IL-18 maturation

continued from previous page

PRRs	Subcellular Compartment	Ligand	Origin of the Ligand	Output (Source)
NLRP3	Cytoplasm	Crystals Membrane integrity M2 ionic channel ss and ds RNA	Asbestos, uric acid Influenza virus SeV, Vaccinia virus, Adenovirus, Varizella zoster	IL-1β, IL-18 maturation
NLRP3	Cytoplasm	Crystals Membrane integrity M2 ionic channel ss and ds RNA	Asbestos, uric acid Influenza virus SeV, Vaccinia virus, Adenovirus, Varizella zoster	IL-1β, IL-18 maturation
NLRC4	Cytoplasm	Flagellin and others	Type III and type IV secretion systems of bacteria: Salmonella, Shigella, Legionella, Pseudomonas	IL-1β, IL-18 maturation, pyroptosis
NLRP6	Cytoplasm	Unknown	Unknown	Regulation of gut microbiota (Colonic epithelial)
Non-NLR-Inflammasome				
AIM2	Cytoplasm	dsDNA	DNA viruses Intracellular bacteria	IL-1β, IL-18 maturation
CLRs				
Dectin-1	Plasma membrane	β-Glucan	Fungi	Cytokines, phagocytosis (DC and Mϕ)
Dectin-2	Plasma membrane	High mannose	Fungi	Cytokines (DC and Mϕ)
MINCLE	Plasma membrane	α-Mannose	Fungi	Cytokines (DC and Mϕ)

Table 1. Overview of PAMPs and PRRs

A wide variety of PAMPs is detected by PRRs that are generally categorized into TLRs, RLRs, NLRs and CLRs. For expansion of the used abbreviations please refer to the list of abbreviations on page 1.

In the following I will focus only on classes of PRRs involved in virus detection with special emphasis on the cytosolic nucleic acid receptors of the RLR family. Virus detection poses a particular challenge to the host as they barely offer features in line with the original definition of PAMPs, i. e. invariant structures that are essential for the survival of the pathogen. With few notable exceptions viral proteins mutate easily without being functionally compromised. Moreover, viruses are obligate parasites that lack their own metabolism. The evolutionary solution to this dilemma is to recognize viral nucleic acids, either virus genomes or replication intermediates. PRRs discriminate between four virally derived nucleic acid species: single-stranded (ss) RNA, double-stranded (ds) RNA, ssDNA and ds DNA. Clearly, nucleic acids are not a PAMP that is unique to viruses and thus virus detection comes at the cost of the potential for autoimmunity [14].

TLRs are membrane - bound pattern recognition receptors of immune cells

To date, 10 human and 12 murine TLRs have been identified. TLR1-9 are conserved in both species, mouse TLR10 is non-functional and humans lack the genes for TLR11-13. TLRs contain a horse shoe-shaped ligand sensing domain comprised of leucine rich repeats (LRR), a transmembrane domain and a carboxyterminal cytoplasmic tail harboring a Toll - interleukin 1 receptor (TIR) domain. Despite the similarity of their ectodomains, TLRs recognize an impressive variety of PAMPs including lipids, lipoproteins, proteins and nucleic acids (Table 1). With respect to their cellular localization and their specificity TLRs are divided into two subgroups. However, regardless of their locale both subgroups detect infectious agents present outside the cell that may or may not have been endocytosed. TLR1, TLR2, TLR4, TLR5, and TLR6 are expressed on the cell surface with their ligand binding domain facing the extracellular space [15]. Overall, these TLRs are not linked to antiviral immunity notwithstanding exceptions. Mϕs and DCs produce various proinflammatory cytokines (but not type I IFN) when TLR2/1 and TLR2/6 are activated by bacterial lipoprotein [16-18]. However, a small subset of bone marrow resident immune cells, termed inflammatory monocytes, produce type I IFN in a TLR2-dependent manner in response to infection with vaccinia virus, even though the identity of the actual ligand molecule remains elusive [19]. LPS from gram-negative bacteria is the stereotypical ligand for TLR4 [20], but TLR4 is also activated by viral proteins such as the respiratory syncytial virus (RSV) fusion protein or the mouse mammary tumor virus (MMTV) envelope protein [21, 22]. In contrast to the former group, TLR3, TLR7/8 and TLR9 are well established sensors for viral infection. They are found within the endolysosomal compartments where they probe endocytosed material for the presence of nucleic acids derived from viruses and bacteria, but also endogenous nucleic acid in pathological settings [13]. The intracellular localization of the nucleic acid sensing TLRs may represent one precautionary measure to prevent autoimmunity through self-nucleic acids [14].

TLR3 is a sensor for dsRNA and was originally identified as a receptor for the synthetic compound polyinosinic-polycytidylic acid (polyI:C) that mimics viral infection [23]. As such it detects the genomic dsRNA of reovirus, and dsRNA replication intermediates of ssRNA viruses such as encephalomyocarditis virus (EMCV), West Nile virus (WNV), and RSV [15]. TLR7 and TLR8 are closely related. ssRNA is the natural agonist of both murine TLR7 and human TLR7/8 [24, 25], but they can also be activated by imidazoquinoline derivatives, i. e. antiviral drugs such as imiquimod or R-848 [26]. Vesicular stomatitis virus (VSV), influenza A

virus and human immunodeficiency virus (HIV) are examples of RNA viruses that elicit a TLR7/8-dependent IFN-response [24, 25, 27]. TLR 9 recognizes unmethylated 2′-deoxyribo cytidine-phosphateguanosine (CpG) DNA motifs that are frequently found in bacteria and viruses, but are rare in mammalian cells [28, 29]. Thus TLR9 senses infection with DNA viruses such as mouse cytomegalovirus virus (MCMV), herpes simplex virus 1 (HSV-1) and HSV-2 [30-32].

TLR3 is present in Mϕs and DCs and when stimulated induces both type I IFN and proinflammatory cytokines [12]. TLR7 and TLR9, but not TLR3, are highly expressed in plasmacytoid DCs (pDCs), a cell type that is predisposed to producing copious amounts of IFN-α due to constitutive expression of the transcription factor interferon regulatory factor 7 (IRF7) [33]. TLR8 is mainly found in cells of myeloid lineage - predominantly monocytes, but also Mϕs and DC - and leads to secretion of proinflammatory cytokines, but not type I IFN [13].

RLRs detect viral infections in the cytosol of most cell types

The ability to detect cytosolic viruses depends on the RLR family of proteins. In contrast to TLRs, RLRs read, if a particular cell is infected or not. As such RLRs operate in most cell types and detect viruses containing RNA (and in some cases DNA) genomes [34-36]. The two best characterized RLRs, retinoic acid inducible gene I (RIG-I) and melanoma differentiation -associated gene 5 (MDA-5), recognize structurally distinct RNA species. The RIG-I ligand comprises a ssRNA molecule with two features: a 5'-triphosphate [37, 38] and base pairing at the 5' end due to secondary RNA structures such as hairpin or panhandle conformations [39]. However, short synthetic dsRNA without a 5'-triphosphate was reported to activate RIG-I as well [40, 41]. Notably, the antiviral protein RNaseL (see below), can cleave ssRNA of virus or host origin and thereby generate ligands for RIG-I and MDA-5 [42]. MDA-5 preferentially binds to longer dsRNA that presumably adopts a weblike conformation much like the synthetic RNA analog polyI:C [38, 40]. The different ligand specificity of RIG-I and MDA-5 is reflected by the largely non-overlapping pattern of virus susceptibility of mice deficient in either of the two RLRs. RIG-I is required for IFN responses to many ssRNA viruses. Among these are the negative-stranded viruses of the orthomyxovirus (such as influenza A virus), paramyxovirus (such as Newcastle disease virus (NDV) and Sendai virus (SeV)) and rhabdovirus (VSV) families and positive-stranded flaviviruses like hepatitis C virus (HCV) and Japanese encephalitis virus (JEV) [43, 44]. MDA-5 is indispensable for protection from

picornaviruses (such as EMCV, poliovirus and Theiler's virus) [44, 45]. Some viruses such as WNV, Dengue virus and reovirus [46, 47] trigger both RIG-I- and MDA-5-dependent innate immune responses. Moreover, recognition of cytoplasmic DNA can also feed into the RIG-I pathway. RIG-I does not detect DNA directly, but can do so after RNA polymerase III-mediated transcription of AT-rich DNA. IFN induction in response to infection with DNA viruses such as adenovirus, HSV and Epstein-Barr virus (EBV) relies on this pathway [34, 35, 40]. Similarly, Vaccinia virus, a dsDNA virus of the poxvirus family, activates MDA-5 via an unknown mechanism [48].

RIG-I and MDA-5 are similar in structure: They share two N-terminal caspase activation and recruitment domains (CARD) followed by a DExD/H box-containing helicase domain and a C-terminal repressor domain (RD). The activation of RLR signaling is best understood for RIG-I. In resting cells RIG-I is in a "closed" conformation. Its RD is associated with the CARDs through intramolecular interactions which prevents the CARDs from engaging with downstream signaling molecules [49]. Binding of 5'-triphosphate RNA to the RD induces a conformational change that releases the RD from the CARDs and leads to dimerization of RIG-I, which allows signal transduction [50]. In line with this model of autoregulation RIG-I mutants that lack the RD are constitutively active, whereas those that lack the CARDs exhibit a dominant negative phenotype [36, 51].

The third member of the RLR family, laboratory of genetics and physiology 2 (LGP2), lacks a CARD domain. Devoid of a signaling domain LGP2 was proposed to be a negative regulator of RLR signaling [51, 52]. Findings obtained from LGP2-deficient mice [53, 54] strongly contradict the previous data generated by *in vitro* studies and implicate LGP2 as a positive regulator. In the absence of LGP2 both RIG-I and particularly MDA-5-dependent responses to RNA virus infection are impaired, whereas responses to synthetic ligands of these RLRs are unaffected [54]. Presumably LGP2 facilitates binding of viral RNA – potentially in complex with protein – to its cognate receptor, whereas the affinity of RIG-I and MDA-5 is sufficiently strong to bind to "naked" synthetic agonists. Structural analysis of the binding interface of RNA with the C-terminal domain of RIG-I supports this model, as it predicts weaker affinity of MDA-5 than RIG-I to its ligand [55]. Nonetheless further clarification is required to determine the role of LGP2 in RLR signaling.

Although RIG-I and MDA-5 have specificities for different ligands, both induce a common signaling pathway that triggers the expression of type I IFNs, ISGs and proinflammatory cytokines (Figure 2). Generally, it is thought that RLRs induce the expression of IFNs that act in both autocrine and paracrine manners to amplify ISG expression. However, ISGs can also be induced directly upon viral infection, without the need for IFN signaling [56, 57].

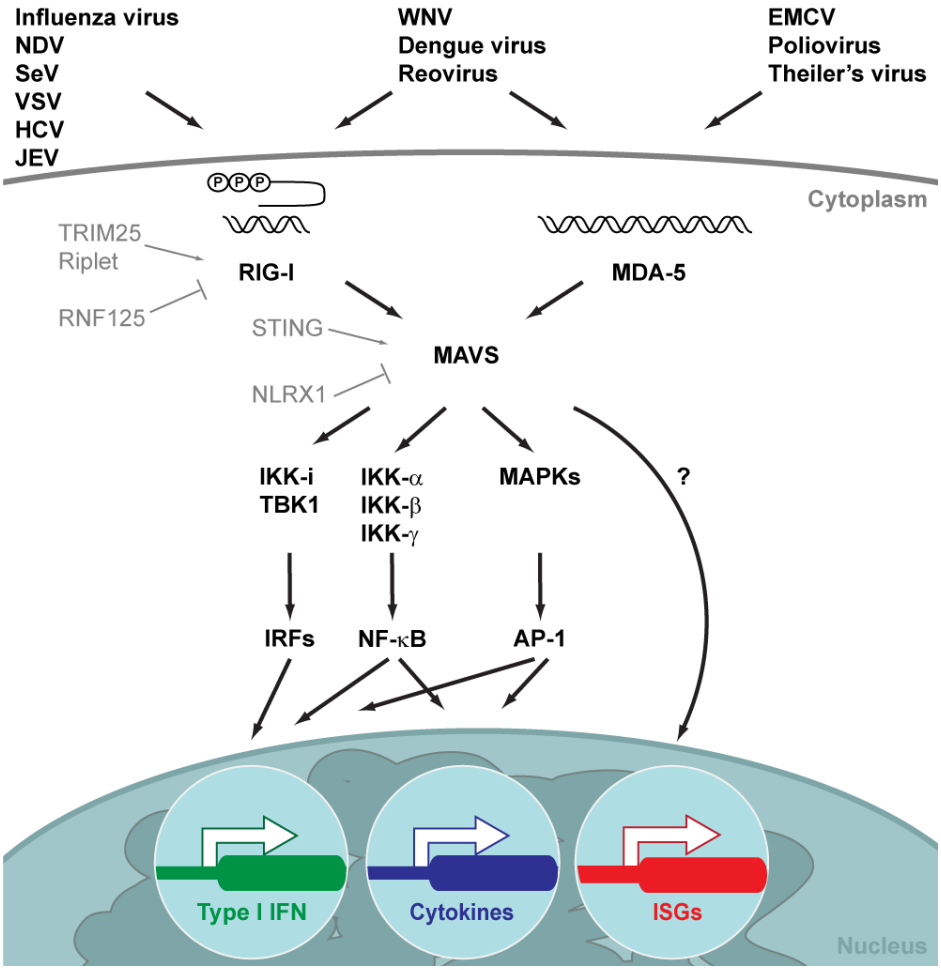

Figure 2. Recognition of RNA viruses by RLRs

RIG-I and MDA-5 are cytosolic receptors for short ds or 5'-triphosphate RNA and long RNA, respectively. MAVS links the receptors to the downstream kinases TBK1 or IKK-i that activate transcription factors of the IRF family to induce IFN-β transcription.

At the receptor-proximal level, RLR-dependent responses are regulated by the adapter mitochondrial antiviral signaling protein (MAVS, also called IPS-1, Cardif or VISA) [58]. MAVS was identified as a CARD-containing protein that is tail-anchored to the outer mitochondrial membrane [59]. Upon virus detection RIG-I or MDA-5 bind to MAVS through homotypic interactions between their CARD domains. MAVS comprises a node from which RLR signaling branches in several directions in order to promote the activation of nuclear

factor-κB (NF-κB, through the canonical IκB kinases (IKKs)-α, β and γ), activator protein 1 (AP-1, through mitogen-activated protein kinase (MAPK) activation) and various IRFs (through the non-canonical IKKs TANK binding kinase 1 (TBK1) and inducible IKK (IKK-i)). These transcription factors act in concert to create an antiviral state in the cell (see below).

Several proteins regulate RLR signaling along the pathway. Tripartite motif-containing protein 25 (TRIM25) and RING finger protein leading to RIG-I activation (Riplet, also known as RNF135 or REUL) are E3 ubiquitin ligases. In addition to ligand binding activation of RIG-I requires lysine 63-linked ubiquitination through TRIM25 or Riplet at its N- or C-terminus, respectively [60-63]. In contrast RNF125 mediates lysine 48-linked ubiqitination that targets RIG-I for degradation and thus acts as a negative regulator [64]. Very recently, zincfinger antiviral protein shorter isoform (ZAPS) was identified as a cofactor for RIG-I signaling. ZAPS is a member of the poly (ADP-ribose) polymerase (PARP) family, but lacks the PARP-like domain present in ZAP due to alternative splicing. ZAPS was shown to directly associate with RIG-I in a ligand-dependent manner and to amplify downstream signaling events such as activation of the transcription factors IRF3 and NF-κB and induction of type I IFN. As a result ZAPS inhibited viral replication after infection with RIG-I-dependent viruses like influenza virus or NDV [65]. While a continuously growing number of accessory proteins that modify RIG-I signaling activity emerges, the interplay between these proteins and the order in which they act upon RIG-I remains elusive until further systematic studies are done to address these questions.

At the level of MAVS, RLR signal transduction is controlled by stimulator of interferon genes (STING, also known as MITA, MPYS or ERIS) [66-69] and NLRX1 (also known as Nod9)[70]. STING was controversially found to localize to the endoplasmic reticulum (ER) [66, 69] and the outer mitochondrial membrane via five transmembrane domains [67, 68]. STING directly interacts with RIG-I, MAVS and TBK1 to mediate antiviral responses, but is dispensable for MDA-5 signaling after polyI:C stimulation. Interestingly, mouse embryonic fibroblasts (MEF) derived from STING-deficient mice failed to induce IFN in response to transfected interferon stimulatory DNA (ISD) and infection with HSV-1 or the bacterium *Listeria monocytogenes*, which implicates STING in DNA sensing as well (see below) [66, 71]. The role of NLRX1 in RLR signaling is a matter of debate. NLRX1 was reported to reside at the outer mitochondrial membrane from where it physically disrupts the virus-induced RLR-MAVS interaction [70]. Alternatively, NLRX1 was found to be localized within the mitochondrial matrix which

deems impossible the proposed function as a direct interactor of MAVS to modulate its activity. Rather it was shown that NLRX1 promotes the generation of reactive oxygen species (ROS) [72, 73]. Interestingly, several lines of evidence implicate ROS as modulators of RLR signaling. Cells deficient in autophagy accumulate dysfunctional mitochondria which entails increased ROS levels and display enhanced RLR signaling. Treatment with antioxidant reverses the effect [74]. Conversely, mitochondrial uncoupling – a process by which ROS generation is decreased – reduced RLR signaling [75]. Additional research is required to delineate the mechanism by which ROS regulate RLR-dependent antiviral responses.

NLRs and inflammasomes are cytosolic sensors of infection

Nucleotide-binding, oligomerization domain (NOD)-like receptor (NLR) proteins are a large family of proteins that are characterized by the presence of a nucleotide-binding and oligomerization domain commonly flanked by a leucine rich repeat (LRR) domain. Typically NLRs contain an additional domain for protein-protein interaction such as a CARD or pyrin domain (PYD). Among the 22 human NLRs many remain to be functionally characterized. The CARD-containing NLRs, NOD1 and NOD2 both recognize components of bacterial cell walls, specifically the building blocks of peptidoglycan mesodiaminopimelic acid and muramyl dipeptide, respectively and induce proinflammatory cytokine production [76]. Interestingly, NOD2 was shown to detect viral ssRNA and to trigger type I IFN expression in a MAVS and IRF3 dependent manner. Accordingly NOD2 deficient mice are more susceptible to RSV infection and produce less IFN-β after infection with influenza virus [77].

Many viruses are known to stimulate IL-1β secretion. This cytokine is implicated in the host inflammatory response and in the induction of fever [78]. In contrast to type I IFN, the production of bioactive IL-1β requires at least two signals for induction and maturation. Signal 1 is provided by proinflammatory signaling such as TLR ligation and activates transcription of the *IL1B* gene resulting in the inactive pro-IL-1β protein. Signal 2 initiates the assembly of multiprotein complexes termed inflammasomes to stimulate caspase-1 activity, that is required for proteolytic maturation of IL-1β. Several NLRPs, a different subfamily of NLRs harboring a pyrin domain, participate in inflammasome formation and determine their specificity. Known inflammasomes are composed of one of several NLRs (including NLRP1, NLRP3, NLRC4 or NLRP6) or non-NLR proteins (including AIM2) and function as cytosolic danger sentinels. Of these the NLRP3 and AIM2 inflammasomes are implicated in antiviral

immunity. The NLRP3 inflammasome is activated by a bewildering variety of PAMPs such as ss and dsRNA, non-infectious host-derived danger signals – termed danger-associated molecular patterns (DAMP) in analogy to PAMPs – such as extracellular ATP or environmental irritants such as asbestos [79, 80]. IL-1β production in response to influenza virus [81-83], SeV [84] and adenovirus [85] infection was shown to depend on the NLRP3 inflammasome. The diversity of stimuli that is detected by NLRP3 and the lack of evidence for direct interaction suggests that these ligands bind indirectly. It is of note that RIG-I was recently shown to activate caspase-1 by a mechanism that is independent of MAVS and NLRP3 [86]. Absent in melanoma 2 (AIM2) directly binds to cytosolic dsDNA [87-90] of viral (e. g. vaccinia virus [88]), bacterial, mammalian or synthetic origin. Ligation of AIM2 causes its oligomerization, recruitment of the adapter protein apoptosis-associated speck-like protein containing a CARD (ASC) and activation of caspase-1. AIM2-deficient macrophages fail to generate an inflammasome after transfection of synthetic DNA or infection with the bacterium *Francisella tularensis*, vaccinia virus or MCMV. In keeping with the in vitro data MCMV infected AIM2 -/- mice suffer from a higher viral burden than wild-type mice, which is accompanied by lower serum levels of IL-18 (another cytokine that requires proteolytic maturation through caspase-1), and reduced IFN-γ secretion by NK cells [91, 92].

Intracellular DNA recognition

In homeostatic cells DNA is sequestered away from the cytosol. It is well appreciated that appearance of DNA in the cytosol during an infection or after tissue damage induces the production of inflammatory mediators. In summary, cytoplasmic DNA activates three different pathways: i) DNA can activate several partially redundant DNA receptors that trigger expression of type I IFN and proinflammatory cytokines. ii) AT-rich DNA can be transcribed by RNA polymerase III into immune stimulatory RNA that feeds into the RIG-I pathway (see above), and iii) DNA can induce assembly of the AIM2 inflammasome that regulates proteolytic maturation of pro-IL-1β (see above) [93]. DAI was the first DNA sensor to be reported. DAI binds to DNA in its predominant right-handed B-conformation, which induces interaction with the kinase TBK1 and the transcription factor IRF3 and as a consequence type I IFN expression [94]. However, DAI-deficient mice had no apparent phenotype when stimulated with DAI ligands such as polydAdT:dTdA and plasmid DNA, or infected with DNA virus [95]. More recently Ifi16, like AIM2 a member of the PYHIN protein family (pyrin and HIN200 domain-containing proteins), was identified as a cytosolic receptor

for DNA [96]. In contrast to AIM2 Ifi16 is not involved in inflammasome formation and acts independently of DAI and TLRs. As suggested by previous studies that characterized the DNA sensing pathway Ifi16 signals through the adapter protein STING and the kinase TBK-1 [71]. The generation of knockout mice will be required to determine, if Ifi16 is the long sought for cytosolic DNA receptor.

Interferons are key players in antiviral immunity

The IFN family consists of 3 classes of cytokines

Human type I IFNs are encoded by intron-less genes and include 12 IFN-α subtypes, a single IFN-β protein, and the lesser known IFN-ε, IFN-κ and IFN-ω. IFN-γ is the only type II IFN [97]. The most recently identified group of type III IFNs belongs to the superfamily of IL-10 cytokines and includes IFN-λ1, -λ2 and -λ3 that are also designated as interleukin (IL)-29, IL-28A and IL-28B, respectively [98, 99]. Type I and III IFNs are produced by most cell types and despite binding to distinct receptors both directly interfere with viral replication through expression of similar sets of ISGs. However, the expression pattern of one of the type III IFN receptor chains, IFN-λR1 (also known as IL-28RA), suggests that type III IFN excerts its antiviral activity on epithelial surfaces [100]. In contrast IFN-γ, binding to yet a different surface receptor called IFNGR, is secreted by immune cells such as natural killer (NK) cells, $CD4^+$ T helper 1 (T_H1) cells and $CD8^+$ cytotoxic T cells. It is not a potent antiviral cytokine, but functions as an effector cytokine for macrophage activation and enhances antigen presentation as well as antibody isotype switching to induce a T_H1 adaptive immune response [101].

Regulation of type I IFN gene transcription

The clinical use of type I IFN for the treatment of viral infections, various cancers and multiple sclerosis is accompanied by severe side effects including inhibition of hematopoesis, neuropsychiatric effects and influenza-like symptom, which demonstrates the wide range of beneficial and detrimental effects of this cytokine [102-104]. Hence, it is of fundamental importance for the organism that IFN production is tightly controlled. An array of PRR ensures efficient recognition of viruses and triggers signaling cascades many of which converge on the activation of IFN genes.

Type I IFNs can be produced by most cell types in the body in response to stimulation of an adequate PRR. Their expression is exclusively regulated at the transcriptional level, i. e. IFN-α and IFN-β genes are silent in resting cells, but upon viral challenge or in response to other pathogenic stimuli they are rapidly and transiently induced [105]. The best-studied example for type I IFN induction is the activation of Ifnb1, the murine IFN-β gene, in fibroblasts. Optimal induction of IFN-β requires the coordinate activation of three distinct sets of transcription factors: IRFs, NF-κB and AP-1 (a heterodimer of c-Jun/ATF-2). AP-1 is activated by the MAPK pathway. NF-κB is sequestered in the cytosol by inhibitor of NF-κB (IκB). Viral infection is one of numerous signals that trigger IκB phosphorylation by the IKK complex, its subsequent ubiquitination and proteasomal degradation. Dissociation of IκB from NF-κB exposes the nuclear localization signal (NLS) of the p65 subunit of NF-κB and allows nuclear translocation [106].

The critical players in the transcription of IFN genes are the members of the IRF family of transcription factors. IRFs are responsible for specificity as activation of NF-κB and AP-1 is not sufficient for type I IFN induction. There are nine IRFs, called IRF1-9, all of which contain a well-conserved N-terminal DNA binding domain that forms a helix-turn-helix motif and is characterized by 5 tryptophan repeats. Except for IRF1 and IRF2, each IRF harbors a C-terminal IRF association domain (IAD) that allows homo- and heterodimeric interaction between other family members or distinct transcription factors and thus accounts for its unique biological function [107]. IRF1 is the founding member of this family of transcription factors [108]. While IRF1 was originally shown to interact with regulatory DNA sequences of IFN-β and ISGs *in vitro* and to induce IFN-β expression upon overexpression in reporter assays, studies with IRF1-deficient MEFs revealed that IRF1 is not required for IFN-α and IFN-β induction upon viral infection and thus is not a key regulator of the IFN system [109, 110]. Nevertheless IRF1 plays various roles in a broader context of host defense against microbial infection such as induction of the nitric-oxide synthase 2 (Nos2) gene in LPS- and IFNγ - stimulated macrophages [111], differentiation into T_H1 and development of $CD8^+$ T as well as NK cells.

IRF3 and IRF7 are the essential transcription factors for Ifnb1 induction. They reside in the cytosol in their latent forms. Viral infection activates the non-canonical IKKs TBK1 and IKK-i. In fibroblasts TBK1 is the critical serine/threonine kinase for phosphorylation of IRF3 and IRF7, while the contribution of IKK-i is minor [112]. IRF3 is a 427 aa protein [113], with the

key phosphorylation sites being serine 385 and 386 as well as the serine/threonine cluster between residue 396 and 405. The highly homologous IRF7 is phosphorylated at serine residues 471/472 and 477/479. Phosphorylation causes a conformational change leading to hetero- or homodimerization and exposure of an NLS that allows translocation to the nucleus [114].

The IFN-β promoter contains a virus-inducible enhancer element that is located within a 57 bp stretch between -100 and -44 relative to the transcription start site and accommodates four cis-acting elements called positive regulatory domains (PRDI - IV). The PRDs direct the highly ordered assembly of the IRF3/7, NF-κB and AP-1 transcription factors and the architectural protein HMG I(Y) into a large multi-protein complex termed the enhanceosome (Figure 3) [115-117]. The enhanceosome modifies and repositions a nucleosome and as a consequence allows formation of a preinitiation complex at the Ifnb1 transcription start site [105, 118].

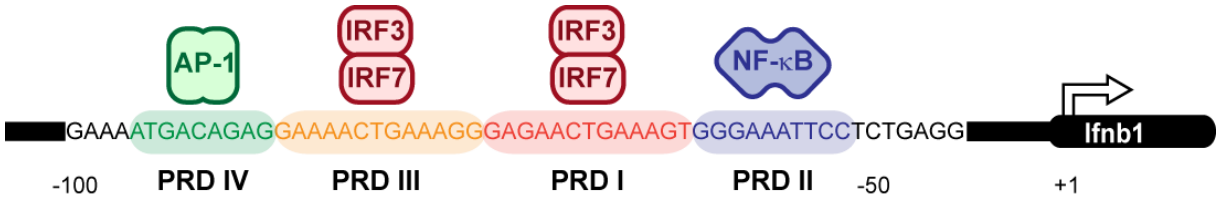

Figure 3. PRDs direct the assembly of the enhanceosome

IFN-β induction requires the coordinate activation of the AP-1, IRF3/7and NF-κB transcription factors that bind to their respective binding sites, termed PRDs, within the enhancer element. These and other factors assemble into the enhanceosome, a higher order multi-protein complex, to activate transcription of the Ifnb1 gene.

IRF 3 is constitutively and ubiquitously expressed, whereas most cells have low levels of IRF7. Constitutive expression of IRF7 is restricted to B cells and pDCs [119, 120], in other cells, IRF-7 is virus- and IFN-inducible. The current model for type I IFN induction in fibroblasts by RLR signaling describes a positive feedback loop, where in the early phase IRF3/7 heterodimers induce small amounts of IFN-β and IFN-α4, the 'primary' IFN genes [121]. Secreted IFN stimulates IRF7 expression. In the later phase of IFN induction activation of the homodimers of newly synthesized IRF7 amplifies transcription of the primary IFN genes and allows transcription of the remaining IFN-α genes, the 'secondary' IFN genes [119, 122]. IRF3 homodimers may contribute to induction of other genes, such as the chemokine CXCL10 (also called IP-10) [123].

ISGs are the workhorses of the innate antiviral response

Type 1 IFN does not only mediate antiviral effects through induction of ISG expression as discussed below, it also modulates the adaptive immune response and has cytostatic and proapoptotic effects. The functional maturation of DCs, upregulation of MHC class I presentation and activation of NK cell and antigen-specific cytotoxic T lymphocytes (CTL) all depend on IFN-α/β [105, 106]. The antiproliferative effect is due to a growth arrest at the G1/S transition point in many cell types, which is the rationale behind the use of IFNs in cancer therapy [106]. Type I IFN alone is not sufficient to induce apoptosis, rather it seems to sensitize cells for apoptotic stimuli through poorly characterized mechanisms [124].

IFNAR signals through the JAK/STAT signaling pathway

Once IFN-α/β is secreted it acts in an autocrine and paracrine manner and excerts its effects through activation of the Janus kinase (JAK) - signal transducer and activator of transcription (STAT) signaling pathway. The type I IFN receptor consists of two distinct subunits, the IFN-α receptor 1 (IFNAR1) and IFNAR2 chains that are permanently associated with members of the JAK family of tyrosine kinases, i. e. TYK2 and JAK1, respectively. Ligand binding to the receptor leads to receptor dimerization and stimulates autophosphorylation of the kinases which activates the receptor complex through creation of phosphotyrosines required for recruitment of STAT1 and STAT2. The same kinases mediate tyrosine phosphorylation of the STAT proteins which allows dimer formation by reciprocal use of their Src homology 2 (SH2) domains [125]. Two distinct species of transcription factors are generated and activate different regulatory elements, namely IFN-stimulated response elements (ISRE) or gamma-IFN activated sites (GAS), both or either of which are present in the regulatory sequences of ISGs: i) Most importantly, the STAT1-STAT2 heterodimer interacts with IRF9 giving rise to a trimeric complex called IFN-stimulated gene factor 3 (ISGF3). In the nucleus ISGF3 activates promoters containing an ISRE. ii) STAT1 homodimers bind to GAS. IFN-γ also activates GAS through STAT1 homodimers. While their role is crucial in the IFN-γ signaling pathway, the contribution of STAT1 homodimers in response to type I IFN in the context of viral infections is ill understood [126].

ISGs are the effectors of the antiviral state

Exposure of cells to IFN-α/β induces expression of a set of several hundred ISGs. Despite their name sake ISGs may also be induced independently of a preceding secretion of type I IFN. Human cytomegalovirus (HCMV) was shown to strongly induce ISG54 (also called IFIT-2) mRNA, but not other IFN-inducible genes, as early as 2 h post infection in the absence of protein synthesis [127]. Gene expression profiling of HSV-1 infected fibroblasts revealed a panel of genes that are induced independently from type I IFN upon infection. Most of these genes are known ISGs and collectively induce an antiviral state that protects cells from superinfection with several RNA and DNA viruses [57]. Furthermore, it was demonstrated that the IFN-independent antiviral state induced by non-replicating HSV-1, NDV or VSV is dependent on IRF3, but not IRF1, IRF7 or IRF9 [56].

No single ISG is sufficient to combat an infection, rather a subset of proteins of a redundant repertoire is required to fight a given pathogen. Many ISGs function as direct antiviral effectors, acting to prevent viral genome replication, viral particle assembly, or virion release from infected cells, others encode components of signaling pathways such as receptors for pathogen recognition or transcription factors resulting in a stronger IFN response and thereby creating a positive feedback loop. However, the majority of ISGs await detailed functional characterization. To date the best-studied examples of ISGs with antiviral capacity are PKR, the 2' 5' OAS/RNaseL system and the Mx protein GTPases [106].

Protein kinase R (PKR)

PKR is a member of a small family of kinases that are activated by stress-related stimuli (such as oxidative or ER stress, amino acid starvation, viral infection) and whose activity blocks *de novo* protein synthesis by interfering with the start of translation. PKR is expressed as an inactive monomer. Viral infection regulates PKR activity at two levels. First, IFN induction significantly increases PKR expression. Second, viral dsRNA activates the kinase as ligand binding induces a conformational change that allows autophosphorylation and dimerization. PKR excerts its antiviral effect by phosphorylating serine 51 of the α-subunit of eukaryotic translational initiation factor (eIF2α) thereby inhibiting the action of the guanine exchange factor eIF2B. As a consequence eIF2a remains in the inactive GDP-bound form and translation initiation stalls [128].

2',5'-Oligoadenylate Synthetase (OAS) and RNaseL

Like PKR, OAS requires the viral PAMP dsRNA as a cofactor for its catalytic activity. Active OAS polymerizes ATP in oligomers of adenylate linked by unique 2'-5'phophodiesterbonds (2-5A), which in turn activate the latent endonuclease RNaseL. The RNaseL is a constitutively expressed protein that dimerizes upon recognition of 2-5A. The active dimer degrades cellular and viral RNAs – specifically, it cleaves within single-stranded regions of RNA molecules after UA or UU dinucleotides – and thus constitutes a translational block for host and virus. Oligoadenylates are rapidly degraded which counterbalances the potent RNase activity [129].

Mx protein GTPases

The guanine-hydrolysing Mx proteins belong to the dynamin superfamily that is involved in membrane scission required for vesicle budding, organogenesis and cytokinesis. Mx proteins, designated as Mx1 and Mx2 in mice and MxA and MxB in humans, were first identified by observing inbred mouse strains that were insensitive to an otherwise lethal orthomyxovirus infection. Virus-susceptibility was solely due to a nonfunctional Mx1 (orthomyxovirus resistance gene 1) gene and resistance could be conferred by restoration of Mx1 expression [130, 131]. Moreover, overexpression of MxA fully protected IFNAR1-deficient mice from infection with several viruses such as Thogoto, La Crosse and Semliki Forest [132]. In general RNA viruses of the orthomyxovirus, paramyxovirus, rhabdovirus, thogavirus and bunyavirus families are susceptible to the activities of Mx proteins, but also hepatitis B virus (HBV) of the Hepadnaviridae family. The precise mechanism of action of Mx proteins is unknown. However, it is believed that Mx proteins recognize nucleocapsid structures and intercept trafficking of essential viral proteins. By trapping viral components Mx GTPases disrupt the nuclear replication phase of RNA viruses to interfere with their life cycle [128].

Other proteins that are dramatically induced by IFN include ISG15, members of the IFIT family and viperin. Despite being among the most prominently induced ISGs – which suggests a major role in antiviral immunity – little is known about their mode of action.

ISG15

ISG15 is a ubiquitin homologue and like ubiquitin is covalently attached to protein targets involving the catalytic activity of 3 enzymes in analogy to ubiquitination, namely UBE1L (ubiquitin-activating enzyme, E1), UBECH8 (ubiquitin-conjugating enzyme, E2) and HERC5

(ubiquitin ligase, E3). All proteins in the ISGylation pathway are coordinately induced by type I IFN including those hydrolyzing ISG15 such as ubiquitin specific peptidase 18 (Usp18) [133]. The impact of ISGylation rather resembles the lysine 63-linked ubiquitination that has activating effects on target proteins in contrast to the lysine 48-linked ubiquitination that labels for proteasomal degradation. It is believed that ISGylation increases the overall efficiency of the IFN response. In addition to its intracellular role ISG15 also acts as a secreted cytokine [106, 128].

Interferon-induced proteins with tetratricopeptide repeats (IFITs)

In humans the IFIT family comprises 4 members, IFIT1 (also called ISG56), IFIT2 (ISG56), IFIT3 and IFIT5. Until recently the antiviral function of IFIT proteins was only broadly characterized as being inhibitors of translation [134, 135], but now a mechanism for this effect was proposed. IFIT1 and IFIT5 specifically and directly bind to 5'-triphosphorylated RNA and thereby interfere with translation of viral RNA by sequestration of template. In contrast to IFIT5 IFIT1 acts in complex with IFIT2 and IFIT3. Thus, RIG-I and IFITs bind to 5'-triphosphorylated RNA. However, RIG-I arms the cell for an antiviral response by promoting IFN secretion, whereas IFITs execute antiviral defense mechanisms. As a consequence, IFIT1-deficient cells accumulated more VSV particles, but not EMCV particles in keeping with the notion that this virus does not generate 5'-triphosphorylated RNA during its replication cycle [136]. A different study revealed that IFIT2 interferes with negative strand synthesis of WNV. Importantly this antiviral effect depends on the absence of 2'O methylation of the 5'cap structure of the viral mRNA. 2'O methylation is a common modification of mRNAs in higher eukaryotes, but many viruses (e. g. flaviviruses like WNV) have evolved strategies to obtain such a modification – in the light of this data – probably in order to evade the innate immune response [137]. Thus, both 5'-triphosphorylated RNA and a 2'O methylated 5'cap facilitate discrimination of self from non-self RNA by the host innate immune response.

Virus inhibitory protein, endoplasmic reticulum-associated, interferon-inducible (Viperin)

Viperin (also called cig5 and RSAD2) is an ISG that has recently gained much attention. It ranks high among the strongly IFN-induced proteins, but much like the Mx proteins is undetectable in absence of infection, which makes it an ideal marker for IFN activity. Viperin harbours an N-terminal amphipathic α-helix followed by a CX_3CX_2C-motif typical of radical

S-adenosyl methionine (SAM) enzymes. The amphipathic helix is required for localization of the protein to the cytosolic face of the ER, perhaps through association with other proteins, and is necessary and sufficient for its antiviral activity [106, 138]. Ectopic expression of viperin was shown to inhibit replication of HCMV [139], HCV [140], HIV [141] and influenza A virus [142]. How and where viperin exerts its antiviral activity depends on the pathogen. While it disrupts lipid rafts to prevent budding of influenza virus particles from the plasma membrane [142], it localizes to lipid droplets to interfere with assembly and budding in case of HCV infection [143]. While overexpression of viperin prior to HCMV infection negatively affected viral replication, upregulation of viperin expression by HCMV infection increased infectivity of the virus. It was demonstrated that viperin interacts with the viral protein vMIA that redirects viperin from the ER to mitochondria. There it lowers ATP generation which leads to a disruption of the actin cytoskeleton and enhancement of infection [144].

Cell biological framework of pattern recognition

A fundamental feature of eukaryotic cells is the use of membrane-bound organelles to compartmentalize activities and serve as scaffolds for signal transduction. The best-characterized signaling pathways involve membrane-bound receptors that respond to extracellular or lumenal stimuli. In these instances, the spatial separation of an extracellular stimulus from the cytosol mandates the use of organelles as signaling platforms, as transmembrane receptors must transmit information across a lipid bilayer.

An example for how subcellular compartments are repurposed as signaling platforms is found in TLR signaling. TLR signal transduction is initiated by the recruitment of the signaling adapters myeloid differentiation primary response protein 88 (MYD88) [145] or TIR domain-containing adapter protein inducing IFNβ (TRIF, also called TICAM1) [146, 147]. In some instances the sorting adapters TIR domain-containing adapter protein (TIRAP, also called MAL) [148, 149] and TRIF-related adapter molecule (TRAM, also called TICAM2) [150, 151] are required for proper localization of MYD88 (TLR2 and TLR4) and TRIF (TLR4), respectively. Receptors and adapters associate through homophilic interactions between their TIR domains. All TLRs use MYD88 as an adapter except for TLR3, which uses TRIF. Solely TLR4 relies on both MYD88- and TRIF-dependent signaling pathways. TLR4 is also unique among the TLRs in the way it induces proinflammatory cytokines and type I IFN in a sequential manner from distinct subcellular compartments [152]. The sorting adapter TIRAP is localized to discrete

phosphatidylinositol 4,5 bisphosphate (PIP2)-rich regions of the plasmamembrane by its PIP2 binding domain and functions to recruit MYD88. Upon ligand engagement TLR4 (and TLR2) signaling is initiated at these specific plasmamembrane subdomains [153]. This first phase of TLR4 signaling drives the MYD88-dependent activation of MAPK and NF-κB that are required for induction of proinflammatory cytokines. TLR4 is then internalized, which is accompanied by a drop in PIP2 concentration of the nascent vesicle and as a consequence dissociation of the TIRAP-MYD88 adapter pair. Once TLR4 has been delivered to early endosomes the TRAM-TRIF complex engages the TIR domain of TLR4. The TRIF-dependent pathway maintains NF-κB and MAPK signaling and activates IRF3 in a TRAF3 dependent manner to induce type I IFN expression in the second phase of TLR4 signaling [152]. Thus, the output of TLR4 signaling is strictly dependent on its location within the cell.

However, an important gap exists in our knowledge of how stimuli from the cytosol are able to initiate specific signaling events. Is the encounter of ligand and receptor or downstream signaling molecules purely stochastic? How common is the use of organelles in signal transduction from cytosolic receptors? An example of this situation can be found in the study of intracellular virus detection, which is accomplished by RLRs. Although much has been learned about the genetics of RLR signaling, less is known about where within the cell signal transduction occurs. Identifying the sites of RLR signal transduction is critical to understanding how antiviral networks are integrated into the general cellular infrastructure within which they operate.

The first clue that cytosolic RLR signaling may occur from organelles came from studies of the MAVS adapter. MAVS contains a C-terminal transmembrane domain that anchors it to the mitochondrial outer membrane [59]. It is from this location that MAVS is thought to engage active RLRs and induce signal transduction. Whether mitochondria are the only organelles that promote RLR-mediated signaling has not been addressed.

Mitochondria have long been appreciated to have an intimate functional relationship with peroxisomes [154]. Both are membrane-bound organelles found in mammalian cells and are involved in the metabolism of lipids and reactive oxygen species. However, while mitochondria are well-established sites of both antiviral signaling and antiviral apoptosis, peroxisomes are thought to function solely as metabolic organelles. Recently, several mitochondrial proteins have been found to reside also on peroxisomes. Included in this group

are the outer membrane proteins Fission 1 homolog (Fis1) and mitochondrial fission factor (Mff), which regulate the morphology of both organelles [155, 156]. Interestingly, Fis1, Mff and MAVS all have similar domain structures: each contains an N-terminal effector domain and a C-terminal localization motif, which consists of a transmembrane domain and a short lumenal tail containing basic amino acids. That other so-called "tail-anchored" mitochondrial outer membrane proteins operate from peroxisomes raised the possibility that MAVS may also function from these organelles.

AIM

The two RLRs, RIG-I and MDA-5, are bona fide receptors for cytosolic RNA and as such act as pattern recognition receptors for viruses that trigger type I interferon production upon infection. During the last few years tremendous progress has been made towards the identification of the molecular components of this signaling pathway. The adapter protein MAVS is strictly required for signal transduction initiated by RLRs. MAVS has been demonstrated to be tail-anchored to the outer mitochondrial membrane. Recent advances in the field of peroxisome biology revealed a close relationship between peroxisomes and mitochondria, which prompted me to re-examine the subcellular localization of MAVS and as a consequence to further the understanding of how RLR signaling is embedded in the cellular infrastructure.

The aim of this thesis is to address the following three modular questions:

1. Is MAVS expressed on peroxisomes?
2. Does peroxisomal MAVS mediate an antiviral response?
3. Does peroxisomal signaling differ from mitochondrial signaling?

MATERIALS AND METHODS

Buffers and media

TAE buffer: 40 mM Tris, 20 mM acetic acid, 1 mM EDTA pH 8,4

5 x DNA loading buffer: 60 % glycerol, bromphenol blue, xylene cyanol

LB-media: 1 % tryptone, 0,5 % yeast extract, 1 % NaCl, autoclaved

LB-agar plates: 1 % tryptone, 0,5 % yeast extract, 1 % NaCl, 1,5 % agar, autoclaved

Lysis buffer: 50 mM Tris-HCl pH 7,4, 150 mM NaCl, 10 % glycerol, 1 % NP-40

7 x Complete stock: Dissolve 1 tablet Complete Mini (Roche, Basel, Switzerland) in 1,5 ml water.

Complete lysis buffer: add Complete stock to lysis buffer fresh before use.

6 x SDS sample buffer: 750 mM Tris-HCl pH 6,8, 12 % SDS, 60 % glycerol, 600 mM DTT

SDS running buffer: 25 mM Tris, 192 mM glycine, 0,1 % SDS, pH 8,3

Transfer buffer: 25 mM Tris, 192 mM glycine, 0,1 % SDS, pH 8,3, 20 % methanol

PBS: 8,1 mM Na2HPO4, 1,76 mM KH2PO4, 137 mM NaCl, 27 mM KCl, pH 7,4

PBS-T: PBS with 0,1 % Tween 20

5 % milk: 5 % non-fat dry milk powder in PBS-T

PFA: 2% PFA in PBS

Triton X-100: 0,1 % in PBS

Block buffer: 2% goat serum, 50 mM ammonium chloride in PBS

Molecular biology

Cloning strategies

All pMSCV MAVS IRES GFP constructs were generated by cloning the respective MAVS sequence into pMSCV IRES GFP. Briefly, pMSCV IRES GFP was cut with XhoI and NotI at the multiple coning site. The vector was dephosphorylated, purified by gel extraction and

ligated with the insert. The inserts for MAVS-WT and MAVS-Cyto were amplified from pEF-HA-MAVS by PCR. The chimeric alleles MAVS-Pex, MAVS-Mito and MAVS-Mimic were generated by overlap extension PCR, where first the MAVS 1-500 sequence was amplified including the first 25-30 bp of the chimeric transmembrane domain of Pex13, Fis1 or OMP25, respectively. In a separate PCR the 3 transmembrane domains were amplified from either plasmid DNA (Pex13) or cDNA (Fis1 and OMP25). The transmembrane fragment and the appropriate MAVS fragment were then pooled at an equimolar ratio and a third PCR performed for amplification of the chimeric insert. All MAVS inserts were cut with XhoI and NotI and gel-purified prior to ligation.

pMSCV Pex19 IRES GFP was cloned similarly. Pex 19 was amplified from EGFP-Pex19 and inserted into pMSCV IRES GFP using BglII and HindIII restriction sites.

I screened for properly cloned constructs by colony PCR and verified identified clones by restriction digestion. Sequence analysis of all plasmids was performed at the Dana-Farber/ Harvard Cancer Center DNA Resource Core.

Plasmids

Plasmid name	Features	Source
pCMV-Flag-IPS1	expression vector, N-terminally Flag-tagged huMAVS	Shizuo Akira
pEF-HA-MAVS	expression vector, N-terminally HA-tagged huMAVS	Zhijian Chen
5xmyc-Mff	expression vector, N-terminally myc-tagged huMff	Alexander van der Bliek
DsRed-PTS1	expression vector for peroxisome marker, DsRed fused to peroxisomal targeting signal 1	Marc Fransen
Pex19 / EGFP-PTS1	bicistronic expression vector for huPex19 and peroxisome marker, EGFP fused to peroxisomal targeting signal 1	Marc Fransen
Pex19	expression vector for huPex19	Marc Fransen
EGFP-Pex19	expression vector, EGFP-huPex19 fusion protein	Marc Fransen

Pex13-EGFP	expression vector, huPex13-EGFP fusion protein	Marc Fransen
pCMV TIRAP-Flag	expression vector, C-terminally Flag-tagged huTIRAP	Tiffany Horng
pMSCV IRES GFP	retroviral vector containing an internal ribosomal entry site for GFP	Jonathan Kagan
pMSCV MAVS WT IRES GFP	retroviral vector expressing MAVS WT and GFP from bicistronic mRNA	self cloned
pMSCV MAVS 1-500 IRES GFP	retroviral vector expressing MAVS-Cyto and GFP from bicistronic mRNA	self cloned
pMSCV MAVS/OMP25 IRES GFP	retroviral vector expressing MAVS-Mimic and GFP from bicistronic mRNA	self cloned
pMSCV MAVS/Fis1 IRES GFP	retroviral vector expressing MAVS-Mito and GFP from bicistronic mRNA	self cloned
pMSCV MAVS/Pex13 IRES GFP	retroviral vector expressing MAVS-Pex and GFP from bicistronic mRNA	self cloned
pMSCV Pex19 IRES GFP	retroviral vector expressing Pex19 and GFP from bicistronic mRNA	self cloned
pCL-Eco	packaging plasmid encoding gag, pol and env	Jonathan Kagan

I am grateful to those who provided plasmids: Shizuo Akira (Osaka University, Osaka, Japan), Zhijian Chen (Southwestern Medical Center, Dallas, TX, USA), Alexander van der Bliek (UCLA, Los Angeles, CA, USA), Marc Fransen (Katholieke Universiteit Leuven, Belgium) and Tiffany Horng (Harvard School of Public Health, Boston, MA, USA).

DNA oligos (Primers)

Oligo name	Sequence (5' to 3')
fw MAVS	atCTCGAGatgccgtttgctgaagacaa
rev MAVS WT	atGCGGCCGCctagtgcagacgccgccggt
rev MAVS 1-500	atGCGGCCGCttacttccggtcggcttgtggcc
rev MAVS for OMP25	tccactcggctctccgtcgcctcgatgcttccggtcggcttgtggcctggggccgcc
rev MAVS for Fis1	acccagggccatgcctcccacgatggccttccggtcggcttgtggcctggggccgcc

rev MAVS for Pex13	actgacagaggcaaatgcatgcacaatcttccggtcggcttgtggcctggggccgcc
fw OMP25 aa109-145	catcgaggcgacggagagcc
rev OMP25 aa109-145	atagtttaGCGGCCGCtcagagctgctttcggtatc
fw Fis1 aa128-152	gccatcgtgggaggcatggc
rev Fis1 aa128-152	atGCGGCCGCtcaggatttggacttggaca
fw Pex13 aa136-233	attgtgcatgcatttgcctc
rev Pex13 aa136-233	atGCGGCCGCttaagattttgctgaggtagctg
fw Pex19	ctcAGATCTgccgccaccatggccgccgctgaggaaggctgtagtg
rev Pex19	tcgAAGCTTtcacatgatcagacactgttcaccact

Oligos were designed according to the following sequences: Human MAVS (BC044952), human Pex13 (NM_002618) residues 136-233, human Fis1 (NM_016068) residues 128-152, rat OMP25 (NM_022599) 109-145, and human Pex19 (NM_002857). Capital letters indicate restriction sites. Sequences required for overlap extension PCR are underlined. All oligos listed were purchased from Eurofins MWG Operon (Huntsville, AL, USA)

RNA extraction and reverse transcription

RNA extraction was performed using the RNA-Bee reagent (ams Biotechnology, Abingdon, UK) according to manufacturer's instructions. Extracted RNA was reverse transcribed using SuperScript III reverse transcriptase (Invitrogen, Carlsbad, CA, USA):

Component	Stock or amount	Volume	Source
total RNA	10 pg -5 µg	9 µl	
oligo(dT)$_{18}$	100 µM	1 µl	(Fermentas, Burlington, Canada)
70°C for 10 min (primer annealing)			
4°C for 10 min			
first-strand buffer	5x	5 µl	(SS III kit)
DTT	100 µM	1 µl	(SS III kit)
dNTPs	10 mM ea	1,25 µl	(Fermentas, Burlington, Canada)
RNaseOUT	40 U/µl	0,20 µl	(Invitrogen, Carlsbad, CA, USA)
SuperScript RT	200 U/µl	0,50 µl	(SS III kit)
RNase-free water	ad 25 µl	7,05 µl	(Ambion, Austin, TX, USA)
50°C for 1 h (reverse transcription)			

70°C for 15 min (inactivation)

Polymerase chain reaction (PCR)

PCR reactions for cloning purposes were performed with Phusion DNA polymerase (New England Biolabs, Ipswich, MA, USA):

Component	Stock/amount	Volume	Source
template	≈ 10 ng pDNA - or - cDNA	variable 2 µl	
HF buffer	5x	10 µl	(Phusion kit)
dNTPs	10 mM ea	1 µl	(Phusion kit)
forward primer	10 µM	2,5 µl	
reverse primer	10 µM	2,5 µl	
$MgCl_2$	50 mM	3 µl	(Phusion kit)
Phusion polymerase	2 U/µl	0,5 µl	(Phusion kit)
water	ad 50 µl	28,5 µl	

DNA was amplified using the following PCR program:

Cycle step	Temperature	Duration	Cycles
Initial denaturation	98°C	30 s	1
Denaturation	98°C	10 s	
Annealing	Tm + 3°C	20 s	
Extension	72°C	20 s/kb	30
Final extension	72°C	10 min	1
Cooling	4°C	10 min	1

For all other purposes such as colony PCR or other semiquantitative analyses Tsg DNA polymerase (Lamda Biotech, St. Louis, MO, USA) was used as follows:

Component	Stock/amount	Volume	Source
template	colony sample	-	
buffer	10x	2 µl	(Tsg kit)
dNTPs	2 mM ea	2 µl	(Tsg kit)

forward primer	10 µM	0,4 µl	
reverse primer	10 µM	0,4 µl	
$MgCl_2$	25 mM	0,8 µl	(Tsg kit)
Tsg polymerase	5 U/µl	0,2 µl	(Tsg kit)
water	ad 20 µl	14,2 µl	

DNA was amplified using the following PCR program:

Cycle step	Temperature	Duration	Cycles
Initial denaturation	95°C	2 min	1
Denaturation	95°C	15 s	
Annealing	55-65°C	30 s	
Extension	74°C	1 min/kb	30
Final extension	74°C	5 min	1
Cooling	4°C	10 min	1

Gel electrophoresis

For > 500 bp fragments 1% (w/v) and for < 500 bp fragments 2% (w/v) agarose gels were prepared with TAE-buffer by heating in a microwave oven. After addition of 1 µg/ml ethidium bromide (Sigma-Aldrich, St. Louis, MO, USA) the solution was poured into a gel tray equipped with an appropriate comb. Once solidified the gels were submerged in a running chamber filled with TAE-buffer and DNA samples mixed with DNA loading buffer were applied to the gel. Gel electrophoresis was commonly performed at 100-120 V for 1 h. DNA was visualized on a UV transilluminator.

Extraction of DNA fragments from agarose gels

DNA fragments of desired size were excised from agarose gels and purified with the Silica bead gel extraction kit (Fermentas, Burlington, Canada): The gel slice was dissolved in Binding buffer using 3 times the volume of its weight by heating at 55°C. After addition of the Silica bead suspension binding was allowed for 5 min at 55°C. The beads were then washed 3 times with ice cold Wash buffer. DNA was eluted from air-dryed beads in 40 µl water by heating to 55°C.

Restriction digests

For preparative or analytical purposes restriction digests were performed with reagents purchased from New England Biolabs (NEB, Ipswich, MA, USA) according to the manufacturer's instructions. Briefly, 0,5 – 2 µg of DNA was added to a mix containing 2-20 Units of restriction endonuclease in the appropriate buffer and incubated at the indicated temperature. When checking for plasmid integrity 0,5 µg DNA was digested for 2 h in a final volume of 15 µl, whereas reactions for cloning purposes prepared with 2 µg of DNA in 50 µl were incubated overnight.

Dephosphorylation of DNA

In order to prevent re-ligation of the vector phosphates were removed on the 5' termini by addition of 1 Unit shrimp alkaline phosphatase (USB, Cleveland, OH, USA) to the restriction reaction after complete digestion. Dephosphorylation was carried out at 37°C for 1 h for and terminated by inactivation of the enzyme at 65°C for 15 min.

Ligation of DNA fragments

Prior to ligation known amounts of vector and insert were run on an agarose gel to estimate the concentration of the preparations by comparison with DNA marker bands of similar size. Rapid DNA ligation (Fermentas, Burlington, Canada) was carried out according to manufacturer's instructions:

Component	Amount
vector	50 ng
insert	3 x molar excess*
5x rapid ligation buffer	2 µl
5 U/µl T4 DNA ligase	0,5 µl
water	ad 10 µl
room temperature for 15 min	

*Calculation of volume of insert:

$$V_I = \frac{m_V * 3 * M_I}{M_V * conc_I}$$

V_I	…	volume of insert	[µl]
m_V	…	amount of vector	[ng]
M_I	…	molecular weight of insert	[g/mol]
M_V	…	molecular weight of vector	[g/mol]
$conc_I$	…	concentration of insert	[ng/µl]

Transformation of competent *E. coli*

An aliquot of 50 µl One Shot competent *E. coli* (Invitrogen, Carlsbad, CA, USA) was thawed on ice and mixed with 3 µl ligation reaction or approximately 10 ng of plasmid DNA. After incubation on ice for 30 min the bacteria were heat-shocked in a 42°C waterbath for 30 sec, then put on ice for 1 min. 700 µl LB-media were added and the suspension was incubated in a heating block at 37°C for 1 h under constant gentle shaking (500 rpm). Bacteria were plated on LB-agar plates containing 100 µg/ml of the appropriate antibiotic for selection (ampicillin or kanamycin, both Sigma-Aldrich, St. Louis, MO, USA) and incubated overnight at 37°C.

Plasmid purification from bacteria

5 ml LB-media containing the appropriate antibiotic were inoculated with single colonies and incubated overnight at 37°C in a shaker. 1,5 ml of the culture was spun for 2 min at 8000 x g to harvest bacteria. Plasmid DNA was isolated using the Wizard plus SV miniprep kit (Promega, Madison, WI, USA) according to the manufacturer's instructions.

For large scale plasmid isolation bacteria were grown in 200 ml cultures and DNA purified using the PureLink HiPure midiprep kit (Invitrogen, Carlsbad, CA, USA) following the manufacturer's protocol.

Cell biology

Cells

MAVS KO MEFs, PEX19 deficient human skin fibroblasts and L929 cells stably expressing an ISRE-luciferase reporter were kindly provided by Zhijian Chen (Southwestern Medical

Center, Dallas, TX, USA), Ronald Wanders (University of Amsterdam, The Netherlands) and Bruce Beutler (The Scripps Research Institute, La Jolla, CA, USA), respectively. All cell lines including wildtype MEFs, Huh-7, 293T, MDCK and Vero were cultured in DMEM supplemented with 10% (vol/vol) fetal bovine serum, 2 mM L-glutamine, 1 mM sodium pyruvate and 100 U/ml penicillin/streptomycin, maintained at 37°C and 5% CO_2 and split regularly before confluency was reached. All cell culture reagents were purchased from Invitrogen (Carlsbad, CA, USA).

Cell stimulation

Cells were plated on 6 well plates 12-16 h before stimulation. Subconfluent cells were stimulated by transfection with 500 ng/ml 5'-triphosphorylated RNA (a kind gift of Andreas Pichlmair, CeMM, Vienna, Austria) or 10 µg/ml polyI:C (Invivogen, San Diego, CA, USA) using Lipofectamine 2000 (Invitrogen, Carlsbad, CA, USA) according to the manufacturer's instructions.

Cell fractionation

Fractionation of HepG2 cells were performed by Marc Fransen (Katholieke Universiteit Leuven, Belgium) as previously described [157]. For fractionation of U937 cells all operations were carried out at 4°C. First, $3x10^8$ cells were lysed in 10 ml homogenization media (0,25 M sucrose, 0,1% v/v ethanol, 1 mM EDTA, 10 mM MOPS, Complete Mini Protease inhibitors [Roche, Basel, Switzerland] pH 7,2) using a ball-bearing homogenizer. Lysates were subjected to differential centrifugation consisting of a 10 000 x g (10K) and a 40 000 x g (40K) centrifugation step to enrich for mitochondria and peroxisomes. The 40 K pellet was resuspended in 5 ml homogenization media and mixed with 5ml 50 % Optiprep working solution (5 volumes Optiprep [Axis-Shield, Oslo, Norway] in 1 volume dilution media [0,25 M sucrose, 0,6% v/v ethanol, 6 mM EDTA, 60 mM MOPS, Complete Mini protease inhibitors, pH 7,2]). The suspension was centrifuged in a near-vertical fixed-angle rotor at 180 000 x g for 3 h to allow gradient formation. Fractions were collected by tube puncture.

Transient transfection

MEFs and Huh-7 were transfected using Fugene 6 (Roche Applied Science, Indianapolis, IN, USA) according to the manufacturer's recommendations, i. e. for cells grown to 50% confluency on a 24 well plate 1,5 µl Fugene 6 were diluted in 50 µl serum-free media and incubated for 5 min. After addition of 500 ng plasmid DNA the transfection mix was incubated for another 15 min prior to application to cells. When other size culture vessels were used the amount of plasmid DNA was adjusted proportionally to the surface area and the transfection mix was scaled up according to the following guidelines: 3 µl Fugene 6/µg plasmid DNA, 33 µl serum-free media/µl Fugene 6.

For transfection of PEX19 deficient human skin fibroblasts Lipofectamine 2000 in combination with Plus Reagent (both Invitrogen, Carlsbad, CA, USA) was used. For 70% confluent cells on a 24 well plate 800 ng plasmid DNA and 0,8 µl Plus Reagent were diluted in 50 µl serum-free medium and incubated for 5 min at room temperature. 4 µl Lipofectamine 2000 were diluted in 50 µl serum-free medium and incubated for max. 5 min. Diluted DNA and diluted Lipofectamine 2000 were then combined and incubated for 20 min to allow complex formation. In the meanwhile the media of target cells was changed to 500 µl medium without serum. 4 h after transfection 55 µl fetal bovine serum were added.

Generation of stable cell lines and cell sorting

293T were used as packaging cells and plated at 70 % confluency on 10 cm dishes. 6 h later cells were transfected with 4 µg retroviral construct of interest (e. g. pMSCV MAVS WT IRES GFP) and 4 µg packaging plasmid (pCL Eco) for a total of 8 µg plasmid DNA using Fugene 6 as described for transient transfection. The following day media was changed with 8 ml fresh media and target cell lines (e. g. MAVS KO MEFs) were seeded on a 6 well plate to be 30 - 50% confluent the next day. Two days after transfection the virus supernatant of the packaging cells was filtered through a 0,45 µm syringe filter. For MEFs 4 µl Lipofectamine 2000/ml supernatant were added to facilitate infection and incubated for 10 min at room temperature. Target cells were provided with 2 ml fresh media before addition of the virus supernatant. Packaging cells were supplied with 8 ml fresh media. The next day a second infection cycle was carried out as described above. For cell sorting, cells from 15 cm dish were washed, resuspended in serum free media and strained through a 35 µm nylon mesh. All

flow cytometric procedures were carried out by Betsy Boush (Children's Hospital Boston, MA, USA)

Virus infections

Reovirus

Reovirus Type 3 Dearing clone C was provided by Max Nibert (Harvard Medical School, Boston, MA, USA). Infections were carried out by Steeve Boulant (Harvard Medical School, Boston, MA, USA). In brief, reovirus was propagated on L929 cells and plaque purified as previously described [158]. Cells were seeded 12-16 h prior to infection on 6-well plates. The day of infection, medium was replaced by addition of 2 ml of fresh medium containing virions at a multiplicity of infection (MOI) of 100. Where indicated cells were preincubated with 20 μg/ml brefeldin A (Invitrogen) and infections were carried out in the presence of the drug. Alternatively, type 1 IFN activity was blocked by addition of 250 neutralizing units/ml rat anti-murine IFN-β (clone RMMB-1, PBL InterferonSource, Piscataway, NJ, USA) and 500 neutralizing units/ml rat anti-murine IFN-α (clone RMMA-1, PBL InterferonSource, Piscataway, NJ, USA) antibodies at the time of infection.

Influenza virus

Influenza virus (A/Puerto Rico/8/34, H1N1) lacking the NS1 gene (originally a gift from Adolfo Garcia-Sastre, Mount Sinai School of Medicine, New York, NY, USA) was provided by Nir Hacohen (Broad Institute, Cambridge, MA, USA), infections were carried out by Bennett Shum (Broad Institute, Cambridge, MA, USA). ΔNS1 virus was propagated in Vero cells as previously described [159] and titrated by plaque assay on MDCK cells. For infection, cell monolayers were incubated with ΔNS1 virus at an MOI of 5 for 1 h at 37ºC in DMEM supplemented with 0,3 % BSA, washed and incubated with growth media.

VSV

VSV (Indiana) was provided by Sean Whelan (Harvard Medical School, Boston, MA, USA). Infections were carried out by Amy Lee (Harvard Medical School, Boston, MA, USA). Virus was amplified in BHK-21 cells, purified on a linear 15-45% sucrose gradient and titrated by plaque assay on Vero cells as previously described [160]. For infection cell monolayers were incubated with VSV at an MOI of 0,01 and virus was removed after 1 h.

Plaque assays

To assess reovirus replication in MEF cell lines, purified virions were diluted in 100 µl of attachment buffer (PBS with 2 mM $MgCl_2$) and incubated with cell monolayers at indicated MOIs for 1 h at room temperature. After removal of unabsorbed virus by two washes with attachment buffer, cells were incubated in DMEM containing 10% FBS at 37° C for 0, 16, 24, 48 and 72 h. Next, cells were lysed by freezing and thawing, and infectious titers in the lysates were measured by serial dilution onto L929 cell monolayers as described previously [161]. Plaque assays were performed by Steeve Boulant (Harvard Medical School, Boston, MA, USA). VSV plaque assays were performed in analogy by Amy Lee (Harvard Medical School, Boston, MA, USA) [162].

Type I IFN bioassay

To measure type 1 IFN activity L929 cells stably expressing an ISRE-driven luciferase reporter were stimulated with known concentrations of recombinant murine IFN-β (PBL InterferonSource, Piscataway, NJ, USA) or cell supernatants. 9 h later cells were lysed and assayed for luciferase activity using Bright-Glo Luciferase Assay System (Promega, Madison, WI, USA).

Protein biochemistry and immunofluorescence

Antibodies for immunoblotting and immunofluorescence

Primary antibodies					
Antibody (clone)	Reactivity	Host	Source	Dilution	
anti-MAVS	human	rabbit	Bethyl Laboratories	IB IF	1:5000 1:1000
anti-myc (9E10)	-	mouse	Steen Hansen	IF	1:100
anti-Flag (M2)	-	mouse	Sigma-Aldrich	IF	1:500
anti-Pex14	human	rabbit	Marc Fransen	IB IF	1:1000 1:200
anti-mtHSP70 (JG1)	human, mouse	mouse	ABR affinity reagents	IB IF	1:500 1:250

anti-Fis1 (FL-152)	human, mouse	rabbit	Santa Cruz Biotech	IB	1:200
anti-viperin	human, mouse	mouse	Peter Cresswell	IB	1:250
Secondary antibodies for immunoblotting					
anti-mouse-HRP			Invitrogen	IB	1:3000
anti-rabbit-HRP			Invitrogen	IB	1:3000
Secondary antibodies for immunofluorescence conjugated to the following fluorophores: Alexa Fluor 488 (green) Alexa Fluor 594 (red) Alexa Fluor 647 (far red)					
anti-mouse			Invitrogen	IF	1:400
anti-rabbit			Invitrogen	IF	1:400

I am grateful to those who provided antibodies: Steen Hansen (Children's Hospital Boston, MA, USA), Marc Fransen (Katholieke Universiteit Leuven, Belgium) and Peter Cresswell (Yale University School of Medicine, New Haven, CT, USA).

Cell lysates and protein quantitation

Cells grown on a 6-well plate were washed with cold PBS (Invitrogen, Carlsbad, CA, USA) before addition of 100 µl chilled complete lysis buffer. Extracts were collected by scraping the culture dish and cells were lysed for 15 min shaking at 4°C. The lysate was obtained by centrifugation of the extracts for 15 min at 13000 rpm at 4°C. The total protein concentration of the lysate was determined using the BCA protein assay kit (Pierce/Thermo Fisher Scientific, Rockford, IL, USA). The BCA working reagent was prepared by diluting reagent B 1:50 in reagent A. 2 µl lysate or known amounts of BSA (series ranging from 2 to 20 µg per reaction) were then added to 1 ml BCA working reagent. Each reaction was incubated for 20 min at 65°C, afterwards placed on ice. The absorbance of each reaction was measured at 562 nm in a spectrophotometer and protein concentrations of samples were calculated in reference to the BSA standard curve.

SDS-PAGE and immunoblotting

An aliquot of cell lysate typically corresponding to 40 µg total protein was mixed with an appropriate amount of 5x SDS sample buffer and heated at 95° for 3 min. PageRuler Prestained Protein Ladder (Fermentas, Burlington, Canada) was used as a molecular weight marker. Marker and samples were loaded on handcast discontinuous polyacrylamide gels consisting of a 10 % resolving gel and a 4 % stacking gel prepared as follows:

10 % Resolving gel			
Component	Stock	Volume	Source
ProtogGel resolving buffer	4 x	2,5 ml	(National Diagnostics)
ProtoGel acrylamide/methylene bisacrylamide	30 %	3,3 ml	(National Diagnostics)
water	ad 10 ml	4,2 ml	
Ammonium persulfate	10 %	100 µl	(Sigma)
TEMED		10 µl	(Bio-Rad)

4 % Stacking gel			
Component	Stock	Volume	Source
ProtogGel stacking buffer	4 x	0,8 ml	(National Diagnostics)
ProtoGel acrylamide/methylene bisacrylamide	30 %	0,4 ml	(National Diagnostics)
water	ad 3 ml	1,8 ml	
Ammonium persulfate	10 %	30 µl	(Sigma)
TEMED		4,5 µl	(Bio-Rad)

Gels were run in SDS running buffer at 120 V for approximately 1,5 h.

Proteins were blotted onto a methanol-activated Immobilon-P PVDF membrane (Millipore, Billerica, MA, USA). To this end, the protein gel was covered with membrane and sandwiched between transfer buffer-soaked filter paper. This stack was placed with the protein gel facing the cathode in a semi-dry blotting apparatus. Proteins were transferred for 1,5 h at 1 mA/cm².

Blots were washed briefly in PBS-T and blocked with 5% milk for at least 30 min at room temperature. Primary antibodies were diluted in 5% milk and incubated with the membrane overnight. After 3 washes with PBS-T, appropriate secondary antibodies diluted in 5% milk were added for another hour. After 3 more washes blots were developed using the SuperSignal West Femto Maximum Sensitivity Substrate (Pierce/Thermo Fisher Scientific, Rockford, IL, USA) and chemiluminescence was analyzed using a GeneGnome HR (Syngene, Frederick, MD, USA) for imaging.

Immunofluorescence staining

For localization studies cells were seeded on coverslips, transfected as described above and and incubated for 24 h at 37°C. Where indicated, cells were incubated with 250 nM MitoTracker Deep Red FM (Invitrogen, Carlsbad, CA, USA) for 30 min at 37°C prior to fixation with PFA for 20 min at 25°C. Samples were permeabilized for 10 min with Triton X-100 and treated with block buffer for 30 min. After incubation with antibodies diluted in block buffer, samples were washed and antibody binding was detected using anti-mouse or anti-rabbit fluorophore conjugated secondary antibodies. Samples were imaged on a TE-2000 inverted microscope (Nikon, Melville, NY, USA) fitted with a video-rate confocal system consisting of a spinning disk confocal head (Yokogawa, Newnan, GA, USA). Slidebook software (Intelligent Imaging Innovations, Denver, CO, USA) was used to drive image capture as well as to perform image analysis and processing. Using a 100x oil immersion objective with a numerical aperture of 1,4 , confocal images were collected as a 3D stack with a focal step size of 0,27 µm. Micrographs were processed using Adobe Photoshop.

Genomic analyses

RNA extraction for expression profiling

Cells were grown on a 6-well plate and treated as indicated. RNA was purified using QIAShredder and the RNeasy Mini Kit in conjunction with the RNase-free DNase set (all Qiagen, Valencia, CA, USA) according to the manufacturer's instructions. RNA concentration was determined by measuring the absorbance at 260 nm (Nanodrop Technologies, Wilmington DE, USA).

Gene arrays and bioinformatic analysis

Microarray studies were performed by the Molecular Genetics Core Facility at Children's Hospital Boston supported by NIH-P50-NS40828, and NIH-P30-HD18655. Briefly, total RNA was reversely transcribed in cDNA, in vitro transcribed into biotin-labeled cRNA, hybridized onto Mouse WG-6 Expression BeadChips and scanned with a BeadArray Reader according to the manufacturer's instructions (Illumina, San Diego, CA, USA).

Microarray data processing and subsequent bioinformatic analyses were performed by Yijing Zhang: Quantile normalization was used for signal extraction and normalization. Two criteria were applied to identify differentially regulated genes: i) statistical significance of $P>0.05$ and ii) fold change of greater than 2 (ratio >2.0 or <0.5). In total, 5111 genes passed both criteria for at least one of the assayed conditions. Samples are clustered based on the Pearson's correlation coefficient for the profile of those 5111 genes. The Pearson correlation, hierarchical clustering and heat map were generated using R functions 'cor', 'hclust' and 'heatmap', respectively. Signal intensity that reflected mRNA expression was presented on heatmaps or scatterplots on a log scale according to a color-coded intensity scale with R software (The R Project for Statistical Computing, Vienna, Austria).

mRNA detection and analysis with nCounter

All nCounter (Nanostring Technologies, Seattle, WA, USA) analyses were performed by Kevin Bonham and Jonathan Kagan (both Children's Hospital Boston, MA, USA). nCounter CodeSets were constructed to detect genes selected by the Gene-Selector algorithm and additional controls as described. 240 000 cells were lysed in RLT buffer (Qiagen, Valencia, CA, USA) supplemented with β-mercaptoethanol (Sigma-Aldrich, St. Louis, MO, USA). 5 % of the lysate was hybridized for 16 h with the CodeSet and loaded onto the nCounter prep station, followed by quantification with the nCounter Digital Analyzer. To allow for side-by-side comparisons of nCounter experiments, the nCounter data was normalized in two steps. First small variations in the efficiency of processing were controlled for by normalizing measurements from all samples analyzed on a given run to the levels of chosen positive controls provided by the nCounter instrument. Second, the data obtained for each sample was normalized to the expression of nine control genes (Gapdh, Ik, Mea1, Ndufs5, Ndufa7, Rbm6, Shfm1, Tomm7 and Ywhaz). These genes were described to be unchanged in cells exposed to

a variety of infectious conditions [163]. For every sample, the weighted average of the mRNA counts of the nine control transcripts was computed and the sample was normalized by multiplying each transcript count by the weighted average of the controls.

RESULTS

MAVS is located on both mitochondria and peroxisomes

Both Fis1 [156] and Mff [155] participate in mitochondrial and peroxisomal morphology by regulating the fission and/or fusion of these cell organelles and display a similar domain architecture. The topology of Fis1 and Mff comprises an N-terminal functional domain exposed to the cytosol, a transmembrane domain inserted into the outer mitochondrial or peroxisome membrane and a short lumenal tail, and therefore are termed tail-anchored proteins. MAVS has a domain organization similar to Fis1 and Mff. Therefore I speculated that MAVS in analogy to other tail-anchored membrane proteins that function from mitochondria and peroxisomes resides not only on mitochondria, but peroxisomes as well. The subcellular localization of overexpressed MAVS was examined MEFs whose peroxisomes were marked by a DsRed allele containing a type 1 peroxisomal targeting sequence (PTS1). In addition to staining structures that appeared to be mitochondria, MAVS was detected on PTS1-positive peroxisomes scattered throughout the cell (Figure 4A). A similar staining pattern was seen for Mff (Figure 4B). In contrast, the TLR adapter protein TIRAP [148, 149] was not detected on peroxisomes (Figure 4C). To confirm that the peroxisomal staining was distinct from mitochondria, cells were additionally stained with the mitochondrial dye MitoTracker. Although no co-staining was detected between PTS1 and MitoTracker, MAVS was detected on both PTS1-positive peroxisomes and MitoTracker-positive mitochondria (Figure 4D).

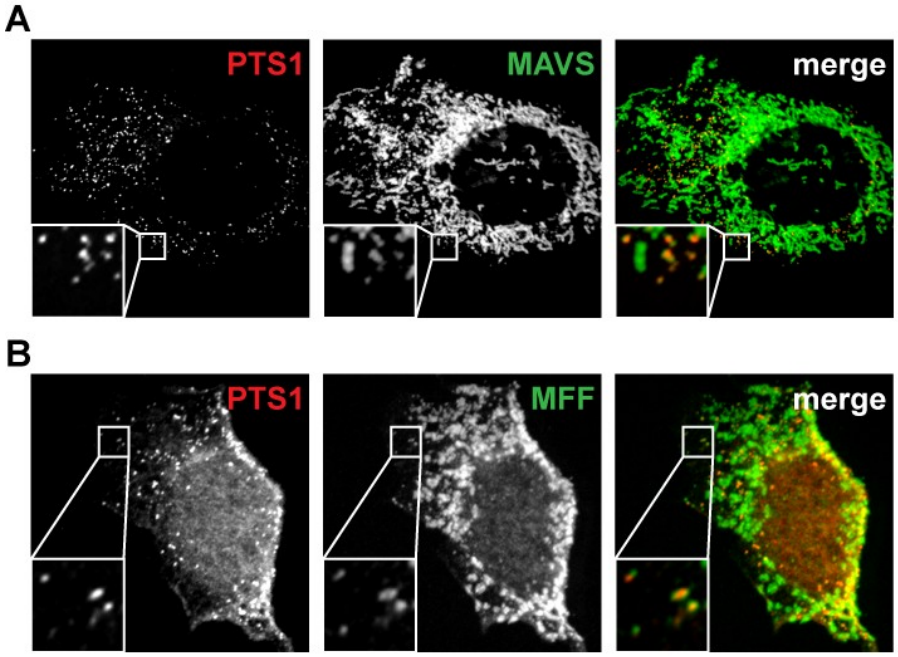

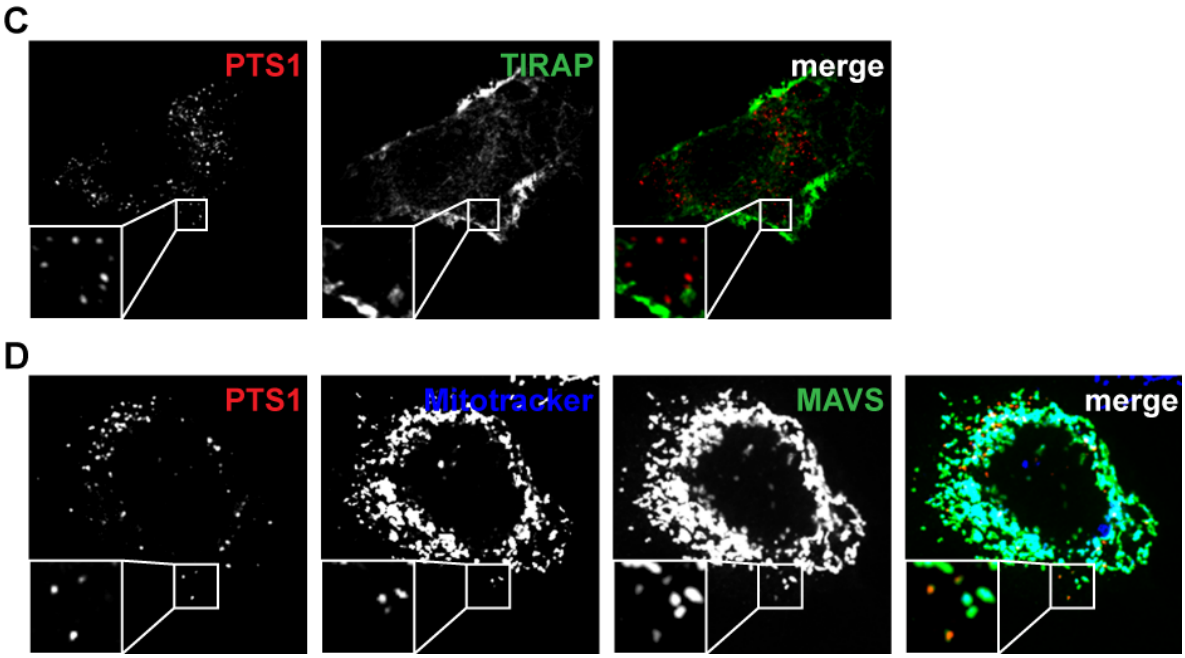

Figure 4. MAVS resides on mitochondria and peroxisomes when overexpressed in MEFs

(A-C) MEFs were transfected with the peroxisomal marker DsRed-PTS1 and Flag-MAVS (A), myc-MFF (B), or Flag-TIRAP (C). Cells were stained with anti-MAVS, anti-myc, or anti-Flag antibodies, respectively.

(D) MEFs expressing Flag-MAVS as well as EGFP-PTS1 and Pex19 from a bicistronic construct were stained with anti-MAVS antibody and MitoTracker to visualize mitochondria.

Next, I examined the localization of endogenous MAVS to exclude that the distribution of MAVS to peroxisomes is due to mistargeting caused by high overexpression levels. In hepatocytes endogenous MAVS co-localized with PTS1-positive peroxisomes (Figure 5A) similarly to the above described localization studies with overexpressed MAVS.

As an independent means of assessing MAVS localization, hepatocytes were biochemically fractionated to separate peroxisomes and mitochondria, which were respectively distinguished by Pex14 and mtHSP70 (Figure 5B). Both MAVS and Fis1 (a protein that occupies both organelles [156]) were detected in fractions containing peroxisomes or mitochondria. Moreover,

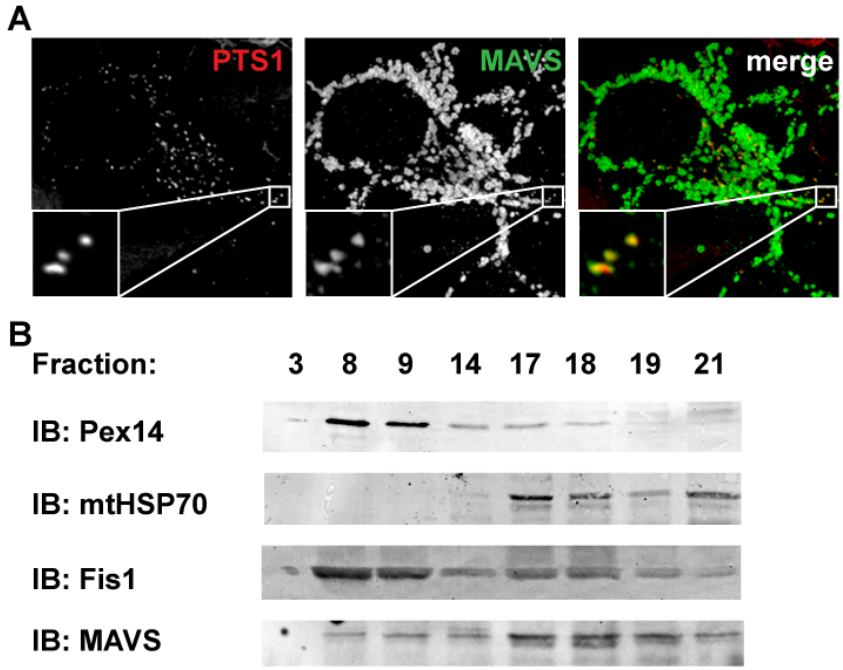
A
PTS1
MAVS
merge
B
Fraction: 3 8 9 14 17 18 19 21
IB: Pex14
IB: mtHSP70
IB: Fis1
IB: MAVS

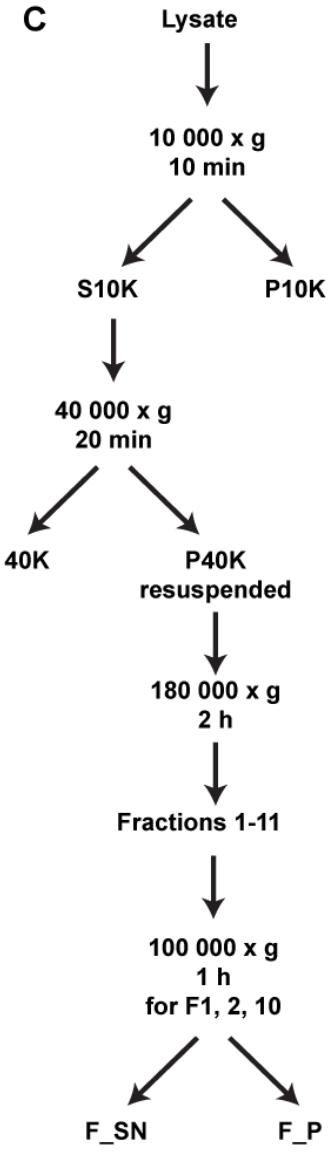
C
Lysate
10 000 x g
10 min
S10K
P10K
40 000 x g
20 min
40K
P40K
resuspended
180 000 x g
2 h
Fractions 1-11
100 000 x g
1 h
for F1, 2, 10
F_SN
F_P

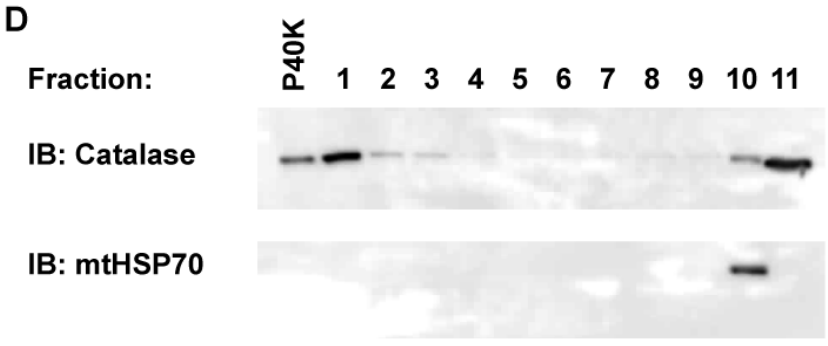
D
Fraction: P40K 1 2 3 4 5 6 7 8 9 10 11
IB: Catalase
IB: mtHSP70

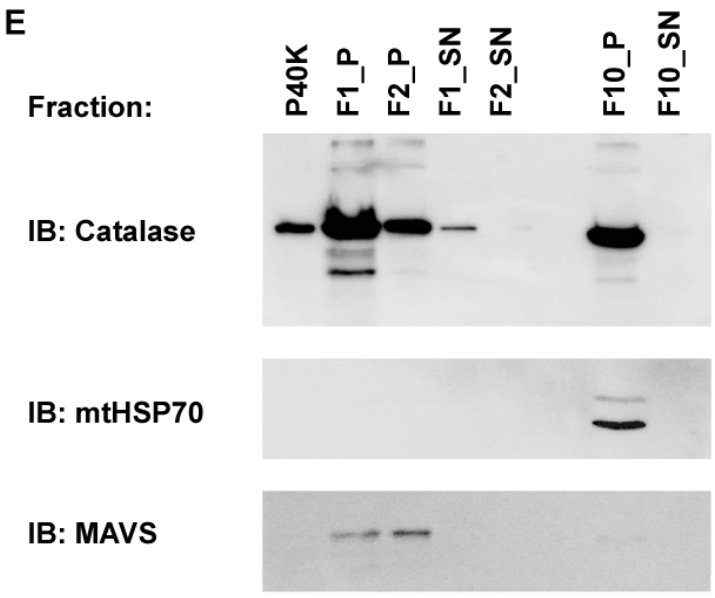
E
Fraction: P40K F1_P F2_P F1_SN F2_SN F10_P F10_SN
IB: Catalase
IB: mtHSP70
IB: MAVS

Figure 5. Endogenous MAVS displays dual localization on mitochondria and peroxisomes

(A) Huh-7 hepatocytes were transfected with DsRed-PTS1 and endogenous MAVS was detected with anti-MAVS antibody.

(B) Peroxisomes were separated from mitochondria on a Nycodenz gradient with HepG2 hepatocyte lysates. Selected fractions of the gradient were analyzed by immunoblotting with Pex14, mtHSP70, Fis1 or MAVS antisera.

(C) Centrifugation scheme of peroxisome purification from U937 lysates

(D) Peroxisomes were separated from mitochondria on a self-generating Optiprep gradient with U937 monocyte lysates and each gradient fraction was analyzed by immunoblotting with catalase or mtHSP70 antisera.

(E) Fraction 1, 2, and 10 were enriched for membranes by a last centrifugation step and pellets (P) and supernatants (SN) were analyzed for the presence of catalase, mtHSP70 or MAVS by immunoblotting.

when cell fractionations were performed with monocytes (Figure 5C and D), MAVS was co-fractionated with peroxisomes, indicated by the presence of catalase, and mitochondria, visualized by the marker protein mtHSP70 (Figure 5E). Overall, based on studies in both human and mouse cells aimed to investigate the localization of overexpressed and endogenous MAVS protein, I concluded from these data that peroxisomes are a second *bona fide* reservoir of MAVS.

One possible reason why MAVS is present on peroxisomes is that newly synthesized MAVS might first pass through peroxisomes en route to mitochondria. To address this possibility, I used human fibroblasts from a patient lacking a functional Pex19 protein. Pex19 controls peroxisome biogenesis, and thus Pex19-deficient cells contain no peroxisomes or peroxisomal remnant structures [164, 165]. Notably, MAVS was delivered to mitochondria in Pex19-KO cells (Figure 6A), indicating that the pathway to mitochondria does not require a peroxisomal intermediate. Moreover, MAVS localized to both peroxisomes and mitochondria in Pex19-KO cells that expressed Pex19 after transient transfection (Figure 6B) or retroviral gene transfer (Figure 6C). It is therefore unlikely that localization of MAVS to peroxisomes is the result of a biosynthetic pathway for delivering outer membrane proteins to mitochondria.

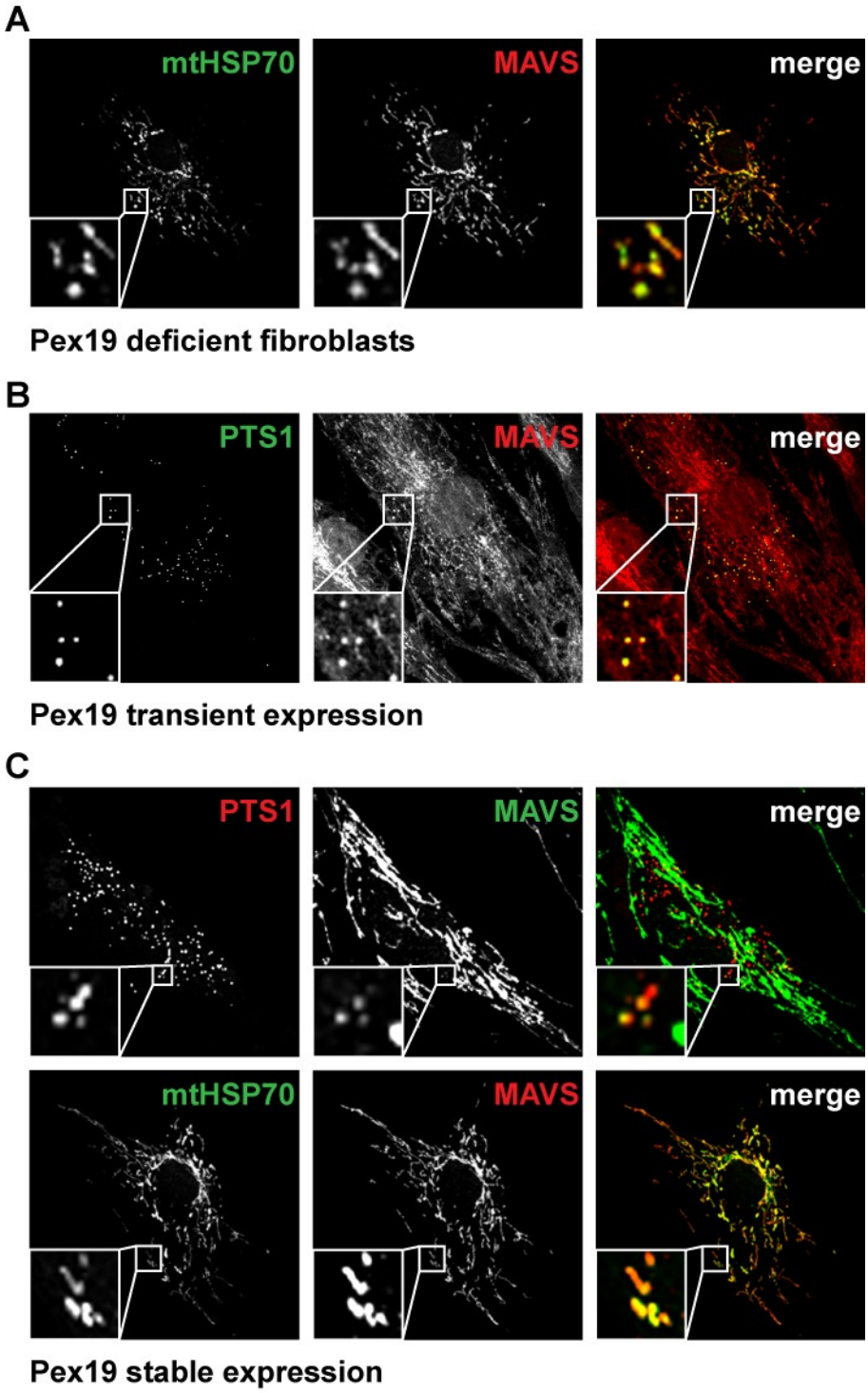

Figure 6. MAVS is delivered to peroxisomes generated de novo

(A-C) Pex19-deficient human fibroblasts were stained for endogenous MAVS before (A) and after transient (B) or stable (C) expression of a functional Pex19 allele. Mitochondria were stained with anti-mtHSP70 antibody. Peroxisomes were visualized by transfection with a bicistronic construct encoding EGFP-PTS1 and Pex19.

A systematic strategy to separate functions of peroxisomal and mitochondrial MAVS

The finding that MAVS is located on peroxisomes raised the possibility that these organelles serve as a site of antiviral signal transduction. I first considered using Pex19-deficient cells to address sufficiency of mitochondrial MAVS in antiviral signaling, but since peroxisomes are required for biochemical processes that occur in mitochondria, Pex19-KO cells have profound defects in mitochondrial function [166]. I therefore used the alternative approach of genetically separating putative mitochondrial and peroxisomal functions of MAVS. This was accomplished by replacing the previously defined MAVS localization motif [59] harboured within the C-terminal 40 residues with a set of domains that instead direct the protein to a single compartment (Figure 7A). Using the localization motif of the peroxin Pex13 [167], I created a protein called MAVS-Pex. By deleting the MAVS localization motif, I also created a cytosolic allele (MAVS-Cyto) [59]. Because the fidelity of mitochondrial sorting signals is not always transferrable to other proteins [168], I lastly created two different alleles of MAVS containing a sorting signal derived from proteins inserted in the mitochondrial outer membrane, either OMP25 or Fis1 [156, 169].

I introduced the WT and mutant MAVS alleles into MAVS-KO MEFs by retroviral gene transfer. Co-translation of MAVS and the fluorescent selection marker from the retroviral expression vector allowed to identify transduced cells, which were sorted for equal fluorescent brightness (Figure 7B). Accordingly, the resultant cell lines expressed comparable levels of each MAVS allele (Figure 7C).

The subcellular localization of the truncated and chimeric MAVS proteins was determined by microscopy. Full-length MAVS (MAVS-WT) was located on both mitochondria and peroxisomes (data not shown), and MAVS-Cyto was found on neither organelle (Figure 8D). As expected, MAVS-Pex was found exclusively on peroxisomes (Figure 8A). Of the alleles containing the putative mitochondrial targeting sequences, the allele harboring the Fis1 transmembrane domain was found primarily on mitochondria (Figure 8B), whereas the one containing the OMP25 transmembrane domain was located on both mitochondria and peroxisomes (Figure 8C). I therefore refer to the mitochondria-specific allele as MAVS-Mito to indicate its exclusive localization to mitochondria and the allele found on both organelles as MAVS-Mimic to indicate its ability to copy the localization pattern of MAVS-WT.

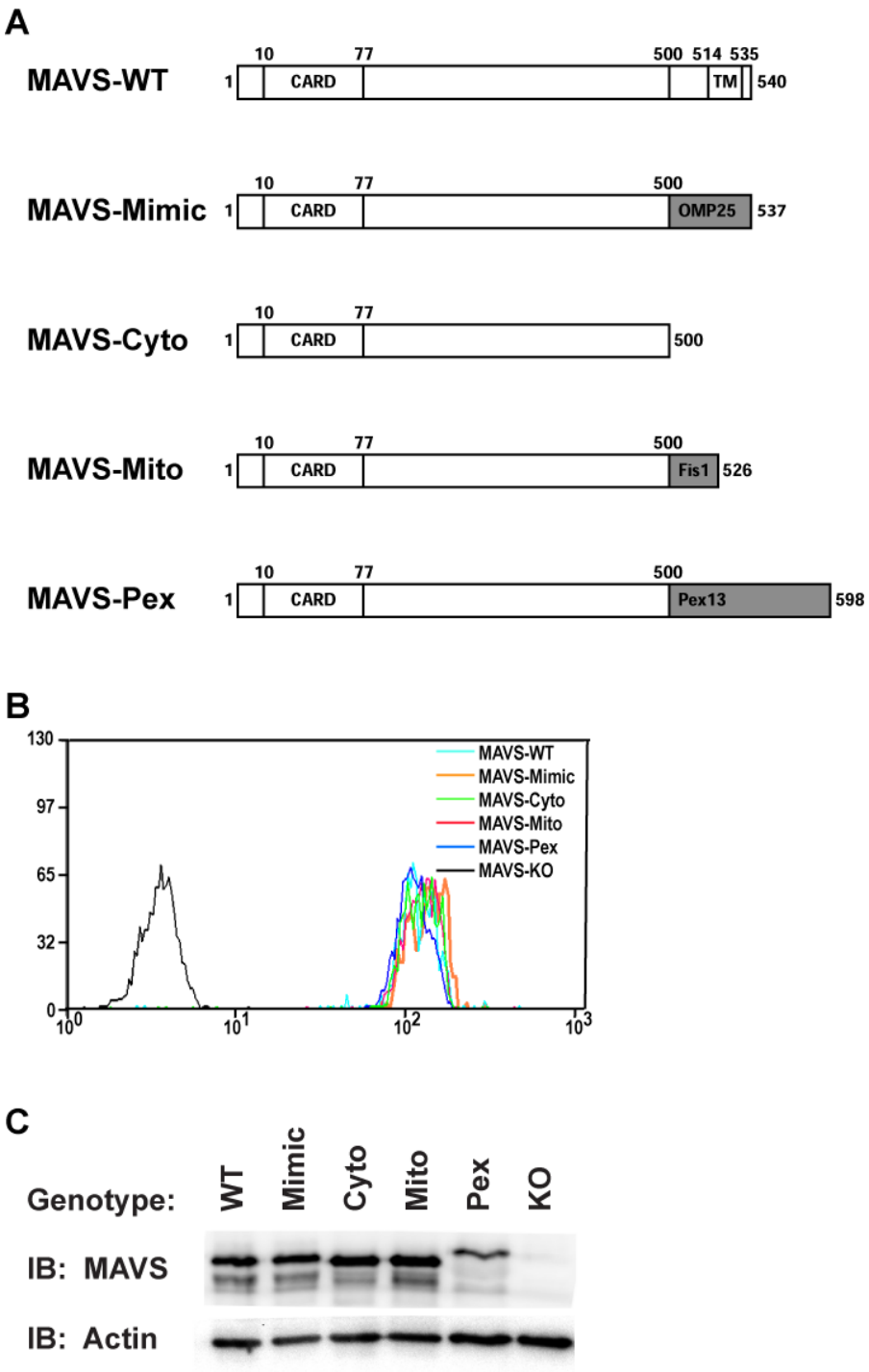

Figure 7. Targeting of MAVS to distinct subcellular compartments by replacement of its transmembrane domain

(A) Schematic of wild-type and mutant MAVS alleles to be tested for signaling from peroxisomes and mitochondria.

(B) Stable cell lines expressing the MAVS alleles listed in (A) were generated by retroviral transduction of MAVS-KO cells. Resulting transgenic cells expressed a MAVS allele and GFP, whose translation is directed by an IRES. Shown are overlaid histograms of stable populations of each cell line expressing equivalent levels of the bicistronic mRNAs encoding MAVS and GFP.

(C) Lysates from stable cell lines described in (B) and parental MAVS KO MEFs were analyzed by immunoblotting with anti-MAVS antibody.

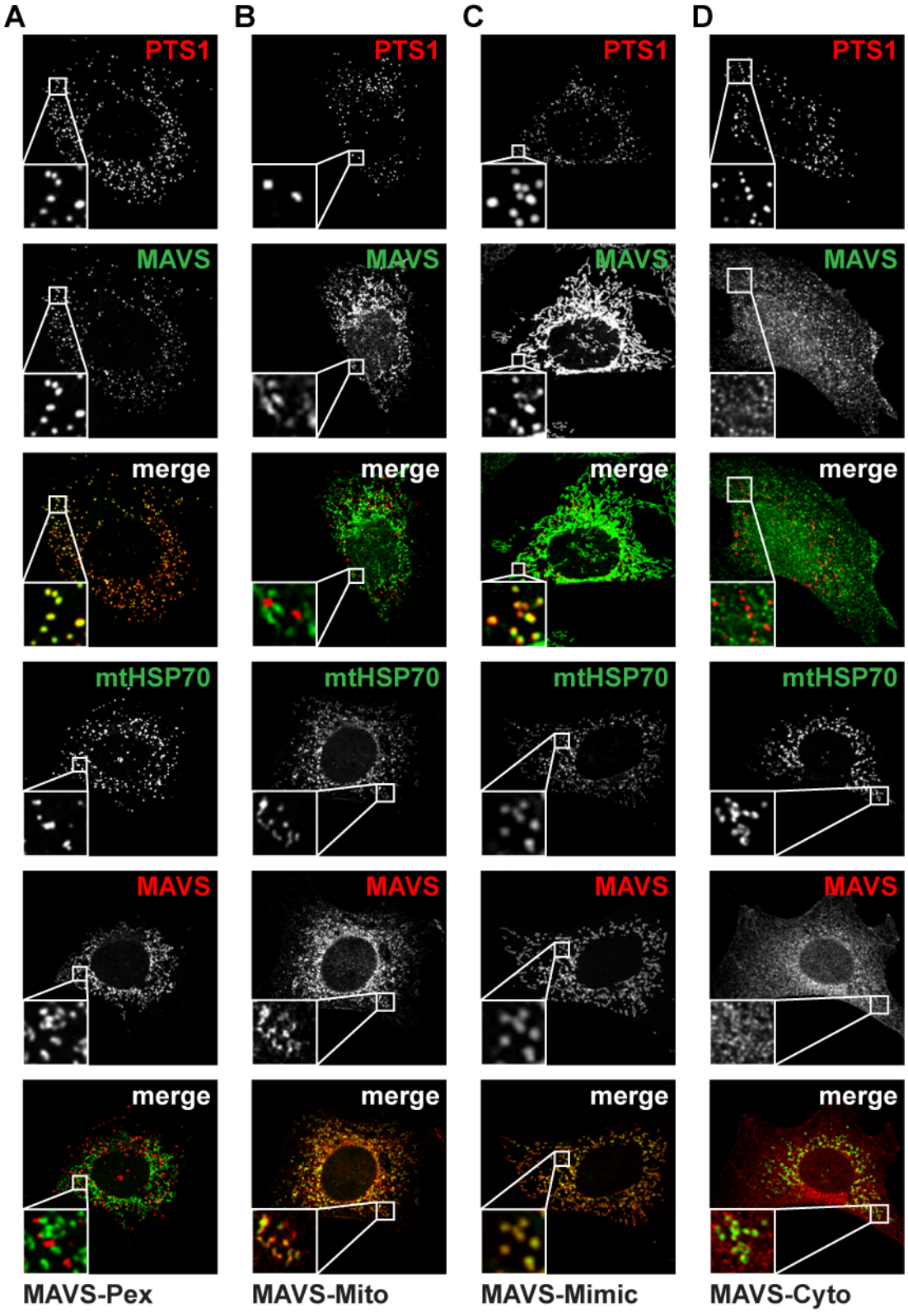

Figure 8. Subcellular distribution of MAVS in chimeric cell lines

Micrographs of MAVS-Pex (A). MAVS-Mito (B), MAVS-Mimic (C) and MAVS-Cyto (D) cell lines stained with anti-MAVS antibody. Mitochondria were stained with anti-mitochondrial HSP70 antibody. Peroxisomes were visualized by transfection with DsRed-PTS1. Note that MAVS-Pex exclusively resides on peroxisomes, MAVS-Mito is located on mitochondria, MAVS-Mimic on both organelles and MAVS-Cyto on neither of the two organelles.

Collectively, this set of MAVS-expressing MEF lines differs only in the subcellular positioning of the signaling domain of MAVS and thereby provides an ideal system to determine the relative roles of mitochondrial and peroxisomal localization in MAVS-dependent signal transduction.

MAVS-dependent signaling occurs from both peroxisomes and mitochondria

To address the function of peroxisomal MAVS, I monitored the expression of antiviral factors in response to infection with reovirus. I chose reovirus because it is a known inducer of both RIG-I and MDA-5 signaling pathways [47], allowing direct examination of both RLRs in a single experiment. Cells were infected with reovirus, and extracts were examined at various times for expression of viperin, a well-characterized ISG [139, 170]. MAVS-WT, -Mimic or -Mito expressing cells induced viperin expression in response to infection (Figure 9A). This response was MAVS dependent, as MAVS-KO cells showed no change in viperin expression (Figure 9A). MAVS-Cyto cells were unable to induce viperin expression, confirming that membrane localization is necessary for MAVS function [59]. Interestingly, despite the fact that MAVS-Pex is found only on peroxisomes, MAVS-Pex cells induced viperin expression after infection (Figure 9A). An examination of the kinetics of ISG induction indicated that cells containing MAVS on peroxisomes (MAVS-WT, -Mimic and -Pex) induced viperin expression within 4 h of infection. In contrast, exclusive localization to mitochondria (MAVS-Mito) resulted in viperin expression with delayed kinetics (Figure 9A). These results suggest that localization of MAVS to either peroxisomes or mitochondria is sufficient to induce antiviral signaling, but that peroxisomal residence allows for more rapid expression of ISGs. Interestingly, rapid expression of ISGs by MAVS-Pex appeared transient, as viperin expression decreased at later times of infection (Figure 9A).

To determine if peroxisomal signaling by MAVS requires signaling by both RIG-I and MDA-5, I performed similar experiments using influenza virus, which activates the RIG-I pathway exclusively [44, 171]. A similar pattern of viperin expression was observed with influenza as with reovirus, although the kinetic differences between MAVS-Pex and -Mito were even more pronounced with influenza (Figure 9B). Thus, RIG-I signaling alone is sufficient to induce MAVS-dependent signaling from peroxisomes. In sum, these data indicate that peroxisomal MAVS induces rapid but transient viperin expression, whereas

mitochondrial MAVS induces delayed but stable viperin expression. Signaling from both organelles thus contributes to the rapid and stable expression of viperin that is detected in MAVS-WT cells.

Peroxisomal MAVS triggers an IFN-independent pathway that promotes ISG expression

The different kinetics of viperin induction by peroxisomal and mitochondrial MAVS suggest that more than one mechanism of RLR-induced ISG expression may operate in virus-infected cells. ISG expression can be induced directly, or indirectly through the action of secreted type I IFNs [56, 57]. To determine if IFNs contribute to expression of ISGs induced by mitochondrial or peroxisomal MAVS, I monitored the rate of IFN production by virally infected cells. As expected, IFN production upon reovirus infection was dependent on mitochondrial localization of MAVS. All mitochondrial MAVS proteins (MAVS-WT, -Mimic and -Mito) triggered IFN production, albeit with delayed kinetics in the case of MAVS-Mito (Figure 9C). These data indicate that in the case of the mitochondria-localized MAVS proteins, IFN expression coincides with ISG induction. Surprisingly, no detectable IFNs were produced by MAVS-Pex cells (Figure 9C). Similar results were obtained with cells infected with influenza as with reovirus (Figure 9D), although the relative amounts of IFNs produced with these two viruses differed dramatically, reflecting unique aspects of each.

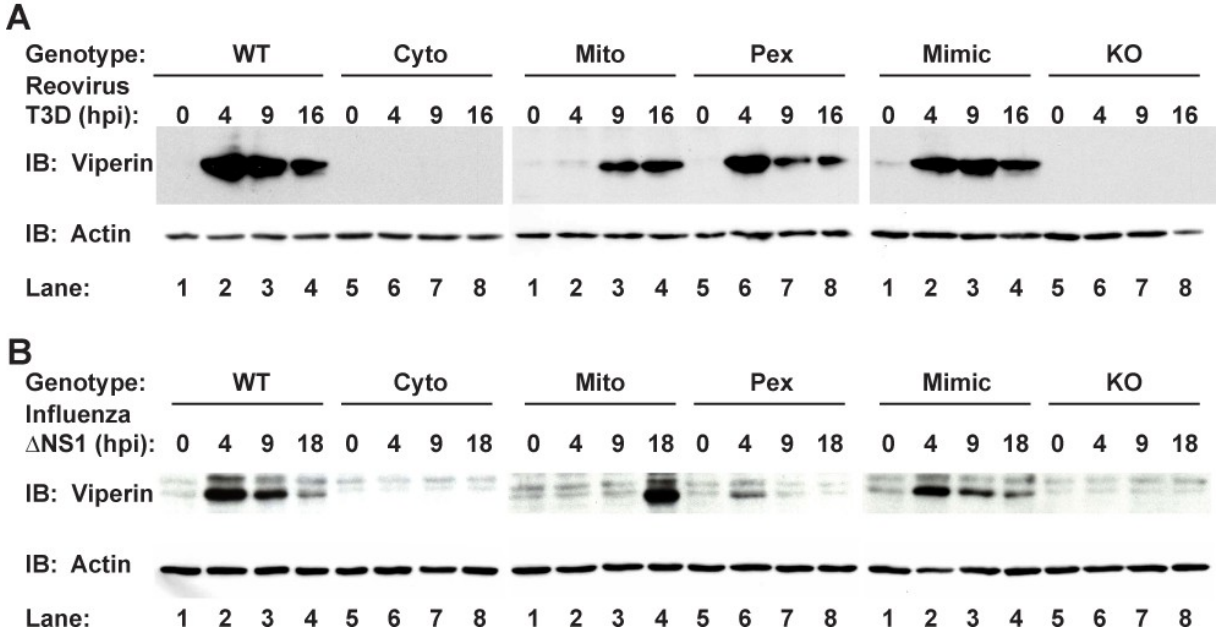

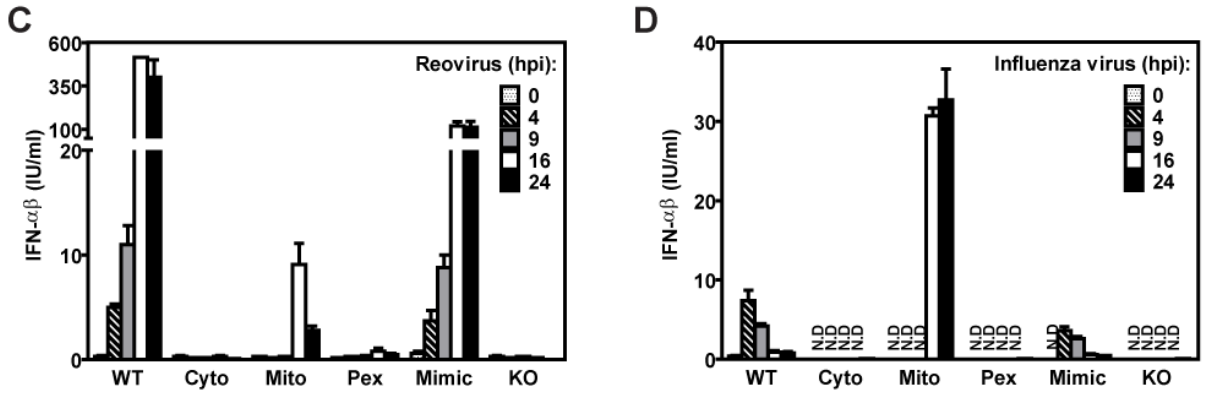

Figure 9. Peroxisomal MAVS mediates ISG expression, but does not induce type I IFN secretion after viral challenge

(A) MAVS-expressing MEFs and parental MAVS-KO cells were infected with reovirus at an MOI of 100). At indicated times, cell-associated ISG expression was determined by immunoblotting with an anti-viperin antibody.
(B) Similar to (A) except for infection with influenza virus ΔNS1 at an MOI 5 in lieu of reovirus.
(C and D) Cell culture media from (A) and (B) were tested for type I IFN activity using a bioassay, respectively.

To confirm the inability of MAVS-Pex cells to secrete IFNs I stimulated cells by transfection with the ligands for RIG-I and MDA-5, 5'-triphosphosphate RNA (Figure 10A) and polyI:C, respectively (Figure 10B). For both stimuli I observed the same phenotype as with viral infection, namely a lack of detectable IFN expression when MAVS is localized exclusively at peroxisomes.

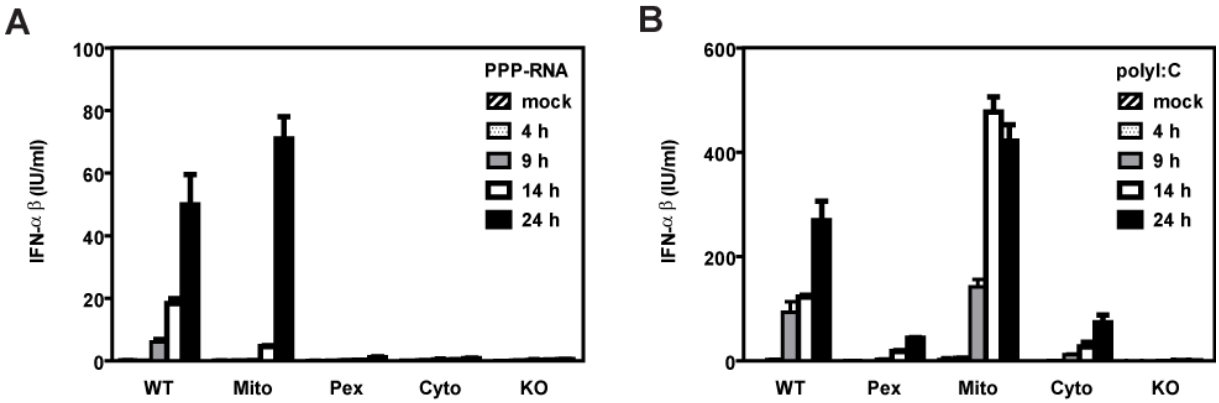

Figure 10. Neither stimulation with 5'-triphosphate RNA nor with polyI:C induces IFN secretion in MAVS-Pex cells.

(A and B) MAVS-expressing MEFs and parental MAVS-KO cells were transfected with 500 ng/ml 5'-triphosphorylated RNA (A) or 10 µg/ml polyI:C (B). At indicated times, cell culture media were tested for type I IFN activity using a bioassay.

My inability to detect a role for IFNs in promoting viperin expression in MAVS-Pex cells was not due to an inability of the cells to respond to IFNs, however, because addition of

recombinant IFN-β was sufficient to induce viperin expression in all cells examined (Figure 11A).

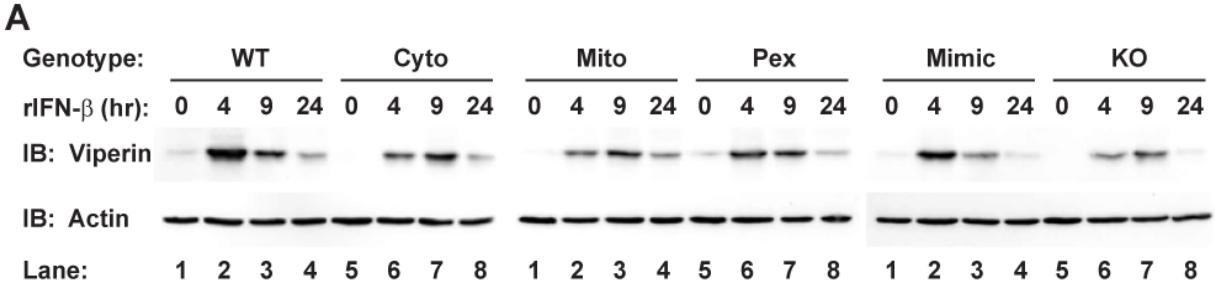

Figure 11. Type I IFN signaling is intact in all cell lines

(A) MAVS-expressing MEFs and parental MAVS-KO cells were treated with 100 IU/ml IFN-β. At indicated times, cell-associated ISG expression was determined by immunoblotting with anti-viperin antibody.

The observation that viperin can be expressed in the absence of type I IFN induction suggests that IFNs may not contribute to ISG expression induced by peroxisomal MAVS. I tested this possibility by infecting cells under conditions in which the functions of IFNs are prevented by either disrupting protein secretion with brefeldin A (BFA) or by utilizing neutralizing antibodies to secreted IFN. Cells were infected with reovirus in the presence of excess of either inhibitor. Both treatments disrupted the activity of type I IFNs produced during reovirus infection (Figure 12A, B) and inhibited the expression of viperin by cells expressing mitochondrial MAVS (MAVS-WT, -Mimic, -Mito) (Figure 12C, D). These data indicate that signaling by IFNs promotes viperin expression but, because these treatments did not completely abolish viperin expression, that an IFN-independent pathway of viperin induction also exists. Interestingly, MAVS signaling from peroxisomes primarily utilized the IFN-independent pathway, as viperin expression within MAVS-Pex cells was largely resistant to these treatments (Figure 12C, D).

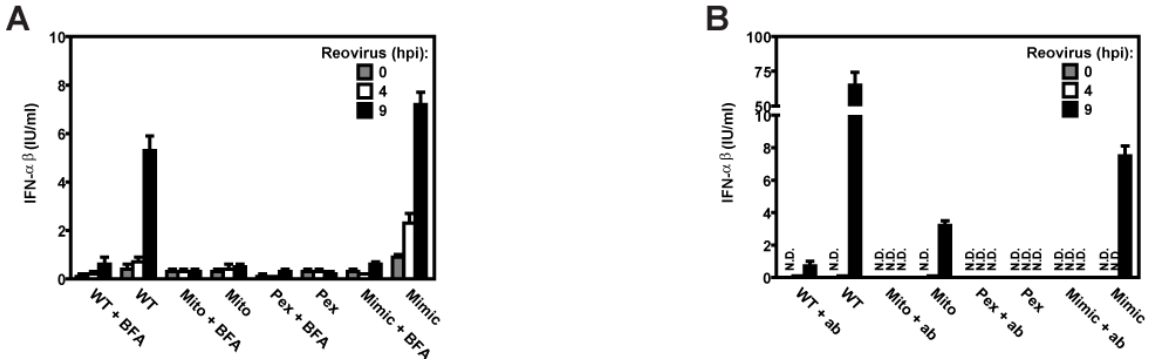

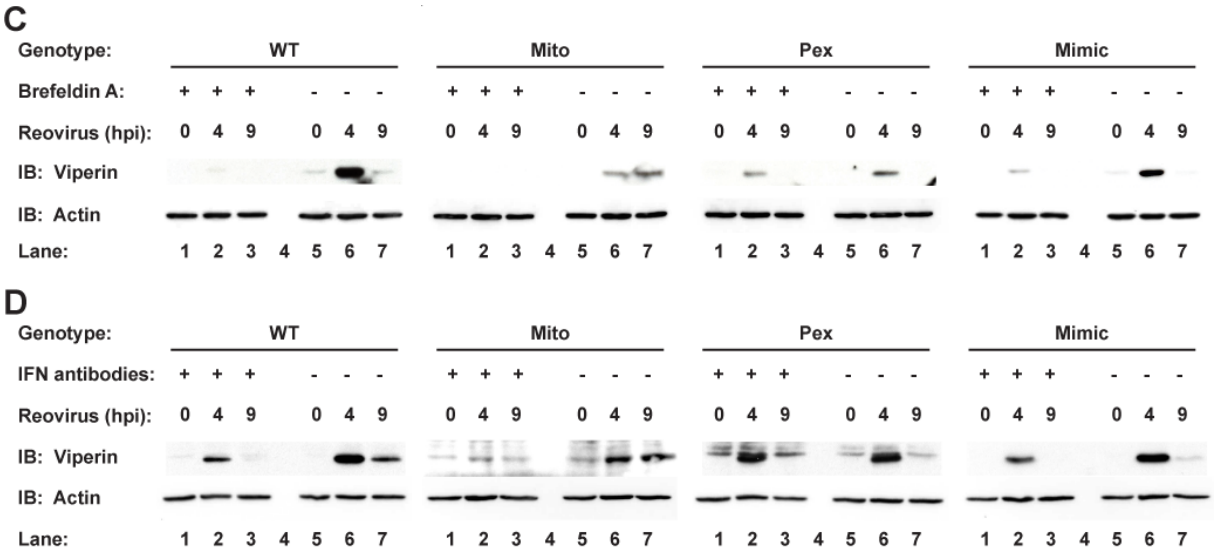

Figure 12. Peroxisomal MAVS directly induces viperin expression

(A) MAVS-expressing MEFs and MAVS-KO cells were pretreated with 20 μg/ml BFA before infection with reovirus in presence of the drug. At indicated times, cell supernatants were tested for type I IFN activity via a bioassay.

(B) Similar to (A) except type I IFN activity was blocked by addition of 250 NU/ml anti-IFN-β and 500 NU/ml anti-IFN-α antibodies after infection with reovirus.

(C and D) Cell lysates from (A) and (B) were tested for ISG expression by immunoblotting with anti-viperin antibody.

These data therefore indicate that the subcellular positioning of MAVS determines the type of signaling pathway activated during viral infection. Peroxisomal MAVS induces the rapid and direct expression of viperin, which is followed by mitochondrial MAVS triggering viperin expression directly, as well as indirectly through the IFN-mediated feed-forward loop.

The global transcriptional response to reovirus infection is mediated by the collective actions of MAVS-dependent peroxisomal and mitochondrial signaling

Based on the set of candidate genes examined, my data suggests that peroxisomal and mitochondrial MAVS each induce a complementary set of genes that are collectively induced by MAVS-WT. To determine if this is the case, microarrays were performed on reovirus infected cells. Infections were performed for 3, 9, or 16 h and RNA was collected for genome-wide expression analysis. At all times examined, similar expression profiles were observed when comparing MAVS-WT or MAVS-Mimic cells, confirming that similarities in MAVS localization are predictive of similarities in MAVS function (Figure 13A, B). These cells

induced the expression of numerous ISGs, IFNs, and chemokines, but no proinflammatory cytokines (Figure 13C and data not shown). MAVS-Cyto cells were most similar to MAVS-KO cells (Figure 13B, C), further confirming that membrane localization of MAVS is critical for its function in antiviral signaling. Interestingly, MAVS-Pex or -Mito expressing cells displayed a transcriptome that each partially overlapped with that of MAVS-WT cells, but were distinct from one another (Figure 13B, C). For example, at 16 h post-infection, MAVS-Mito cells upregulated genes encoding chemokines, ISGs, IFN-β, and several IFN-α family members (Figure 13C). MAVS-Pex cells also induced the expression of chemokines and ISGs, but without any detectable changes in IFN expression and with much faster kinetics (within 3 h) (Figure 13C). Thus, on a global scale, peroxisomal MAVS induces the rapid expression of ISGs without inducing IFN expression, whereas mitochondrial MAVS promotes IFN and ISG expression but with delayed kinetics.

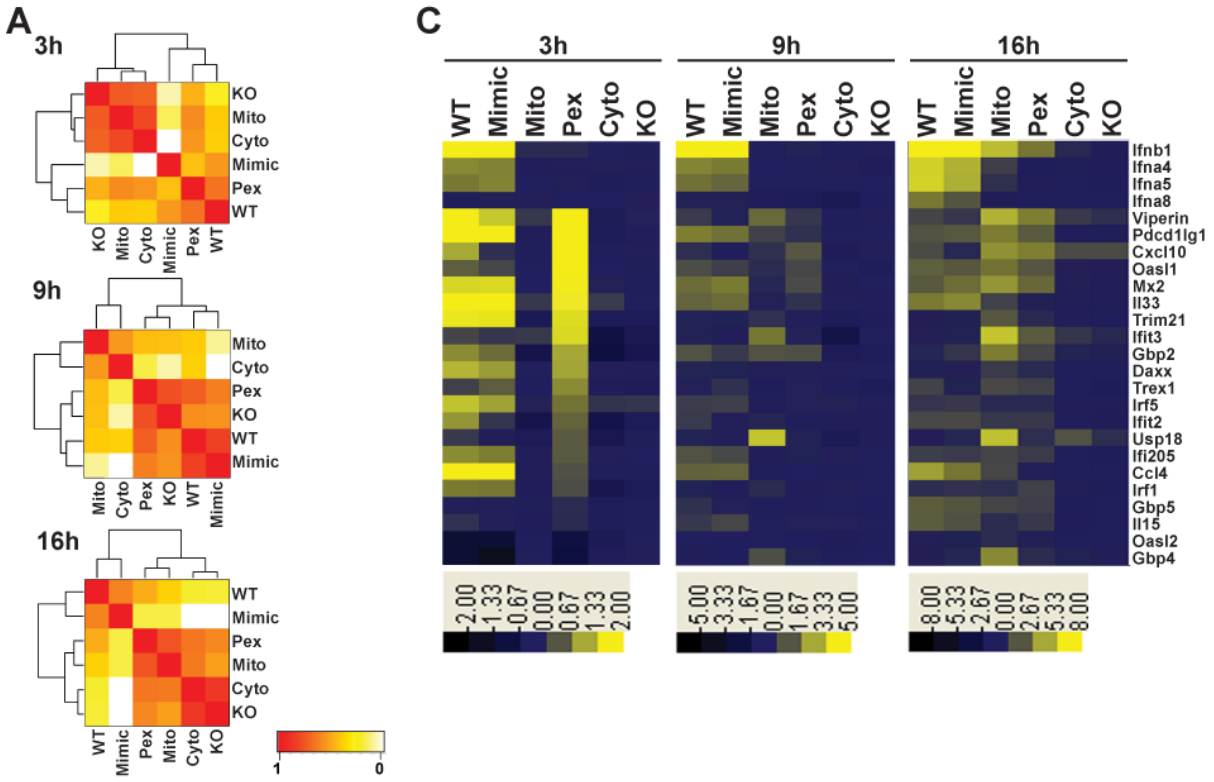

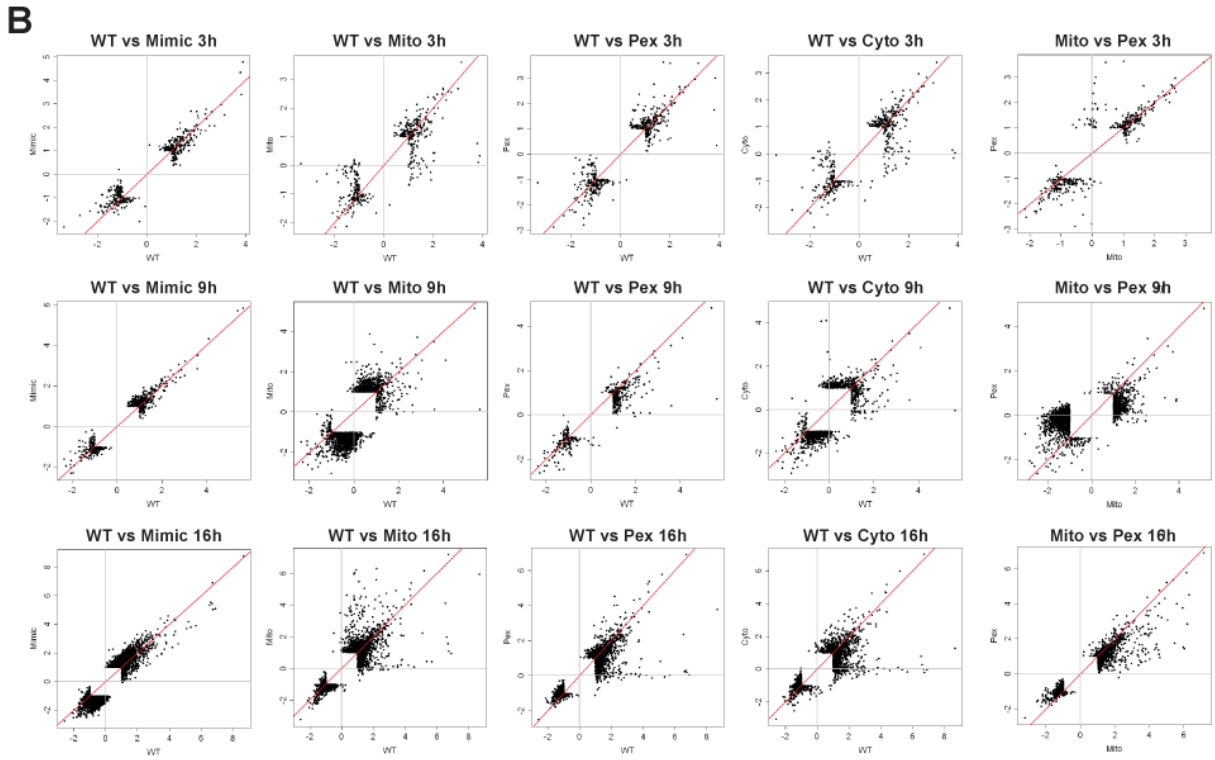

Figure 13. Genome-wide transcriptome analysis reveals a general role for peroxisomal and mitochondrial MAVS in antiviral gene expression

(A) RNA from MAVS-expressing MEFs and parental MAVS-KO cells after infection with reovirus for 3, 9 or 16 h was subject to microarray analysis. The similarity of the overall gene expression profiles mediated by the indicated MAVS alleles is displayed as Pearson correlation coefficient-based heat map. Samples are clustered along both axes based on their correlation value.

(B) Pairwise comparisons of indicated cell lines based on 4089 significantly regulated genes depicted in a log-log scale scatter plot. Each data point indicates a gene whose expression level exhibited a change of greater than 2-fold.

(C) Heat map of selected genes based on their expression ratios across all six cell lines and during all time points upon reovirus infection.

Genes are colored according to a log2-based color bar depicted underneath each heat map.

I verified these results by examining the expression of several candidate IFNs and ISGs using the nCounter technology, which allows for multiplex analysis of gene expression with the sensitivity of quantitative RT-PCR [172]. It is of note that this method allows measurement of the absolute number of a given transcript within a cell as opposed to a relative increase in abundance derived from microarray analyses. As expected the number of both primary and secondary IFN transcripts (Ifnb1 and Ifna4, respectively) in uninfected cells is extremely low (Figure 14A). MAVS-WT and MAVS-Mimic cells rapidly induce transcription as early as 3 h after infection and accumulate tens of thousands of transcripts by 16 h, whereas transcript

counts of the negative controls MAVS-KO and MAVS-Cyto are barely affected throughout the infection. MAVS-Mito cells achieve strong induction of IFN-β and IFN-α4 only 16 h after infection. In contrast, MAVS-Pex cells never significantly induce IFN-α4 and display rather moderate induction of IFN-β as late as 16 h post infection. It is most important to note though, that an increase of viperin transcripts in MAVS-Mito cells coincides with type I IFN upregulation, whereas MAVS-Pex cells induce viperin despite an evident lack of IFN induction. MAVS-WT and MAVS-Mimic combine these two phenomena as they display highest viperin transcript counts 3 h after infection, when IFN transcripts are still relatively low and maintain high transcript numbers later in infection, when IFN transcripts become abundant. For direct comparison with the microarray data fold changes were calculated from transcript counts as obtained by the nCounter system. Despite a discrepancy in magnitude likely due to the higher sensitivity of the nCounter [172] the pattern of IFN and viperin induction revealed by the microarray analysis was confirmed by the nCounter assay (Figure 14B).

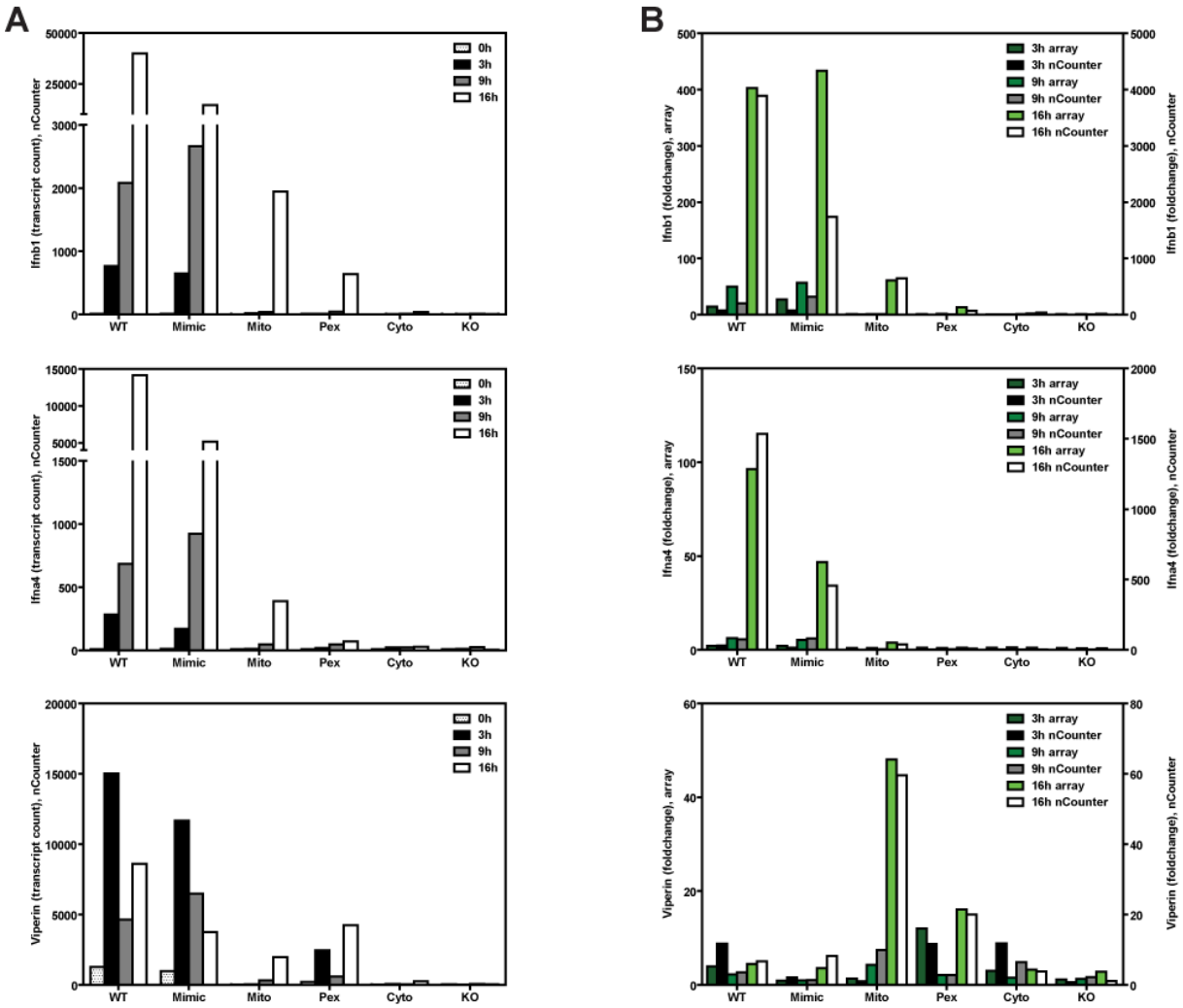

Figure 14. Confirmation of the microarray data using the nCounter platform

(A) RNA from MAVS-expressing MEFs and parental MAVS-KO cells after infection with reovirus for 3, 9 or 16 h was subject to nCounter analysis.

(B) For side by side comparison of microarray with nCounter data fold changes in relation to uninfected cells were calculated for all time points and each of the cell lines. Foldchanges obtained by both methods were plotted in one graph.

Overall, at all times examined, the genes expressed by either peroxisomal or mitochondrial MAVS were induced by MAVS-WT or -Mimic (Figure 13B, C). These data therefore support a model whereby the host transcriptional response is the result of MAVS signaling from both mitochondria and peroxisomes. I do note however, that the magnitude of antiviral gene expression induced by cells expressing MAVS-WT or MAVS-Mimic was greater than the magnitude induced by cells where MAVS was restricted to a single organelle, which suggests that signaling from both organelles may be coordinated to ensure maximal antiviral gene expression.

Peroxisomal signal transduction creates a transient but functional antiviral state

MAVS-dependent signaling promotes an antiviral state, which is functionally defined as the ability of cells to restrict multiplication of viruses. To determine the significance of mitochondrial or peroxisomal signaling pathways in this regard, I asked if signaling from either organelle is sufficient to restrict viral replication. This was addressed by infecting MAVS-expressing cells with reovirus and measuring production of infectious virions over time. As expected, MAVS-WT and -Mimic cells were most resistant to infection and MAVS-KO and -Cyto cells were most susceptible (Figure 15A). These data indicate that MAVS signaling is required to limit viral replication. Interestingly, cells expressing MAVS-Pex or MAVS-Mito exhibited an unusual biphasic behavior (Figure 15A). Over the first 24 h, these cells restricted viral replication as well as MAVS-WT, but this capacity diminished, and by 72 h were most similar to the MAVS-KO cells. These data establish that signaling from either peroxisomes or mitochondria is sufficient to induce a functional antiviral response, but signaling from both organelles is necessary for maximal containment of reovirus replication.

VSV is one of many viruses that interfere with type I IFN expression as part of their pathogenic lifecycle. However, VSV infection is known to induce ISG expression in the

absence of IFNs [173] (Figure 15B), which accurately reflects the hallmark of peroxisomal MAVS signaling. I therefore speculated that VSV engages selectively the peroxisomal pathway, while the mitochondrial pathway is blocked by viral inhibitory proteins. Under such circumstances the IFN-independent means of signaling that is induced by peroxisomal MAVS may be particularly important in controlling infection. Therefore I sought to determine the relative importance of peroxisomal and mitochondrial signaling in protecting cells from VSV infection by measuring the replication of this virus. Consistent with this idea, MAVS-Mito cells were as susceptible to VSV infection as MAVS-KO or -Cyto cells (Figure 15C), suggesting that in the absence of IFN production, the mitochondrial signaling pathway is functionally defective. Most notably, MAVS-Pex cells were nearly as effective at controlling VSV as MAVS-WT cells (Figure 15C). These results suggest that MAVS signaling from peroxisomes is the primary means of controlling viruses that interfere with IFN expression, thus underscoring the importance of this organelle in host defense.

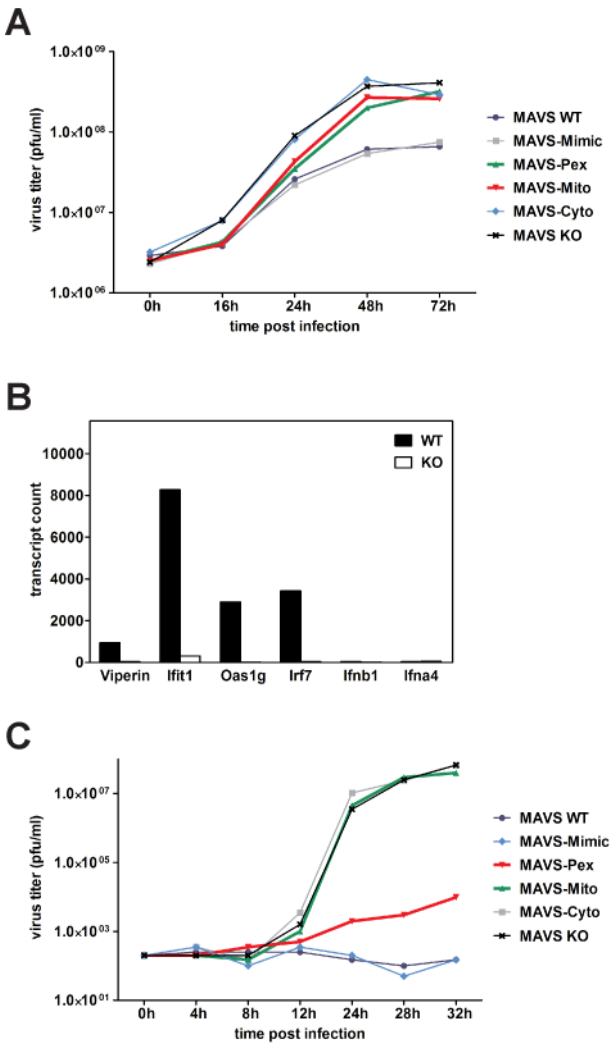

Figure 15. Peroxisomal MAVS Elicits a Functional Antiviral Response

(A) MAVS-expressing MEFs and MAVS-KO MEFs were infected with reovirus at an MOI of 3. At the indicated times, virus titers were determined by plaque assay.

(B) MAVS-WT and MAVS-KO MEFs were infected with VSV at an MOI of 3. After 8 h, RNA was isolated and analyzed for ISG and type I IFN expression using an nCounter.

(C) MAVS-expressing MEFs and parental MAVS-KO cells were infected with VSV at an MOI of 0.01. At the indicated times, virus titers were determined by plaque assay.

DISCUSSION

The best-characterized sensors of cytosolic viruses are members of the RLR family, which enlist the adaptor protein MAVS to initiate antiviral signal transduction [174]. MAVS is one of a growing group of tail-anchored membrane proteins that contain a C-terminal transmembrane domain [59, 155, 156]. This anchor was originally reported to promote localization of MAVS to the mitochondrial outer membrane, providing a landmark of where RLR signaling can occur [59]. This discovery established that cytosolic detection systems, like extracellular detection systems (i. e. TLRs), use membranes as scaffolds for signal transduction. In the TLR network, signaling occurs from a variety of different organelles, not just one [14]. I report here that in addition to mitochondria, MAVS is located on peroxisomes in several human and murine cell types, and represents the first antiviral signaling protein found on this organelle.

In order to address if this newly found localization of MAVS is a site of active antiviral signal transduction I generated chimeric MAVS alleles to be targeted to distinct organelles in analogy to previous studies [59]. The use of MAVS-deficient fibroblasts afforded us the advantage of generating a panel of cell lines that solely differs in the subcellular distribution of MAVS and thus represents an ideal tool to study organelle-specific signaling events. The central finding of this study – that peroxisomes are a site of signal transduction – was established with a complementary set of assays. I demonstrated that infection of fibroblasts with reovirus, a dsRNA virus known to be detected by both RIG-I and MDA-5, results in the strong upregulation of several ISGs such as viperin and members of the Mx and IFIT protein families. Strikingly, genome-wide expression profiling did not reveal type I IFN induction by peroxisomal MAVS in stark contrast to findings from mitochondrial MAVS. Furthermore, I assayed for type I IFN secretion using a luciferase-based bioassay and viperin expression by immunoblot after infection with reovirus or influenza virus, a segmented dsRNA virus, whose detection strictly depends on RIG-I. In line with the genomic data peroxisomal MAVS mediates ISG expression, but not type I IFN expression. Finally, decreased viral titers of fibroblasts infected with reovirus or VSV, the latter eliciting a RIG-I-mediated antiviral response, indicate that peroxisomal MAVS interferes with viral replication. In summary, I measured 1) mRNAs encoding ISGs and IFNs, 2) protein levels of ISGs and IFNs, and 3) induction of a functional antiviral state in cells. In each of these assays, I found that peroxisomes are a site of MAVS-dependent signaling. Moreover, I obtained these results by using several unrelated RNA viruses (i. e. reovirus, influenza virus and VSV) as physiological

triggers of RLR signaling, which suggests that peroxisomal signaling is a fundamental component of the RLR network.

The RLR signaling network now joins the TLRs as pattern recognition systems that signal from multiple organelles. Both systems require that a transmembrane protein be positioned on specific organelles – the receptors themselves in the case of TLRs and the MAVS adaptor in the case of RLRs [14, 175]. Interestingly, when considering these two networks, the function of diversifying signaling locale appears to be distinct. In the case of TLRs, differential receptor placement diversifies the types of pathogens that can be detected: TLRs found on endosomes recognize viruses, while TLRs found on the plasma membrane typically recognize bacteria. In contrast, differential MAVS placement does not diversify the types of viruses detected by RLRs, but diversifies the types of signaling pathways that are activated. In the case of reovirus and influenza virus, peroxisomal MAVS triggers rapid induction of ISGs, whereas mitochondrial MAVS triggers delayed ISG and IFN expression (Figure 16). This diversification is functionally important, as my data indicate that MAVS signaling must occur from both organelles to limit reovirus replication.

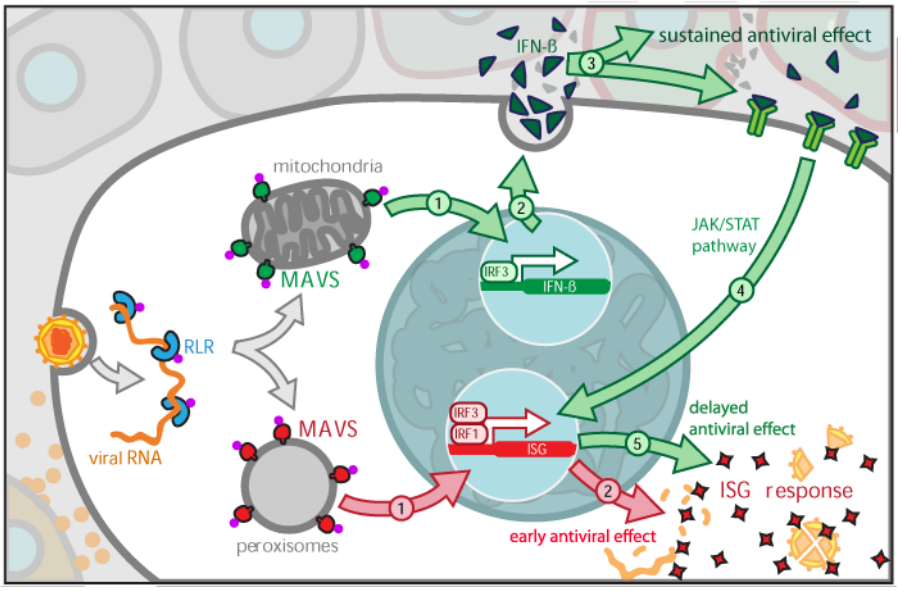

Figure 16. Model of organelle-specific MAVS signaling in fibroblasts

Peroxisomal MAVS is essential for rapid ISG expression independent of type I IFN, whereas mitochondrial MAVS induces ISGs with delayed kinetics and primarily dependent on type I IFN secretion. Therefore, peroxisomal MAVS mediates immediate and transient antiviral effects, while mitochondrial MAVS promotes a sustained response later during infection.

My finding that peroxisomal localization of MAVS is required for rapid but transient induction of antiviral ISGs, whereas mitochondrial MAVS promotes ISG expression with

delayed kinetics, is especially intriguing. The kinetic differences of ISG expression were explained by the observation that peroxisomal MAVS induced a cell-intrinsic means of ISG induction, which occurred in the absence of detectable IFN expression. Mitochondrial MAVS induced cell-intrinsic ISG expression as well, but maximal induction occurred through the actions of secreted IFNs.

The location-specific differences in MAVS signaling are functionally relevant, as we found a remarkably consistent correlation between the rate of ISG expression and the ability of infected cells to restrict viral replication. During reovirus infection, peroxisomal MAVS induces rapid, but transient expression of ISGs, and thereby creates a functional, but short-term antiviral state. Long-term protection requires the additional actions of secreted IFNs, and thus signaling from mitochondria is also important to create the most effective antiviral state. The observation that mitochondrial MAVS can induce most or all of the same genes as WT MAVS, but cannot control reovirus infection, indicates that the timing of ISG expression is critical. These data therefore establish peroxisomes as a *bona fide* functional site of antiviral signal transduction and underscore the importance of non-mitochondrial RLR signaling in innate immunity.

The importance of RLR signaling from peroxisomes was also revealed by experiments with VSV, which interferes with IFN expression and renders the mitochondrial pathway ineffective. As a result, even though MAVS is present on mitochondria and peroxisomes in WT cells, a functional antiviral response against VSV is only induced by the peroxisomal pathway. The experiments with VSV further revealed a probable benefit of utilizing both IFN-dependent and IFN- independent mechanisms of ISG induction: for pathogens that disrupt the expression of IFNs, the peroxisomal pathway retains the ability to induce ISGs and create a functional, albeit temporary antiviral state.

In fibroblasts, the cooperative actions of MAVS on peroxisomes and mitochondria are needed for maximal antiviral immunity, and signaling from each organelle occurs independently of the other. As such, it appears that a simple mathematical equation can be proposed to explain antiviral signal transduction: RLR=Pex+Mito. If either term in this equation is removed, then the RLR signaling network operates inefficiently, and antiviral immunity is compromised. I note however, that maximal ISG and IFN expression requires signaling from both organelles, which likely indicates that crosstalk exists to allow the two pathways to be properly integrated.

The molecular basis for the different signaling capabilities of mitochondria and peroxisomes remains elusive at this point. Arguably different accessory proteins are recruited to these organelles to create a unique signaling scaffold. Perhaps a positive regulator of direct ISG induction is only targeted to peroxisomes or an inhibitor of such a signaling pathway is located on mitochondria. The TLR4 pathway exemplifies how the spatial distribution of signaling components governs the signaling output. For TLR4 signaling TRAF3 was proposed to be limited in its mobility. The inability of TRAF3 to be recruited to TLR4 at the plasma membrane necessitates TLR4 to be endocytosed. It is at the endosome that the TRAM-TRIF adaptor pair is recruited to engage TRAF 3 and to enable type I IFN signaling. Similarly an essential factor for direct ISG induction may be available exclusively at peroxisomes. Experimental evidence for the organelle-specific presence of regulators of RLR signaling comes from NLRX1. My coworkers in Prof. Kagan's laboratory have shown that overexpression of NLRX1, a known negative regulator of MAVS exclusively found on mitochondria, inhibits signaling mediated by mitochondrial MAVS, but not by peroxisomal MAVS (data not shown and [176]).

Initial studies on the differential involvement of transcription factors in peroxisomal and mitochondrial MAVS were not informative. Reporter gene assays for AP-1, NF-κB and ISRE typically indicating IRF3 activity did not reveal an obvious difference in the transcription factors activated by overexpressed peroxisomal vs. mitochondrial MAVS (data not shown). Therefore it remained unclear why signaling from peroxisomes does not result in type I IFN expression. I speculated that selective IRF utilization may be responsible. Indeed, my coworkes were able to confirm this hypothesis by selectively activating the peroxisomal branch of RLR signaling with VSV in cells derived from mice genetically-deficient in IRF1, IRF3 or IRF5. While they found that IRF3 plays a role in ISG expression, this factor is also involved in the regulation of IFN expression [177] and may therefore be considered a more general regulator of antiviral gene expression. In fact IRF3 is also involved in IFN expression induced by non-RLRs [174]. IRF1, on the other hand, is needed for expression of all ISGs that were examined in VSV-infected cells and is not required for IFN expression [178]. IRF1 may thus uniquely control IFN-independent signaling events that lead to ISG expression and antiviral immunity. This statement was independently corroborated for the induction of viperin in response to viral infection [179]. This study identified two IRF1 binding sites in the promotor of the viperin gene and concludes that viperin is induced in a type I IFN dependent

or independent manner, the latter being mediated by IRF1. Interestingly both pathways depend on STAT1.

Since the publication of my data, two more studies addressed the spatial organization of RLR signaling, both of which emphasize a role for mitofusins as essential regulators of antiviral immunity [180, 181]. Onoguchi et al. observed a redistribution of mitochondrial MAVS upon activation of RIG-I signaling either by infection with various RNA viruses or transfection with 5' triphosphate RNA. While some mitochondria accumulate MAVS, others become devoid of it during a process that depends on MFN1. MFN1 is known to regulate mitochondrial dynamics and was already identified as a regulator of antiviral immunity by the authors before MAVS had been discovered. RIG-I is evenly distributed throughout the cytosol in uninfected cells, but is concentrated in foci upon infection. However, no co-localization between RIG-I and MAVS was observed. On the contrary, RIG-I co-localized with viral nucleocapsid. These findings led the authors to propose a model where RIG-I is recruited to virus factories to maximize the chances of receptor-ligand interaction. Mitochondria serve as vehicles that position MAVS. Some mitochondria enrich MAVS through repeated fission and fusion events and surround the foci of active viral replication in order to enable IFN induction. While this model outlines how mitochondrial signaling is optimized to perpetuate IFN induction for the duration of infection and to establish a sustained antiviral immune response, it leaves two important question unanswered. First, what are the kinetics of this process? The earliest and only time point presented in the study is 12 h post infection. Second, what triggers mitochondrial remodeling and accumulation of MAVS? Regardless if activation of RLR signaling or a different stimulus initiates the rearrangement, this model does not explain RNA detection at the very first instant of virus encounter. Much rather it demands additional and disparate means of RLR signaling that ensure an immediate antiviral response until MAVS-enriched mitochondria are recruited to the periphery of virus factories. I propose that signaling through peroxisomal MAVS constitutes a means to protect the cell during the time needed for mitochondrial reorganization for efficient MAVS signaling through mitochondria.

Horner et al. put forward yet another model for the spatial organisation of MAVS signaling. Higher resolution imaging equipment allowed the authors to detect MAVS not only on mitochondria and peroxisomes but also on mitochondria-associated membranes (MAM), a membranous network that links the ER with mitochondria and peroxisomes. HCV is sensed by RIG-I in hepatocytes, but uses its NS3/4A protease to evade the antiviral immune response.

NS3/4A cleaves MAVS from membranes.I and others have shown that cytosolic MAVS is unable to signal [59, 176]. Thus, NS3/4A is a potent inhibitor of RLR signaling. Prompted by the finding that NS3/4A is localized on the MAM, the authors investigated which subcellular pool of MAVS is affected by proteolytic cleavage. Unexpectedly, NS3/4A targeted MAM-resident MAVS, while mitochondrial MAVS remained fully intact. Moreover, RIG-I co-purified with MAM-associated MAVS, but not with mitochondrial MAVS in HCV infected cells. Based upon the findings that HCV infected hepatocytes are unable to mount an IFN response despite functional MAVS on mitochondria and that RIG-I interacts with MAVS on the MAM the authors conclude that - at least for HCV infections - mitochondrial MAVS is dispensable for RLR signaling. According to their model the MAM serves as a signaling synapse that coordinates MAVS-dependent signaling from mitochondria and peroxisomes. Contacts between MAM and mitochondria are known to be maintained by MFN2 [182]. Depletion of MFN2 by RNAi results in destabilization of this synapse, an increase in non-mitochondrial MAVS and an elevated IFN response in HCV and SeV-infected cells as a consequence. The latter observation is not in agreement with my findings, as I do not detect type I IFN expression by peroxisomal MAVS. This might be due to cell type or virus specific differences. As the evidence presented by Horner et al. is fairly indirect, it would be interesting to test the effect of MFN2 on the organelle-specific outcome of RLR signaling in MAVS-Pex and MAVS-Mito cells.

To summarize, these studies convincingly demonstrate that RLR signaling is strictly dependent on its spatial organization. The requirements for the subcellular arrangement of this and other antiviral signaling pathways are only beginning to emerge. Our understanding of cross-talk between different pathways as well as our ability to develop novel antiviral drugs as exemplified by site-specific interference of viral inhibitors with the innate immune response may depend on this knowledge. It seems serendipitous that pathway maps indeed require t information.

In closing, my work establishes a new function for peroxisomes, that of a subcellular compartment that promotes a rapid response to viral infection. I speculate that additional organelles may harbor pathogen detection systems, and my work provides a mandate to expand the search for these organelles.

REFERENCES

1. Benedict, C.A., Norris, P.S. & Ware, C.F. To kill or be killed: viral evasion of apoptosis. *Nat Immunol* **3**, 1013-1018 (2002).

2. Bowie, A.G. & Unterholzner, L. Viral evasion and subversion of pattern-recognition receptor signalling. *Nat Rev Immunol* **8**, 911-922 (2008).

3. Versteeg, G.A. & Garcia-Sastre, A. Viral tricks to grid-lock the type I interferon system. *Curr Opin Microbiol* **13**, 508-516 (2010).

4. Isaacs, A. & Lindenmann, J. Virus interference. I. The interferon. *Proc R Soc Lond B Biol Sci* **147**, 258-267 (1957).

5. Seth, R.B., Sun, L. & Chen, Z.J. Antiviral innate immunity pathways. *Cell Res* **16**, 141-147 (2006).

6. Samuel, C.E. Antiviral actions of interferons. *Clin Microbiol Rev* **14**, 778-809, table of contents (2001).

7. Katze, M.G., He, Y. & Gale, M., Jr. Viruses and interferon: a fight for supremacy. *Nat Rev Immunol* **2**, 675-687 (2002).

8. Hwang, S.Y., Hertzog, P.J., Holland, K.A., Sumarsono, S.H., Tymms, M.J., Hamilton, J.A., Whitty, G., Bertoncello, I. & Kola, I. A null mutation in the gene encoding a type I interferon receptor component eliminates antiproliferative and antiviral responses to interferons alpha and beta and alters macrophage responses. *Proc Natl Acad Sci U S A* **92**, 11284-11288 (1995).

9. Muller, U., Steinhoff, U., Reis, L.F., Hemmi, S., Pavlovic, J., Zinkernagel, R.M. & Aguet, M. Functional role of type I and type II interferons in antiviral defense. *Science* **264**, 1918-1921 (1994).

10. Janeway, C.A., Jr. Approaching the asymptote? Evolution and revolution in immunology. *Cold Spring Harb Symp Quant Biol* **54 Pt 1**, 1-13 (1989).

11. Medzhitov, R. Approaching the asymptote: 20 years later. *Immunity* **30**, 766-775 (2009).

12. Ishii, K.J., Koyama, S., Nakagawa, A., Coban, C. & Akira, S. Host innate immune receptors and beyond: making sense of microbial infections. *Cell Host Microbe* **3**, 352-363 (2008).

13. Takeuchi, O. & Akira, S. Pattern recognition receptors and inflammation. *Cell* **140**, 805-820 (2010).

14. Barton, G.M. & Kagan, J.C. A cell biological view of Toll-like receptor function: regulation through compartmentalization. *Nat Rev Immunol* **9**, 535-542 (2009).

15. Kawai, T. & Akira, S. Toll-like Receptors and Their Crosstalk with Other Innate Receptors in Infection and Immunity. *Immunity* **34**, 637-650 (2011).

16. Ozinsky, A., Underhill, D.M., Fontenot, J.D., Hajjar, A.M., Smith, K.D., Wilson, C.B., Schroeder, L. & Aderem, A. The repertoire for pattern recognition of pathogens by the innate immune system is defined by cooperation between toll-like receptors. *Proc Natl Acad Sci U S A* **97**, 13766-13771 (2000).

17. Takeuchi, O., Sato, S., Horiuchi, T., Hoshino, K., Takeda, K., Dong, Z., Modlin, R.L. & Akira, S. Cutting edge: role of Toll-like receptor 1 in mediating immune response to microbial lipoproteins. *J Immunol* **169**, 10-14 (2002).

18. Takeuchi, O., Kawai, T., Muhlradt, P.F., Morr, M., Radolf, J.D., Zychlinsky, A., Takeda, K. & Akira, S. Discrimination of bacterial lipoproteins by Toll-like receptor 6. *Int Immunol* **13**, 933-940 (2001).

19. Barbalat, R., Lau, L., Locksley, R.M. & Barton, G.M. Toll-like receptor 2 on inflammatory monocytes induces type I interferon in response to viral but not bacterial ligands. *Nat Immunol* **10**, 1200-1207 (2009).

20. Poltorak, A., He, X., Smirnova, I., Liu, M.Y., Van Huffel, C., Du, X., Birdwell, D., Alejos, E., Silva, M., Galanos, C., Freudenberg, M., Ricciardi-Castagnoli, P., Layton, B. & Beutler, B. Defective LPS signaling in C3H/HeJ and C57BL/10ScCr mice: mutations in Tlr4 gene. *Science* **282**, 2085-2088 (1998).

21. Rassa, J.C., Meyers, J.L., Zhang, Y., Kudaravalli, R. & Ross, S.R. Murine retroviruses activate B cells via interaction with toll-like receptor 4. *Proc Natl Acad Sci U S A* **99**, 2281-2286 (2002).

22. Kurt-Jones, E.A., Popova, L., Kwinn, L., Haynes, L.M., Jones, L.P., Tripp, R.A., Walsh, E.E., Freeman, M.W., Golenbock, D.T., Anderson, L.J. & Finberg, R.W. Pattern recognition receptors TLR4 and CD14 mediate response to respiratory syncytial virus. *Nat Immunol* **1**, 398-401 (2000).

23. Alexopoulou, L., Holt, A.C., Medzhitov, R. & Flavell, R.A. Recognition of double-stranded RNA and activation of NF-kappaB by Toll-like receptor 3. *Nature* **413**, 732-738 (2001).

24. Heil, F., Hemmi, H., Hochrein, H., Ampenberger, F., Kirschning, C., Akira, S., Lipford, G., Wagner, H. & Bauer, S. Species-specific recognition of single-stranded RNA via toll-like receptor 7 and 8. *Science* **303**, 1526-1529 (2004).

25. Diebold, S.S., Kaisho, T., Hemmi, H., Akira, S. & Reis e Sousa, C. Innate antiviral responses by means of TLR7-mediated recognition of single-stranded RNA. *Science* **303**, 1529-1531 (2004).

26. Jurk, M., Heil, F., Vollmer, J., Schetter, C., Krieg, A.M., Wagner, H., Lipford, G. & Bauer, S. Human TLR7 or TLR8 independently confer responsiveness to the antiviral compound R-848. *Nat Immunol* **3**, 499 (2002).

27. Lund, J.M., Alexopoulou, L., Sato, A., Karow, M., Adams, N.C., Gale, N.W., Iwasaki, A. & Flavell, R.A. Recognition of single-stranded RNA viruses by Toll-like receptor 7. *Proc Natl Acad Sci U S A* **101**, 5598-5603 (2004).

28. Krieg, A.M., Yi, A.K., Matson, S., Waldschmidt, T.J., Bishop, G.A., Teasdale, R., Koretzky, G.A. & Klinman, D.M. CpG motifs in bacterial DNA trigger direct B-cell activation. *Nature* **374**, 546-549 (1995).

29. Hemmi, H., Takeuchi, O., Kawai, T., Kaisho, T., Sato, S., Sanjo, H., Matsumoto, M., Hoshino, K., Wagner, H., Takeda, K. & Akira, S. A Toll-like receptor recognizes bacterial DNA. *Nature* **408**, 740-745 (2000).

30. Krug, A., Luker, G.D., Barchet, W., Leib, D.A., Akira, S. & Colonna, M. Herpes simplex virus type 1 activates murine natural interferon-producing cells through toll-like receptor 9. *Blood* **103**, 1433-1437 (2004).

31. Krug, A., French, A.R., Barchet, W., Fischer, J.A., Dzionek, A., Pingel, J.T., Orihuela, M.M., Akira, S., Yokoyama, W.M. & Colonna, M. TLR9-dependent recognition of MCMV by IPC and DC generates coordinated cytokine responses that activate antiviral NK cell function. *Immunity* **21**, 107-119 (2004).

32. Lund, J., Sato, A., Akira, S., Medzhitov, R. & Iwasaki, A. Toll-like receptor 9-mediated recognition of Herpes simplex virus-2 by plasmacytoid dendritic cells. *J Exp Med* **198**, 513-520 (2003).

33. Gilliet, M., Cao, W. & Liu, Y.J. Plasmacytoid dendritic cells: sensing nucleic acids in viral infection and autoimmune diseases. *Nat Rev Immunol* **8**, 594-606 (2008).

34. Ablasser, A., Bauernfeind, F., Hartmann, G., Latz, E., Fitzgerald, K.A. & Hornung, V. RIG-I-dependent sensing of poly(dA:dT) through the induction of an RNA polymerase III-transcribed RNA intermediate. *Nat Immunol* **10**, 1065-1072 (2009).

35. Chiu, Y.H., Macmillan, J.B. & Chen, Z.J. RNA polymerase III detects cytosolic DNA and induces type I interferons through the RIG-I pathway. *Cell* **138**, 576-591 (2009).

36. Yoneyama, M., Kikuchi, M., Natsukawa, T., Shinobu, N., Imaizumi, T., Miyagishi, M., Taira, K., Akira, S. & Fujita, T. The RNA helicase RIG-I has an essential function in double-stranded RNA-induced innate antiviral responses. *Nat Immunol* **5**, 730-737 (2004).

37. Hornung, V., Ellegast, J., Kim, S., Brzozka, K., Jung, A., Kato, H., Poeck, H., Akira, S., Conzelmann, K.K., Schlee, M., Endres, S. & Hartmann, G. 5'-Triphosphate RNA is the ligand for RIG-I. *Science* **314**, 994-997 (2006).

38. Pichlmair, A., Schulz, O., Tan, C.P., Naslund, T.I., Liljestrom, P., Weber, F. & Reis e Sousa, C. RIG-I-mediated antiviral responses to single-stranded RNA bearing 5'-phosphates. *Science* **314**, 997-1001 (2006).

39. Rehwinkel, J. & Reis e Sousa, C. RIGorous detection: exposing virus through RNA sensing. *Science* **327**, 284-286 (2010).

40. Kato, H., Takeuchi, O., Mikamo-Satoh, E., Hirai, R., Kawai, T., Matsushita, K., Hiiragi, A., Dermody, T.S., Fujita, T. & Akira, S. Length-dependent recognition of double-stranded ribonucleic acids by retinoic acid-inducible gene-I and melanoma differentiation-associated gene 5. *J Exp Med* **205**, 1601-1610 (2008).

41. Takahasi, K., Yoneyama, M., Nishihori, T., Hirai, R., Kumeta, H., Narita, R., Gale, M., Jr., Inagaki, F. & Fujita, T. Nonself RNA-sensing mechanism of RIG-I helicase and activation of antiviral immune responses. *Mol Cell* **29**, 428-440 (2008).

42. Malathi, K., Dong, B., Gale, M., Jr. & Silverman, R.H. Small self-RNA generated by RNase L amplifies antiviral innate immunity. *Nature* **448**, 816-819 (2007).

43. Sumpter, R., Jr., Loo, Y.M., Foy, E., Li, K., Yoneyama, M., Fujita, T., Lemon, S.M. & Gale, M., Jr. Regulating intracellular antiviral defense and permissiveness to hepatitis C virus RNA replication through a cellular RNA helicase, RIG-I. *J Virol* **79**, 2689-2699 (2005).

44. Kato, H., Takeuchi, O., Sato, S., Yoneyama, M., Yamamoto, M., Matsui, K., Uematsu, S., Jung, A., Kawai, T., Ishii, K.J., Yamaguchi, O., Otsu, K., Tsujimura, T., Koh, C.S., Reis e Sousa, C., Matsuura, Y., Fujita, T. & Akira, S. Differential roles of MDA5 and RIG-I helicases in the recognition of RNA viruses. *Nature* **441**, 101-105 (2006).

45. Barral, P.M., Morrison, J.M., Drahos, J., Gupta, P., Sarkar, D., Fisher, P.B. & Racaniello, V.R. MDA-5 is cleaved in poliovirus-infected cells. *J Virol* **81**, 3677-3684 (2007).

46. Fredericksen, B.L., Keller, B.C., Fornek, J., Katze, M.G. & Gale, M., Jr. Establishment and maintenance of the innate antiviral response to West Nile Virus involves both RIG-I and MDA5 signaling through IPS-1. *J Virol* **82**, 609-616 (2008).

47. Loo, Y.M., Fornek, J., Crochet, N., Bajwa, G., Perwitasari, O., Martinez-Sobrido, L., Akira, S., Gill, M.A., Garcia-Sastre, A., Katze, M.G. & Gale, M., Jr. Distinct RIG-I and MDA5 signaling by RNA viruses in innate immunity. *J Virol* **82**, 335-345 (2008).

48. Pichlmair, A., Schulz, O., Tan, C.P., Rehwinkel, J., Kato, H., Takeuchi, O., Akira, S., Way, M., Schiavo, G. & Reis e Sousa, C. Activation of MDA5 requires higher-order RNA structures generated during virus infection. *J Virol* **83**, 10761-10769 (2009).

49. Saito, T., Hirai, R., Loo, Y.M., Owen, D., Johnson, C.L., Sinha, S.C., Akira, S., Fujita, T. & Gale, M., Jr. Regulation of innate antiviral defenses through a shared repressor domain in RIG-I and LGP2. *Proc Natl Acad Sci U S A* **104**, 582-587 (2007).

50. Cui, S., Eisenacher, K., Kirchhofer, A., Brzozka, K., Lammens, A., Lammens, K., Fujita, T., Conzelmann, K.K., Krug, A. & Hopfner, K.P. The C-terminal regulatory domain is the RNA 5'-triphosphate sensor of RIG-I. *Mol Cell* **29**, 169-179 (2008).

51. Yoneyama, M., Kikuchi, M., Matsumoto, K., Imaizumi, T., Miyagishi, M., Taira, K., Foy, E., Loo, Y.M., Gale, M., Jr., Akira, S., Yonehara, S., Kato, A. & Fujita, T. Shared and unique functions of the DExD/H-box helicases RIG-I, MDA5, and LGP2 in antiviral innate immunity. *J Immunol* **175**, 2851-2858 (2005).

52. Rothenfusser, S., Goutagny, N., DiPerna, G., Gong, M., Monks, B.G., Schoenemeyer, A., Yamamoto, M., Akira, S. & Fitzgerald, K.A. The RNA helicase Lgp2 inhibits TLR-independent sensing of viral replication by retinoic acid-inducible gene-I. *J Immunol* **175**, 5260-5268 (2005).

53. Venkataraman, T., Valdes, M., Elsby, R., Kakuta, S., Caceres, G., Saijo, S., Iwakura, Y. & Barber, G.N. Loss of DExD/H box RNA helicase LGP2 manifests disparate antiviral responses. *J Immunol* **178**, 6444-6455 (2007).

54. Satoh, T., Kato, H., Kumagai, Y., Yoneyama, M., Sato, S., Matsushita, K., Tsujimura, T., Fujita, T., Akira, S. & Takeuchi, O. LGP2 is a positive regulator of RIG-I- and MDA5-mediated antiviral responses. *Proc Natl Acad Sci U S A* **107**, 1512-1517 (2010).

55. Takahasi, K., Kumeta, H., Tsuduki, N., Narita, R., Shigemoto, T., Hirai, R., Yoneyama, M., Horiuchi, M., Ogura, K., Fujita, T. & Inagaki, F. Solution structures of cytosolic RNA sensor MDA5 and LGP2 C-terminal domains: identification of the RNA recognition loop in RIG-I-like receptors. *J Biol Chem* **284**, 17465-17474 (2009).

56. Collins, S.E., Noyce, R.S. & Mossman, K.L. Innate cellular response to virus particle entry requires IRF3 but not virus replication. *J Virol* **78**, 1706-1717 (2004).

57. Mossman, K.L., Macgregor, P.F., Rozmus, J.J., Goryachev, A.B., Edwards, A.M. & Smiley, J.R. Herpes simplex virus triggers and then disarms a host antiviral response. *J Virol* **75**, 750-758 (2001).

58. Nakhaei, P., Genin, P., Civas, A. & Hiscott, J. RIG-I-like receptors: sensing and responding to RNA virus infection. *Semin Immunol* **21**, 215-222 (2009).

59. Seth, R.B., Sun, L., Ea, C.K. & Chen, Z.J. Identification and characterization of MAVS, a mitochondrial antiviral signaling protein that activates NF-kappaB and IRF 3. *Cell* **122**, 669-682 (2005).

60. Oshiumi, H., Miyashita, M., Inoue, N., Okabe, M., Matsumoto, M. & Seya, T. The ubiquitin ligase Riplet is essential for RIG-I-dependent innate immune responses to RNA virus infection. *Cell Host Microbe* **8**, 496-509 (2010).

61. Gack, M.U., Shin, Y.C., Joo, C.H., Urano, T., Liang, C., Sun, L., Takeuchi, O., Akira, S., Chen, Z., Inoue, S. & Jung, J.U. TRIM25 RING-finger E3 ubiquitin ligase is essential for RIG-I-mediated antiviral activity. *Nature* **446**, 916-920 (2007).

62. Oshiumi, H., Matsumoto, M., Hatakeyama, S. & Seya, T. Riplet/RNF135, a RING finger protein, ubiquitinates RIG-I to promote interferon-beta induction during the early phase of viral infection. *J Biol Chem* **284**, 807-817 (2009).

63. Gao, D., Yang, Y.K., Wang, R.P., Zhou, X., Diao, F.C., Li, M.D., Zhai, Z.H., Jiang, Z.F. & Chen, D.Y. REUL is a novel E3 ubiquitin ligase and stimulator of retinoic-acid-inducible gene-I. *PLoS One* **4**, e5760 (2009).

64. Arimoto, K., Takahashi, H., Hishiki, T., Konishi, H., Fujita, T. & Shimotohno, K. Negative regulation of the RIG-I signaling by the ubiquitin ligase RNF125. *Proc Natl Acad Sci U S A* **104**, 7500-7505 (2007).

65. Hayakawa, S., Shiratori, S., Yamato, H., Kameyama, T., Kitatsuji, C., Kashigi, F., Goto, S., Kameoka, S., Fujikura, D., Yamada, T., Mizutani, T., Kazumata, M., Sato, M., Tanaka, J., Asaka, M., Ohba, Y., Miyazaki, T., Imamura, M. & Takaoka, A. ZAPS is a potent stimulator of signaling mediated by the RNA helicase RIG-I during antiviral responses. *Nat Immunol* **12**, 37-44 (2011).

66. Ishikawa, H. & Barber, G.N. STING is an endoplasmic reticulum adaptor that facilitates innate immune signalling. *Nature* **455**, 674-678 (2008).

67. Jin, L., Hill, K.K., Filak, H., Mogan, J., Knowles, H., Zhang, B., Perraud, A.L., Cambier, J.C. & Lenz, L.L. MPYS Is Required for IFN Response Factor 3 Activation and Type I IFN Production in the Response of Cultured Phagocytes to Bacterial Second Messengers Cyclic-di-AMP and Cyclic-di-GMP. *J Immunol* **187**, 2595-2601 (2011).

68. Zhong, B., Yang, Y., Li, S., Wang, Y.Y., Li, Y., Diao, F., Lei, C., He, X., Zhang, L., Tien, P. & Shu, H.B. The adaptor protein MITA links virus-sensing receptors to IRF3 transcription factor activation. *Immunity* **29**, 538-550 (2008).

69. Sun, W., Li, Y., Chen, L., Chen, H., You, F., Zhou, X., Zhou, Y., Zhai, Z., Chen, D. & Jiang, Z. ERIS, an endoplasmic reticulum IFN stimulator, activates innate immune signaling through dimerization. *Proc Natl Acad Sci U S A* **106**, 8653-8658 (2009).

70. Moore, C.B., Bergstralh, D.T., Duncan, J.A., Lei, Y., Morrison, T.E., Zimmermann, A.G., Accavitti-Loper, M.A., Madden, V.J., Sun, L., Ye, Z., Lich, J.D., Heise, M.T., Chen, Z. & Ting, J.P. NLRX1 is a regulator of mitochondrial antiviral immunity. *Nature* **451**, 573-577 (2008).

71. Ishikawa, H., Ma, Z. & Barber, G.N. STING regulates intracellular DNA-mediated, type I interferon-dependent innate immunity. *Nature* **461**, 788-792 (2009).

72. Arnoult, D., Soares, F., Tattoli, I., Castanier, C., Philpott, D.J. & Girardin, S.E. An N-terminal addressing sequence targets NLRX1 to the mitochondrial matrix. *J Cell Sci* **122**, 3161-3168 (2009).

73. Tattoli, I., Carneiro, L.A., Jehanno, M., Magalhaes, J.G., Shu, Y., Philpott, D.J., Arnoult, D. & Girardin, S.E. NLRX1 is a mitochondrial NOD-like receptor that amplifies NF-kappaB and JNK pathways by inducing reactive oxygen species production. *EMBO Rep* **9**, 293-300 (2008).

74. Tal, M.C., Sasai, M., Lee, H.K., Yordy, B., Shadel, G.S. & Iwasaki, A. Absence of autophagy results in reactive oxygen species-dependent amplification of RLR signaling. *Proc Natl Acad Sci U S A* **106**, 2770-2775 (2009).

75. Koshiba, T., Yasukawa, K., Yanagi, Y. & Kawabata, S. Mitochondrial membrane potential is required for MAVS-mediated antiviral signaling. *Sci Signal* **4**, ra7 (2011).

76. Schroder, K. & Tschopp, J. The inflammasomes. *Cell* **140**, 821-832 (2010).

77. Sabbah, A., Chang, T.H., Harnack, R., Frohlich, V., Tominaga, K., Dube, P.H., Xiang, Y. & Bose, S. Activation of innate immune antiviral responses by Nod2. *Nat Immunol* **10**, 1073-1080 (2009).

78. Brennan, K. & Bowie, A.G. Activation of host pattern recognition receptors by viruses. *Curr Opin Microbiol* **13**, 503-507 (2010).

79. Elinav, E., Strowig, T., Henao-Mejia, J. & Flavell, R.A. Regulation of the antimicrobial response by NLR proteins. *Immunity* **34**, 665-679 (2011).

80. Elinav, E., Strowig, T., Kau, A.L., Henao-Mejia, J., Thaiss, C.A., Booth, C.J., Peaper, D.R., Bertin, J., Eisenbarth, S.C., Gordon, J.I. & Flavell, R.A. NLRP6 inflammasome regulates colonic microbial ecology and risk for colitis. *Cell* **145**, 745-757 (2011).

81. Ichinohe, T., Lee, H.K., Ogura, Y., Flavell, R. & Iwasaki, A. Inflammasome recognition of influenza virus is essential for adaptive immune responses. *J Exp Med* **206**, 79-87 (2009).

82. Thomas, P.G., Dash, P., Aldridge, J.R., Jr., Ellebedy, A.H., Reynolds, C., Funk, A.J., Martin, W.J., Lamkanfi, M., Webby, R.J., Boyd, K.L., Doherty, P.C. & Kanneganti, T.D. The intracellular sensor NLRP3 mediates key innate and healing responses to influenza A virus via the regulation of caspase-1. *Immunity* **30**, 566-575 (2009).

83. Allen, I.C., Scull, M.A., Moore, C.B., Holl, E.K., McElvania-TeKippe, E., Taxman, D.J., Guthrie, E.H., Pickles, R.J. & Ting, J.P. The NLRP3 inflammasome mediates in vivo innate immunity to influenza A virus through recognition of viral RNA. *Immunity* **30**, 556-565 (2009).

84. Kanneganti, T.D., Body-Malapel, M., Amer, A., Park, J.H., Whitfield, J., Franchi, L., Taraporewala, Z.F., Miller, D., Patton, J.T., Inohara, N. & Nunez, G. Critical role for Cryopyrin/Nalp3 in activation of caspase-1 in response to viral infection and double-stranded RNA. *J Biol Chem* **281**, 36560-36568 (2006).

85. Muruve, D.A., Petrilli, V., Zaiss, A.K., White, L.R., Clark, S.A., Ross, P.J., Parks, R.J. & Tschopp, J. The inflammasome recognizes cytosolic microbial and host DNA and triggers an innate immune response. *Nature* **452**, 103-107 (2008).

86. Poeck, H., Bscheider, M., Gross, O., Finger, K., Roth, S., Rebsamen, M., Hannesschlager, N., Schlee, M., Rothenfusser, S., Barchet, W., Kato, H., Akira, S., Inoue, S., Endres, S., Peschel, C., Hartmann, G., Hornung, V. & Ruland, J. Recognition of RNA virus by RIG-I results in activation of CARD9 and inflammasome signaling for interleukin 1 beta production. *Nat Immunol* **11**, 63-69 (2010).

87. Roberts, T.L., Idris, A., Dunn, J.A., Kelly, G.M., Burnton, C.M., Hodgson, S., Hardy, L.L., Garceau, V., Sweet, M.J., Ross, I.L., Hume, D.A. & Stacey, K.J. HIN-200 proteins regulate caspase activation in response to foreign cytoplasmic DNA. *Science* **323**, 1057-1060 (2009).

88. Hornung, V., Ablasser, A., Charrel-Dennis, M., Bauernfeind, F., Horvath, G., Caffrey, D.R., Latz, E. & Fitzgerald, K.A. AIM2 recognizes cytosolic dsDNA and forms a caspase-1-activating inflammasome with ASC. *Nature* **458**, 514-518 (2009).

89. Fernandes-Alnemri, T., Yu, J.W., Datta, P., Wu, J. & Alnemri, E.S. AIM2 activates the inflammasome and cell death in response to cytoplasmic DNA. *Nature* **458**, 509-513 (2009).

90. Burckstummer, T., Baumann, C., Bluml, S., Dixit, E., Durnberger, G., Jahn, H., Planyavsky, M., Bilban, M., Colinge, J., Bennett, K.L. & Superti-Furga, G. An orthogonal proteomic-genomic screen identifies AIM2 as a cytoplasmic DNA sensor for the inflammasome. *Nat Immunol* **10**, 266-272 (2009).

91. Fernandes-Alnemri, T., Yu, J.W., Juliana, C., Solorzano, L., Kang, S., Wu, J., Datta, P., McCormick, M., Huang, L., McDermott, E., Eisenlohr, L., Landel, C.P. & Alnemri, E.S. The AIM2 inflammasome is critical for innate immunity to Francisella tularensis. *Nat Immunol* **11**, 385-393 (2010).

92. Rathinam, V.A., Jiang, Z., Waggoner, S.N., Sharma, S., Cole, L.E., Waggoner, L., Vanaja, S.K., Monks, B.G., Ganesan, S., Latz, E., Hornung, V., Vogel, S.N., Szomolanyi-Tsuda, E. & Fitzgerald, K.A. The AIM2 inflammasome is essential for host defense against cytosolic bacteria and DNA viruses. *Nat Immunol* **11**, 395-402 (2010).

93. Hornung, V. & Latz, E. Intracellular DNA recognition. *Nat Rev Immunol* **10**, 123-130 (2010).

94. Takaoka, A., Wang, Z., Choi, M.K., Yanai, H., Negishi, H., Ban, T., Lu, Y., Miyagishi, M., Kodama, T., Honda, K., Ohba, Y. & Taniguchi, T. DAI (DLM-1/ZBP1) is a cytosolic DNA sensor and an activator of innate immune response. *Nature* **448**, 501-505 (2007).

95. Ishii, K.J., Kawagoe, T., Koyama, S., Matsui, K., Kumar, H., Kawai, T., Uematsu, S., Takeuchi, O., Takeshita, F., Coban, C. & Akira, S. TANK-binding kinase-1 delineates innate and adaptive immune responses to DNA vaccines. *Nature* **451**, 725-729 (2008).

96. Unterholzner, L., Keating, S.E., Baran, M., Horan, K.A., Jensen, S.B., Sharma, S., Sirois, C.M., Jin, T., Latz, E., Xiao, T.S., Fitzgerald, K.A., Paludan, S.R. & Bowie, A.G. IFI16 is an innate immune sensor for intracellular DNA. *Nat Immunol* **11**, 997-1004 (2010).

97. Pestka, S., Krause, C.D. & Walter, M.R. Interferons, interferon-like cytokines, and their receptors. *Immunol Rev* **202**, 8-32 (2004).

98. Kotenko, S.V., Gallagher, G., Baurin, V.V., Lewis-Antes, A., Shen, M., Shah, N.K., Langer, J.A., Sheikh, F., Dickensheets, H. & Donnelly, R.P. IFN-lambdas mediate antiviral protection through a distinct class II cytokine receptor complex. *Nat Immunol* **4**, 69-77 (2003).

99. Sheppard, P., Kindsvogel, W., Xu, W., Henderson, K., Schlutsmeyer, S., Whitmore, T.E., Kuestner, R., Garrigues, U., Birks, C., Roraback, J., Ostrander, C., Dong, D., Shin, J., Presnell, S., Fox, B., Haldeman, B., Cooper, E., Taft, D., Gilbert, T., Grant, F.J., Tackett, M., Krivan, W., McKnight, G., Clegg, C., Foster, D. & Klucher, K.M. IL-28, IL-29 and their class II cytokine receptor IL-28R. *Nat Immunol* **4**, 63-68 (2003).

100. Mordstein, M., Neugebauer, E., Ditt, V., Jessen, B., Rieger, T., Falcone, V., Sorgeloos, F., Ehl, S., Mayer, D., Kochs, G., Schwemmle, M., Gunther, S., Drosten, C., Michiels, T. & Staeheli, P. Lambda interferon renders epithelial cells of the respiratory and gastrointestinal tracts resistant to viral infections. *J Virol* **84**, 5670-5677 (2010).

101. Abbas, A.K. & Lichtman, A.H. *Cellular and molecular immunology*, Edn. 5th. (Saunders, Philadelphia, PA; 2005).

102. Sulkowski, M.S., Cooper, C., Hunyady, B., Jia, J., Ogurtsov, P., Peck-Radosavljevic, M., Shiffman, M.L., Yurdaydin, C. & Dalgard, O. Management of adverse effects of

Peg-IFN and ribavirin therapy for hepatitis C. *Nat Rev Gastroenterol Hepatol* **8**, 212-223 (2011).

103. Scott, G.M., Secher, D.S., Flowers, D., Bate, J., Cantell, K. & Tyrrell, D.A. Toxicity of interferon. *Br Med J (Clin Res Ed)* **282**, 1345-1348 (1981).

104. Kieseier, B.C. & Stuve, O. A critical appraisal of treatment decisions in multiple sclerosis--old versus new. *Nat Rev Neurol* **7**, 255-262 (2011).

105. Honda, K., Yanai, H., Takaoka, A. & Taniguchi, T. Regulation of the type I IFN induction: a current view. *Int Immunol* **17**, 1367-1378 (2005).

106. Randall, R.E. & Goodbourn, S. Interferons and viruses: an interplay between induction, signalling, antiviral responses and virus countermeasures. *J Gen Virol* **89**, 1-47 (2008).

107. Honda, K., Takaoka, A. & Taniguchi, T. Type I interferon [corrected] gene induction by the interferon regulatory factor family of transcription factors. *Immunity* **25**, 349-360 (2006).

108. Miyamoto, M., Fujita, T., Kimura, Y., Maruyama, M., Harada, H., Sudo, Y., Miyata, T. & Taniguchi, T. Regulated expression of a gene encoding a nuclear factor, IRF-1, that specifically binds to IFN-beta gene regulatory elements. *Cell* **54**, 903-913 (1988).

109. Matsuyama, T., Kimura, T., Kitagawa, M., Pfeffer, K., Kawakami, T., Watanabe, N., Kundig, T.M., Amakawa, R., Kishihara, K., Wakeham, A. & et al. Targeted disruption of IRF-1 or IRF-2 results in abnormal type I IFN gene induction and aberrant lymphocyte development. *Cell* **75**, 83-97 (1993).

110. Ruffner, H., Reis, L.F., Naf, D. & Weissmann, C. Induction of type I interferon genes and interferon-inducible genes in embryonal stem cells devoid of interferon regulatory factor 1. *Proc Natl Acad Sci U S A* **90**, 11503-11507 (1993).

111. Kamijo, R., Harada, H., Matsuyama, T., Bosland, M., Gerecitano, J., Shapiro, D., Le, J., Koh, S.I., Kimura, T., Green, S.J. & et al. Requirement for transcription factor IRF-1 in NO synthase induction in macrophages. *Science* **263**, 1612-1615 (1994).

112. Hemmi, H., Takeuchi, O., Sato, S., Yamamoto, M., Kaisho, T., Sanjo, H., Kawai, T., Hoshino, K., Takeda, K. & Akira, S. The roles of two IkappaB kinase-related kinases in lipopolysaccharide and double stranded RNA signaling and viral infection. *J Exp Med* **199**, 1641-1650 (2004).

113. Au, W.C., Moore, P.A., Lowther, W., Juang, Y.T. & Pitha, P.M. Identification of a member of the interferon regulatory factor family that binds to the interferon-stimulated response element and activates expression of interferon-induced genes. *Proc Natl Acad Sci U S A* **92**, 11657-11661 (1995).

114. Hiscott, J., Grandvaux, N., Sharma, S., Tenoever, B.R., Servant, M.J. & Lin, R. Convergence of the NF-kappaB and interferon signaling pathways in the regulation of antiviral defense and apoptosis. *Ann N Y Acad Sci* **1010**, 237-248 (2003).

115. Thanos, D. & Maniatis, T. Virus induction of human IFN beta gene expression requires the assembly of an enhanceosome. *Cell* **83**, 1091-1100 (1995).

116. Kim, T.K. & Maniatis, T. The mechanism of transcriptional synergy of an in vitro assembled interferon-beta enhanceosome. *Mol Cell* **1**, 119-129 (1997).

117. Agalioti, T., Lomvardas, S., Parekh, B., Yie, J., Maniatis, T. & Thanos, D. Ordered recruitment of chromatin modifying and general transcription factors to the IFN-beta promoter. *Cell* **103**, 667-678 (2000).

118. Hiscott, J. Convergence of the NF-kappaB and IRF pathways in the regulation of the innate antiviral response. *Cytokine Growth Factor Rev* **18**, 483-490 (2007).

119. Sato, M., Hata, N., Asagiri, M., Nakaya, T., Taniguchi, T. & Tanaka, N. Positive feedback regulation of type I IFN genes by the IFN-inducible transcription factor IRF-7. *FEBS Lett* **441**, 106-110 (1998).

120. Hiscott, J. Triggering the innate antiviral response through IRF-3 activation. *J Biol Chem* **282**, 15325-15329 (2007).

121. Erlandsson, L., Blumenthal, R., Eloranta, M.L., Engel, H., Alm, G., Weiss, S. & Leanderson, T. Interferon-beta is required for interferon-alpha production in mouse fibroblasts. *Curr Biol* **8**, 223-226 (1998).

122. Marie, I., Durbin, J.E. & Levy, D.E. Differential viral induction of distinct interferon-alpha genes by positive feedback through interferon regulatory factor-7. *EMBO J* **17**, 6660-6669 (1998).

123. Honda, K. & Taniguchi, T. IRFs: master regulators of signalling by Toll-like receptors and cytosolic pattern-recognition receptors. *Nat Rev Immunol* **6**, 644-658 (2006).

124. Trinchieri, G. Type I interferon: friend or foe? *J Exp Med* **207**, 2053-2063 (2010).

125. Platanias, L.C. Mechanisms of type-I- and type-II-interferon-mediated signalling. *Nat Rev Immunol* **5**, 375-386 (2005).

126. Decker, T., Muller, M. & Stockinger, S. The yin and yang of type I interferon activity in bacterial infection. *Nat Rev Immunol* **5**, 675-687 (2005).

127. Navarro, L., Mowen, K., Rodems, S., Weaver, B., Reich, N., Spector, D. & David, M. Cytomegalovirus activates interferon immediate-early response gene expression and an interferon regulatory factor 3-containing interferon-stimulated response element-binding complex. *Mol Cell Biol* **18**, 3796-3802 (1998).

128. Sadler, A.J. & Williams, B.R. Interferon-inducible antiviral effectors. *Nat Rev Immunol* **8**, 559-568 (2008).

129. Silverman, R.H. Viral encounters with 2',5'-oligoadenylate synthetase and RNase L during the interferon antiviral response. *J Virol* **81**, 12720-12729 (2007).

130. Arnheiter, H., Skuntz, S., Noteborn, M., Chang, S. & Meier, E. Transgenic mice with intracellular immunity to influenza virus. *Cell* **62**, 51-61 (1990).

131. Lindenmann, J. Resistance of mice to mouse-adapted influenza A virus. *Virology* **16**, 203-204 (1962).

132. Hefti, H.P., Frese, M., Landis, H., Di Paolo, C., Aguzzi, A., Haller, O. & Pavlovic, J. Human MxA protein protects mice lacking a functional alpha/beta interferon system against La crosse virus and other lethal viral infections. *J Virol* **73**, 6984-6991 (1999).

133. Skaug, B. & Chen, Z.J. Emerging role of ISG15 in antiviral immunity. *Cell* **143**, 187-190 (2010).

134. Terenzi, F., Hui, D.J., Merrick, W.C. & Sen, G.C. Distinct induction patterns and functions of two closely related interferon-inducible human genes, ISG54 and ISG56. *J Biol Chem* **281**, 34064-34071 (2006).

135. Hui, D.J., Terenzi, F., Merrick, W.C. & Sen, G.C. Mouse p56 blocks a distinct function of eukaryotic initiation factor 3 in translation initiation. *J Biol Chem* **280**, 3433-3440 (2005).

136. Pichlmair, A., Lassnig, C., Eberle, C.A., Gorna, M.W., Baumann, C.L., Burkard, T.R., Burckstummer, T., Stefanovic, A., Krieger, S., Bennett, K.L., Rulicke, T., Weber, F., Colinge, J., Muller, M. & Superti-Furga, G. IFIT1 is an antiviral protein that recognizes 5'-triphosphate RNA. *Nat Immunol* **12**, 624-630 (2011).

137. Daffis, S., Szretter, K.J., Schriewer, J., Li, J., Youn, S., Errett, J., Lin, T.Y., Schneller, S., Zust, R., Dong, H., Thiel, V., Sen, G.C., Fensterl, V., Klimstra, W.B., Pierson, T.C., Buller, R.M., Gale, M., Jr., Shi, P.Y. & Diamond, M.S. 2'-O methylation of the viral mRNA cap evades host restriction by IFIT family members. *Nature* **468**, 452-456 (2010).

138. Fitzgerald, K.A. The interferon inducible gene: Viperin. *J Interferon Cytokine Res* **31**, 131-135 (2011).

139. Chin, K.C. & Cresswell, P. Viperin (cig5), an IFN-inducible antiviral protein directly induced by human cytomegalovirus. *Proc Natl Acad Sci U S A* **98**, 15125-15130 (2001).

140. Helbig, K.J., Lau, D.T., Semendric, L., Harley, H.A. & Beard, M.R. Analysis of ISG expression in chronic hepatitis C identifies viperin as a potential antiviral effector. *Hepatology* **42**, 702-710 (2005).

141. Rivieccio, M.A., Suh, H.S., Zhao, Y., Zhao, M.L., Chin, K.C., Lee, S.C. & Brosnan, C.F. TLR3 ligation activates an antiviral response in human fetal astrocytes: a role for viperin/cig5. *J Immunol* **177**, 4735-4741 (2006).

142. Wang, X., Hinson, E.R. & Cresswell, P. The interferon-inducible protein viperin inhibits influenza virus release by perturbing lipid rafts. *Cell Host Microbe* **2**, 96-105 (2007).

143. Hinson, E.R. & Cresswell, P. The antiviral protein, viperin, localizes to lipid droplets via its N-terminal amphipathic alpha-helix. *Proc Natl Acad Sci U S A* **106**, 20452-20457 (2009).

144. Seo, J.Y., Yaneva, R., Hinson, E.R. & Cresswell, P. Human cytomegalovirus directly induces the antiviral protein viperin to enhance infectivity. *Science* **332**, 1093-1097 (2011).

145. Medzhitov, R., Preston-Hurlburt, P., Kopp, E., Stadlen, A., Chen, C., Ghosh, S. & Janeway, C.A., Jr. MyD88 is an adaptor protein in the hToll/IL-1 receptor family signaling pathways. *Mol Cell* **2**, 253-258 (1998).

146. Yamamoto, M., Sato, S., Mori, K., Hoshino, K., Takeuchi, O., Takeda, K. & Akira, S. Cutting edge: a novel Toll/IL-1 receptor domain-containing adapter that preferentially activates the IFN-beta promoter in the Toll-like receptor signaling. *J Immunol* **169**, 6668-6672 (2002).

147. Oshiumi, H., Matsumoto, M., Funami, K., Akazawa, T. & Seya, T. TICAM-1, an adaptor molecule that participates in Toll-like receptor 3-mediated interferon-beta induction. *Nat Immunol* **4**, 161-167 (2003).

148. Horng, T., Barton, G.M. & Medzhitov, R. TIRAP: an adapter molecule in the Toll signaling pathway. *Nat Immunol* **2**, 835-841 (2001).

149. Fitzgerald, K.A., Palsson-McDermott, E.M., Bowie, A.G., Jefferies, C.A., Mansell, A.S., Brady, G., Brint, E., Dunne, A., Gray, P., Harte, M.T., McMurray, D., Smith, D.E., Sims, J.E., Bird, T.A. & O'Neill, L.A. Mal (MyD88-adapter-like) is required for Toll-like receptor-4 signal transduction. *Nature* **413**, 78-83 (2001).

150. Fitzgerald, K.A., Rowe, D.C., Barnes, B.J., Caffrey, D.R., Visintin, A., Latz, E., Monks, B., Pitha, P.M. & Golenbock, D.T. LPS-TLR4 signaling to IRF-3/7 and NF-kappaB involves the toll adapters TRAM and TRIF. *J Exp Med* **198**, 1043-1055 (2003).

151. Oshiumi, H., Sasai, M., Shida, K., Fujita, T., Matsumoto, M. & Seya, T. TIR-containing adapter molecule (TICAM)-2, a bridging adapter recruiting to toll-like receptor 4 TICAM-1 that induces interferon-beta. *J Biol Chem* **278**, 49751-49762 (2003).

152. Kagan, J.C., Su, T., Horng, T., Chow, A., Akira, S. & Medzhitov, R. TRAM couples endocytosis of Toll-like receptor 4 to the induction of interferon-beta. *Nat Immunol* **9**, 361-368 (2008).

153. Kagan, J.C. & Medzhitov, R. Phosphoinositide-mediated adaptor recruitment controls Toll-like receptor signaling. *Cell* **125**, 943-955 (2006).

154. Hettema, E.H. & Motley, A.M. How peroxisomes multiply. *J Cell Sci* **122**, 2331-2336 (2009).

155. Gandre-Babbe, S. & van der Bliek, A.M. The novel tail-anchored membrane protein Mff controls mitochondrial and peroxisomal fission in mammalian cells. *Mol Biol Cell* **19**, 2402-2412 (2008).

156. Koch, A., Yoon, Y., Bonekamp, N.A., McNiven, M.A. & Schrader, M. A role for Fis1 in both mitochondrial and peroxisomal fission in mammalian cells. *Mol Biol Cell* **16**, 5077-5086 (2005).

157. Fransen, M., Vastiau, I., Brees, C., Brys, V., Mannaerts, G.P. & Van Veldhoven, P.P. Potential role for Pex19p in assembly of PTS-receptor docking complexes. *J Biol Chem* **279**, 12615-12624 (2004).

158. Furlong, D.B., Nibert, M.L. & Fields, B.N. Sigma 1 protein of mammalian reoviruses extends from the surfaces of viral particles. *J Virol* **62**, 246-256 (1988).

159. Garcia-Sastre, A., Egorov, A., Matassov, D., Brandt, S., Levy, D.E., Durbin, J.E., Palese, P. & Muster, T. Influenza A virus lacking the NS1 gene replicates in interferon-deficient systems. *Virology* **252**, 324-330 (1998).

160. Cureton, D.K., Massol, R.H., Saffarian, S., Kirchhausen, T.L. & Whelan, S.P. Vesicular stomatitis virus enters cells through vesicles incompletely coated with clathrin that depend upon actin for internalization. *PLoS Pathog* **5**, e1000394 (2009).

161. Middleton, J.K., Agosto, M.A., Severson, T.F., Yin, J. & Nibert, M.L. Thermostabilizing mutations in reovirus outer-capsid protein mu1 selected by heat inactivation of infectious subvirion particles. *Virology* **361**, 412-425 (2007).

162. Wong, G.W., Liu, E.K., Leung, T.F., Yung, E., Ko, F.W., Hui, D.S., Fok, T.F. & Lai, C.K. High levels and gender difference of exhaled nitric oxide in Chinese schoolchildren. *Clin Exp Allergy* **35**, 889-893 (2005).

163. Amit, I., Garber, M., Chevrier, N., Leite, A.P., Donner, Y., Eisenhaure, T., Guttman, M., Grenier, J.K., Li, W., Zuk, O., Schubert, L.A., Birditt, B., Shay, T., Goren, A., Zhang, X., Smith, Z., Deering, R., McDonald, R.C., Cabili, M., Bernstein, B.E., Rinn, J.L., Meissner, A., Root, D.E., Hacohen, N. & Regev, A. Unbiased reconstruction of a mammalian transcriptional network mediating pathogen responses. *Science* **326**, 257-263 (2009).

164. Matsuzono, Y., Kinoshita, N., Tamura, S., Shimozawa, N., Hamasaki, M., Ghaedi, K., Wanders, R.J., Suzuki, Y., Kondo, N. & Fujiki, Y. Human PEX19: cDNA cloning by functional complementation, mutation analysis in a patient with Zellweger syndrome, and potential role in peroxisomal membrane assembly. *Proc Natl Acad Sci U S A* **96**, 2116-2121 (1999).

165. Sacksteder, K.A., Jones, J.M., South, S.T., Li, X., Liu, Y. & Gould, S.J. PEX19 binds multiple peroxisomal membrane proteins, is predominantly cytoplasmic, and is required for peroxisome membrane synthesis. *J Cell Biol* **148**, 931-944 (2000).

166. Wanders, R.J. Peroxisomes, lipid metabolism, and peroxisomal disorders. *Mol Genet Metab* **83**, 16-27 (2004).

167. Fransen, M., Wylin, T., Brees, C., Mannaerts, G.P. & Van Veldhoven, P.P. Human pex19p binds peroxisomal integral membrane proteins at regions distinct from their sorting sequences. *Mol Cell Biol* **21**, 4413-4424 (2001).

168. Ingelmo-Torres, M., Gonzalez-Moreno, E., Kassan, A., Hanzal-Bayer, M., Tebar, F., Herms, A., Grewal, T., Hancock, J.F., Enrich, C., Bosch, M., Gross, S.P., Parton, R.G. & Pol, A. Hydrophobic and basic domains target proteins to lipid droplets. *Traffic* **10**, 1785-1801 (2009).

169. Nemoto, Y. & De Camilli, P. Recruitment of an alternatively spliced form of synaptojanin 2 to mitochondria by the interaction with the PDZ domain of a mitochondrial outer membrane protein. *Embo J* **18**, 2991-3006 (1999).

170. Severa, M., Coccia, E.M. & Fitzgerald, K.A. Toll-like receptor-dependent and -independent viperin gene expression and counter-regulation by PRDI-binding factor-1/BLIMP1. *J Biol Chem* **281**, 26188-26195 (2006).

171. Gitlin, L., Barchet, W., Gilfillan, S., Cella, M., Beutler, B., Flavell, R.A., Diamond, M.S. & Colonna, M. Essential role of mda-5 in type I IFN responses to polyriboinosinic:polyribocytidylic acid and encephalomyocarditis picornavirus. *Proc Natl Acad Sci U S A* **103**, 8459-8464 (2006).

172. Geiss, G.K., Bumgarner, R.E., Birditt, B., Dahl, T., Dowidar, N., Dunaway, D.L., Fell, H.P., Ferree, S., George, R.D., Grogan, T., James, J.J., Maysuria, M., Mitton, J.D., Oliveri, P., Osborn, J.L., Peng, T., Ratcliffe, A.L., Webster, P.J., Davidson, E.H., Hood, L. & Dimitrov, K. Direct multiplexed measurement of gene expression with color-coded probe pairs. *Nat Biotechnol* **26**, 317-325 (2008).

173. Ferran, M.C. & Lucas-Lenard, J.M. The vesicular stomatitis virus matrix protein inhibits transcription from the human beta interferon promoter. *J Virol* **71**, 371-377 (1997).

174. Kawai, T. & Akira, S. Antiviral signaling through pattern recognition receptors. *J Biochem (Tokyo)* **141**, 137-145 (2007).

175. Akira, S., Uematsu, S. & Takeuchi, O. Pathogen recognition and innate immunity. *Cell* **124**, 783-801 (2006).

176. Dixit, E., Boulant, S., Zhang, Y., Lee, A.S., Odendall, C., Shum, B., Hacohen, N., Chen, Z.J., Whelan, S.P., Fransen, M., Nibert, M.L., Superti-Furga, G. & Kagan, J.C. Peroxisomes are signaling platforms for antiviral innate immunity. *Cell* **141**, 668-681 (2010).

177. Sato, M., Suemori, H., Hata, N., Asagiri, M., Ogasawara, K., Nakao, K., Nakaya, T., Katsuki, M., Noguchi, S., Tanaka, N. & Taniguchi, T. Distinct and essential roles of transcription factors IRF-3 and IRF-7 in response to viruses for IFN-alpha/beta gene induction. *Immunity* **13**, 539-548 (2000).

178. Tamura, T., Yanai, H., Savitsky, D. & Taniguchi, T. The IRF family transcription factors in immunity and oncogenesis. *Annu Rev Immunol* **26**, 535-584 (2008).

179. Stirnweiss, A., Ksienzyk, A., Klages, K., Rand, U., Grashoff, M., Hauser, H. & Kroger, A. IFN regulatory factor-1 bypasses IFN-mediated antiviral effects through viperin gene induction. *J Immunol* **184**, 5179-5185 (2010).

180. Horner, S.M., Liu, H.M., Park, H.S., Briley, J. & Gale, M., Jr. Mitochondrial-associated endoplasmic reticulum membranes (MAM) form innate immune synapses and are targeted by hepatitis C virus. *Proc Natl Acad Sci U S A* **108**, 14590-14595 (2011).

181. Onoguchi, K., Onomoto, K., Takamatsu, S., Jogi, M., Takemura, A., Morimoto, S., Julkunen, I., Namiki, H., Yoneyama, M. & Fujita, T. Virus-infection or 5'ppp-RNA activates antiviral signal through redistribution of IPS-1 mediated by MFN1. *PLoS Pathog* **6**, e1001012 (2010).

182. de Brito, O.M. & Scorrano, L. Mitofusin 2 tethers endoplasmic reticulum to mitochondria. *Nature* **456**, 605-610 (2008).

CURRICULUM VITAE

Mag. Evelyn Dixit

Personal data

Born:	November 23, 1976, Graz, Austria
Citizenship:	Austrian
E-mail:	evelyndixit@gmail.com

Academic education and scientific experience

Since 12/2007	**Medical University of Vienna** Ph.D. program Cell Communication in Health and Disease
Since 11/2010	maternity leave
12/2007 – 10/2010	**CeMM – Research Center for Molecular Medicine,** **Austrian Academy of Sciences**, Vienna *Ph.D. student* Advisor: Prof. Dr. Giulio Superti-Furga Thesis: „Nucleic Acid Sensing in the Cytosol“
10/2008 – 09/2009	**Children's Hospital Boston and** **Harvard Medical School**, Boston, MA, USA Collaboration with Prof. Dr. Jonathan Kagan
10/2003 – 11/2007	**University of Vienna** Diploma program for Molecular Biology Graduation *cum laude*
11/2006 – 11/2007	**CeMM – Research Center for Molecular Medicine,** **Austrian Academy of Sciences**, Vienna *Diploma student* Advisor: Prof. Dr. Giulio Superti-Furga Thesis: „Functional Proteomics and Genomics of Virus-Induced Innate Immunity Pathways”

General education and professional experience

03/2002 – 08/2003	**SangStat Medical Corporation**, Fremont, CA, USA *Research Associate*
02/1999 – 02/2002	**Baxter AG**, Vienna *Technical Assistant*
06/1998 – 01/1999	**Veterinary University of Vienna** *Technician*
09/1995 – 05/1998	**HBLuVA für chemische Industrie**, Vienna Kolleg für Biochemie, Biotechnologie und Gentechnik Graduation *magna cum laude*
09/1987 – 06/1995	**Neusprachliches Gymnasium der Ursulinen**, Graz Graduation *cum laude*

Awards and scholarships

2010	YSA Publication Award for "Peroxisomes Are Signaling Platforms for Antiviral Innate Immunity" (Dixit et al, Cell 2010)
2007	Scholarship for excellent performance during the academic year 2005/06 awarded by the University of Vienna
2006	Scholarship for excellent performance during the academic year 2004/05 awarded by the University of Vienna
2000	Baxter Values in Action Award for exemplary performance and work ethics, a prize given to 50 out of 45.000 Baxter employees worldwide each year

PUBLICATION LIST

Peer-reviewed publications (under married and maiden names)

Goncalves, A.*, Burckstummer, T.*, **Dixit, E.***, Scheicher, R., Gorna, M.W., Karayel, E., Sugar, C., Stukalov, A., Berg, T., Kralovics, R., Planyavsky, M., Bennett, K.L., Colinge, J. & Superti-Furga, G.
Functional Dissection of the TBK1 Molecular Network.
PLoS One 6, e23971 (2011).
*** Equal contributions** of Dixit, E., Burckstummer, T. and Goncalves, A.

Dixit, E., Boulant, S., Zhang, Y., Lee, A.S., Odendall, C., Shum, B., Hacohen, N., Chen, Z.J., Whelan, S.P., Fransen, M., Nibert, M.L., Superti-Furga, G. & Kagan, J.C.
Peroxisomes Are Signaling Platforms for Antiviral Innate Immunity.
Cell 141, 668-681 (2010).

Burckstummer, T., Baumann, C., Bluml, S., **Dixit, E.**, Durnberger, G., Jahn, H., Planyavsky, M., Bilban, M., Colinge, J., Bennett, K.L. & Superti-Furga, G.
An Orthogonal Proteomic-Genomic Screen Identifies AIM2 as a Cytoplasmic DNA Sensor for the Inflammasome.
Nat Immunol 10, 266-272 (2009).

De Vry, C.G., Valdez, M., Lazarov, M., **Muhr, E.**, Buelow, R., Fong, T. & Iyer, S.
Topical Application of a Novel Immunomodulatory Peptide, RDP58, Reduces Skin Inflammation in the Phorbol Ester-Induced Dermatitis Model.
J Invest Dermatol 125, 473-481 (2005).

Himmelspach, M., Richter, G., **Muhr, E.**, Varadi, K., Turecek, P.L., Dorner, F., Schwarz, H.P. & Schlokat, U.
A Fully Recombinant Partial Prothrombin Complex Effectively Bypasses fVIII In Vitro and In Vivo.
Thromb Haemost 88, 1003-1011 (2002).

Oral presentations

6th PhD Symposium of the Medical University of Vienna, YSA Publication Award Lecture
Vienna, Austria, June 16 – 17, 2010
"Peroxisomes Are Signaling Platforms for Antiviral Innate Immunity"

5th International Symposium of the Austrian Proteomics Platform,
Seefeld, Austria, January 20 – 23, 2008 (invited speaker)
"Nucleic Acids Proteomics and Innate Immunity"

Poster presentations

Toll2008 Meeting - Recent Advances in Pattern Recognition
Lisbon, Portugal, September 24 – 27, 2008

4th PhD Symposium of the Medical University of Vienna
Vienna, Austria, May 28 – 29, 2008